

# UNIVERSITY OF TWENTE.

Faculty of Science and Technology,  
Biomedical Engineering

## High-frequency stimulation and time-frequency analysis for the validation of the MTT-EP protocol

Francesca Marsili

M.Sc. Thesis  
October 2020

---

**Supervisor:**

Dr. ir. J. R. Buitenweg

**Examination Committee:**

Dr. ir. J. R. Buitenweg

Niels Jansen, MSc

Dr. A.D. van der Meer

Biomedical Signals and Systems group  
Faculty of Electrical Engineering,  
Mathematics and Computer Science  
University of Twente  
P.O. Box 217  
7500 AE Enschede  
The Netherlands

---



## *Preface*

This graduation assignment started on January 2020. After few weeks into the project, on March 17th 2020, the University of Twente announced the complete closure of the buildings on campus and the start of remote-working due to the increasing number of Coronavirus cases in the Netherlands. Due to the impossibility to access the facilities or perform any experimental sessions on individuals, data acquisition for the HFS experimental protocol has been put on hold and postponed until further notice. In order to adjust this graduation assignment to a smart-working project, changes have been made including the use of already-available datasets. For these reasons, this graduation assignment will be divided in two main and distinct topics.

At first, the reader will be introduced to background information about pain and its physiology, about pain research and the way pain research is conducted at the University of Twente. *Chapter 3* will address the first topic, part of the graduation assignment conducted prior the closure of the University. Due to discontinuation of the project, Chapter 3 lacks of sections related to data acquisition, analysis and results. Lastly, *Chapter 4* will address the second and new project conducted on a remote-basis. Due to the impossibility of acquiring new data, Chapter 4 lacks of a method and data acquisition section.



# Abstract

Pain is the major cause of disability and disease burden affecting 19% of the European population over 18 years of age. It is a multidimensional experience involving both cognitive and physical mechanisms and characterized by an individual variability of its perceptual processing.

At the University of Twente, research investigating the underlying mechanisms of pain is conducted using the 'Multiple Threshold Tracking and Evoked Potentials' (MTT-EP) protocol. In the MTT-EP protocol, nociceptive stimuli are delivered around the individuals' detection threshold using intra-epidermal electrical stimulation (IES) and neural processing of pain stimuli, transmitted from the periphery to the central nervous system, is simultaneously recorded using EEG.

The effect of stimulus parameters on evoked potentials has been investigated by modelling the collected data using a linear mixed model (LMM). Previous results at the University of Twente demonstrated that stimulus parameters, such as stimulus amplitude and detection, play a significant role in modulating evoked potentials responding to noxious stimuli. While the MTT-EP protocol has been thoroughly investigated and already showed significant results as objective and quantitative measurement of nociception, further studies need to be conducted in order to validate the MTT-EP protocol as diagnostic tool for the assessment of chronic pain conditions.

One way to validate the MTT-EP protocol consists of introducing an experimental pain model, a commonly-used tool in pain research, to induce symptoms on healthy subjects that mimic pathophysiological conditions such as peripheral or central sensitization. For example, high-frequency stimulation (HFS) is known to induce secondary hyperalgesia by delivering electrical stimuli onto the skin of individuals at high frequencies.

For further understanding the mechanisms of nociception, time-frequency analysis can be conducted on EEG data. Evidences from previous pain research revealed the presence of neuronal oscillations at frequencies from 3Hz to 100Hz, carrying functional information on how nociceptive stimuli are integrated in the brain.

In this graduation assignment, an experimental protocol is designed introducing the use of HFS with the MTT-EP protocol. Furthermore, previously-acquired EEG data recorded during the MTT-EP protocol are transformed into time-frequency representations (TFRs) and investigated. Results are then modelled using a Linear Mixed Model (LMM) in order to study the effects of stimulus parameters on neuronal oscillations.

Time-frequency analysis of EEG data recorded during the MTT-EP protocol unveiled the

frequency contents of neuronal activations elicited by nociceptive stimuli; while the LMM identified the effect of stimulus parameters in modulating neuronal oscillations. Results from two datasets were not consistent and showed statistically significant differences. As result of this exploratory analysis, it has been concluded that time-frequency analysis is a useful tool to understand the functional role of neuronal responses and can be used to further understand nociceptive processing by investigating the role of subject characteristics on the TFRs and by including a larger and diverse cohort of both healthy individuals and chronic pain patients.

# Contents

<b>Contents</b>	<b>3</b>
<b>1 Introduction</b>	<b>1</b>
1.1 Problem statement . . . . .	1
1.2 Research goal . . . . .	2
<b>2 Background</b>	<b>4</b>
2.1 Pain . . . . .	4
2.2 The nociceptive system . . . . .	4
2.2.1 The anatomy and physiology of pain . . . . .	5
2.3 Quantitative measure of pain . . . . .	11
2.3.1 Peripheral stimulation . . . . .	11
2.3.2 Nociceptive detection threshold and Psychometric curve . . . . .	11
2.3.3 Peripheral modulation . . . . .	12
2.3.4 Central acquisition . . . . .	14
2.4 The MTT-EP protocol . . . . .	14
2.4.1 Peripheral stimulation . . . . .	14
2.4.2 Multiple threshold tracking . . . . .	15
2.4.3 Central acquisition . . . . .	16
2.4.4 Nociceptive evoked potentials (EPs) . . . . .	16
2.4.5 The MTT-EP Measurement System . . . . .	17
2.5 Frequency-domain analysis of EEG pain-related recordings . . . . .	18
2.5.1 Analysis of neuronal oscillations . . . . .	20
<b>3 High-frequency stimulation (HFS) and the MTT-EP protocol</b>	<b>21</b>
3.1 Methods & Materials . . . . .	21
3.1.1 Participants . . . . .	21
3.1.2 Equipment . . . . .	21
3.1.3 Experimental procedure . . . . .	23
3.1.4 Ethical approval . . . . .	25
<b>4 Frequency-domain analysis of EEG data</b>	<b>26</b>
4.1 Methods & Materials . . . . .	26
4.1.1 Participants . . . . .	26
4.1.2 Equipment . . . . .	27
4.1.3 Experimental procedure . . . . .	27
4.1.4 Time-frequency analysis . . . . .	27
4.1.5 Statistical Analysis . . . . .	28
4.1.6 Comparison analysis . . . . .	29
4.2 Results . . . . .	30
4.2.1 Time-frequency analysis . . . . .	30
4.2.2 Statistical Analysis . . . . .	35
4.2.3 Comparison analysis . . . . .	39
4.3 Discussion . . . . .	54
4.3.1 Time-frequency and statistical analysis . . . . .	54
4.3.2 Comparison analysis . . . . .	55
<b>5 Conclusions</b>	<b>57</b>

<b>Bibliography</b>	<b>59</b>
<b>Appendix A</b>	<b>64</b>

1.1 Problem statement . . . . . 1  
1.2 Research goal . . . . . 2

Pain has been the center of an open debate for decades due to its complex and dual nature, being both an adaptive function to protect the body and a pathological condition. For these reasons, a generally accepted definition and classification of pain and pain-related syndromes has been the topic of many discussions in the scientific community and the major focus of the International Association for the Study of Pain (IASP)<sup>1</sup> [1]. The experience of pain can be classified as nociceptive, neuropathic or nociplastic pain. Nociceptive pain is generally recognized as a symptom and defined as *"the pain arising from actual or threatened damage to non-neural tissue and is due to the activation of nociceptors"*<sup>2</sup>, while neuropathic pain is *"caused by a lesion or a damage of the somatosensory nervous system"*<sup>3</sup>. An altered nociception with no evidence of tissue damage or disease of the somatosensory system is known as nociplastic pain<sup>4</sup>. Nociceptive, neuropathic and nociplastic pain can develop into more acute and chronic states.

The sole presence of symptoms without clear evidence of damages or diseases is often reason for errors in assessment and management of pain, although it negatively affects the quality of life of individuals altering mental health, sleep and personal relationships [1]. In the long term, unrelieved pain also causes physically harmful effects on the endocrine and metabolic system, on the cardiovascular, gastrointestinal and immune system [2]. Lack of adequate management of pain contributes to the occurrence of adverse physical and psychological comorbidity factors (e.g. lack of energy, mood changes and depression).

According to The Global Burden of Disease Study 2016, chronic pain is considered the major cause of disability and disease burden in Europe, affecting 20.27% of the population over 18 years of age [3]. The prevalence of pain varies depending on the country, but 22.47% of the European population affected by pain or pain-related syndromes experiences severe pain and 59.20% experiences moderate pain [4]. For these reasons, the complexity of neuropathic and nociplastic pain syndromes is the source of physical and psychological burden for patients, but also a big economic and social burden for society.

Unraveling the underlying mechanisms of pathological nociception is the major focus of pain researchers who have to deal with many sensory modalities intervening simultaneously, along with influence from perception and emotional states [5]. A physiological and psychological understanding of the nociceptive system is imperative in order to make the correct diagnosis and develop the proper treatments.

## 1.1 Problem statement

Pain, caused by either external or internal factors, is a highly subjective experience merging physical and emotional states such as past experiences and personality [6].

From a physiological point of view, pain is composed of four processes: transduction, transmission, modulation and perception [7]. The first three processes are the result of a complex network involving both the peripheral (PNS)<sup>5</sup> and the central nervous systems (CNS)<sup>6</sup>.

1: IASP: International Association for the Study of Pain

2: nociceptive pain. 2017. In *IASP Terminology*. Retrieved Jul 16, 2020, from <https://www.iasp-pain.org/Education/Content.aspx?ItemNumber=1698#Nociceptivepain>

3: neuropathic pain. 2017. In *IASP Terminology*. Retrieved Jul 16, 2020, from <https://www.iasp-pain.org/Education/Content.aspx?ItemNumber=1698#Neuropathicpain>

4: nociplastic pain. 2017. In *IASP Terminology*. Retrieved Jul 16, 2020, from <https://www.iasp-pain.org/Education/Content.aspx?ItemNumber=1698#Nociplasticpain>

5: PNS: peripheral nervous system

6: CNS: central nervous system

In diagnostics, self-rating instruments, such as Numerical Rating Scores (NRS)<sup>7</sup> are one-dimensional measures assisting patients in quantifying their subjective experience of pain. However, they are also characterized by strong inaccuracies leading to improper diagnosis and treatments [8]. Instead, pain researchers have explored the opportunity of introducing already-available, objective and quantifiable measurements to characterize the nociceptive system and pathological nociception [8]. At the University of Twente, the MTT-EP<sup>8</sup> protocol is used as a tool to describe the modulation of the nociceptive system in response to variable noxious stimuli delivered onto the skin of individuals via intra-epidermal electrical stimulation (IES)<sup>9</sup>. In fact, IES-generated stimuli have an intensity around each individual's detection threshold and are transmitted from the periphery via selective activation of nociceptive A $\delta$ -, and C-fibers to the CNS, projecting on brain regions for an active perception of a sensory sensation. This stimulus-evoked brain activity is also addressed as nociceptive evoked potentials (EPs)<sup>10</sup> and is derived by averaging the EEG signals obtained from multiple trials in the time-domain [9].

Further experimental evidence must be provided in order to validate the MTT-EP protocol. In this regard, clinically-relevant pain symptoms, such as central sensitization and its related characteristics (e.g. hyperalgesia, allodynia) [10], can be experimentally induced on healthy subjects using experimental pain models, such as high-frequency electrical stimulation (HFS), to mimic the presence of neuropathic pain [11],[10],[12]. Previous results have shown that HFS can modulate EPs when applied on the site of HFS-induced sensitization [13].

Frequency content of evoked potentials results into patterns of inhibition and/or excitation and are addressed as neuronal oscillations. These neuronal oscillations have already been crucial biomarkers at the center of attention of clinical researchers for understanding brain functions in cognitive impairments or epilepsy [14],[15]. Brain mapping investigations demonstrated a positive correlation among intensity of pain, cortical activation and neuronal oscillations, and unveiled a hidden network of cortical areas that are likewise involved in integrating pain information [16]. The combination of time-frequency cortical activations (as stimulus-dependent neurophysiological activity) and multiple noxious stimuli provides a proper representation of the relation between neurophysiological activity and nociceptive stimuli. At the University of Twente, nociceptive evoked potentials are currently used to describe the underlying mechanisms of nociceptive processing, while frequency-domain components has never been investigated.

In light of this evidence, pain research at the University of Twente introduces HFS, as a new means for validating their MTT-EP protocol, and frequency-domain analysis, as an alternative to investigate neuronal oscillations responding to nociceptive stimulation.

## 1.2 Research goal

In this report, the stages for conducting a biomedical research are detailed including literature search, experimental design and analysis of the data. Accordingly, the readers will be provided with an overview of the nociceptive system and pain research with specific interest on the role of hyperalgesia in patients with pain-related or chronic pain syndromes.

The first objective of this assignment is to search for existing literature validating the use of high-frequency electrical stimulation as a tool for inducing pain symptoms and to design an experimental protocol combining HFS-induced secondary hyperalgesia with the MTT-EP protocol. HFS is used to induce a temporary

7: NRS: numerical rating scores

8: MTT: multiple threshold tracking

9: IES: intra-epidermal electrical stimulation

10: EPs: Evoked Potentials

change in central pain-processing, mimicking the long-term alterations of the nociceptive system that are relevant in the development of chronic pain states. Characterizing maladaptive cortical activations further validates the MTT-EP protocol as diagnostic tool for the assessment of chronic pain conditions.

#### **First research question**

In which way cortical activations, recorded during the MTT-EP protocol, depict the maladaptive changes in nociceptive processing, caused by HFS-induced secondary hyperalgesia?

Afterwards, specific attention is drawn to the relevance of time-frequency analysis in providing further insights of nociception. The second objective of this assignment is to investigate the content of neuronal oscillations at various frequencies in response to IES-5 stimuli. A signal processing tool for the analysis of electroencephalographic data recorded during the MTT-EP protocol is presented as an alternative to investigate neuronal responses in the frequency domain.

#### **Second research question**

What is the frequency content of cortical activations recorded during the MTT-EP protocol and what is the role of stimulus parameters in modulating these time-frequency representations?

1. What is the frequency content of cortical activations recorded during the MTT-EP experiments?
2. How do stimulus parameters modulate the frequency content of neuronal oscillations as measured via the MTT-EP method?
3. How does the frequency content of cortical activations recorded during the MTT-EP protocol change with respect to subjects characteristics?

- 2.1 Pain . . . . . 4
- 2.2 The nociceptive system . . . . 4
- 2.3 Quantitative measure of pain 11
- 2.4 The MTT-EP protocol . . . . 14
- 2.5 Frequency-domain analysis of EEG pain-related recordings . . . . 18

In this chapter, background information about the nociceptive system, the physiology behind the perception of pain and the current methodology in use for diagnosis and treatment of pain-related diseases are presented to the reader.

## 2.1 Pain

Nowadays, pain is defined by the International Association for the Study of Pain (IASP)<sup>1</sup> as ‘an unpleasant sensory and emotional experience associated with actual or potential tissue damage, or described in terms of such damage’.<sup>2</sup> Its complex and subjective nature leaves an open debate and justifies the adversities in assessing and treating pain.

Pain can be classified into three categories: nociceptive, neuropathic and nociplastic pain. The first arises from damage to non-neural tissue and activates nociceptors, while neuropathic pain is consequence of damaged or injured nociceptive pathways. Nociplastic pain is a term introduced subsequently to describe any maladaptive change in the nociceptive system without clear evidence of tissue damages or disease states [17]. Experiencing pain may be the consequence of one or all three mechanisms concurrently operating at the same time or in the same time course and share many comorbidities, such as depression, sleep disturbances, lack of energy, neurocognitive changes and other vague symptoms including generalized diffuse pain states [18].

Any persistent and long-lasting pain, exceeding healing times for more than 3 to 6 months, is classified as chronic pain and it is the principal cause of disability in Europe, according to The Global Burden of Disease Study 2016 [19], [3], source of not only physical and psychological burden for patients, but also a big economic and social burden for society affecting around 11.17 million people in Europe [4]. The worldwide burden caused by chronic pain syndromes justifies the necessity of understanding the mechanisms underlying nociceptive processing and of developing effective treatments.

## 2.2 The nociceptive system

On a healthy state, the nociceptive system is activated as consequence of selective noxious stimulation producing either physical or cognitive reactions. However, disease states and maladaptive changes can translate into pain experiences without the presence of an external event causing physical harm. This is the result of a complex system involving both the peripheral and the central nervous system. In the next pages, the anatomy and physiology of nociceptive signaling of the human body is introduced, followed by a short introduction to the pathophysiology of pain.

1: IASP - International Association for the Study of Pain

2: pain. 2017. In *IASP - Terminology*. Retrieved Jul 16, 2020, from <https://www.iasp-pain.org/Education/Content.aspx?ItemNumber=1698#Pain>

## 2.2.1 The anatomy and physiology of pain

### The periphery

Organs in the periphery of a human body (e.g. skin, joints and muscles) include four classes of receptors: cutaneous mechanoreceptors, thermoreceptors, nociceptors and chemoreceptors.

Most cutaneous receptors are encapsulated in cellular corpuscles and are the ends of afferent neurons. These neurons, also called *primary afferent sensory neurons* are part of the PNS and transduce information into electrical pulses delivered to the CNS. Each neuron has a morphological and molecular specialization given by their peripheral terminals and responds to specific types of stimuli.

Sensory nociceptive receptors are exclusively activated by noxious stimuli (i.e. mechanical, heat and chemical stimuli) and are connected to primary sensory neurons. Nociceptors have peripheral endings innervating either the dermis and/or epidermis and are divided in four classes [20], Figure 2.1:

- Thermal receptors: activated by extremes temperatures (over 45 °C and lower than 5 °C). They are the peripheral endings of small-diameter, thinly myelinated A $\delta$ -axons conducting at 5 to 30 m/s;
- Mechanical receptors: activated by intense pressure on the skin. They are peripheral endings of thinly myelinated A $\delta$ -axons;
- Polymodal receptors: activated by high-intensity mechanical, chemical or thermal stimuli. They are peripheral endings of small-diameter, unmyelinated C-axons, conducting at 1 m/s;
- Silent receptors: : found in the viscera. Not normally activated by noxious stimuli, but by inflammation or various chemical agents. Their activation is thought to contribute to the emergence of secondary hyperalgesia and central sensitization.

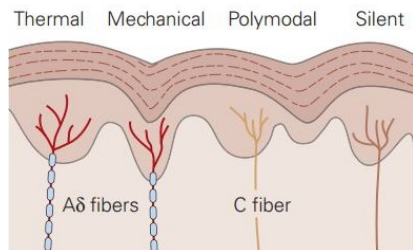


**Figure 2.1:** Four classes of nociceptors are distributed under the skin and in deeper tissues. Their peripheral endings innervate either the dermis and/or epidermis. Reprinted from *Principles of Neural Science* (5th Edition, p. 534), by Eric R. Kandel, James H. Schwartz, Thomas M. Jessel, Steven A. Siegelbaum, A.J. Hudspeth, 2000, USA, The McGraw-Hill Companies [20]

Accordingly, the transmission of nociceptive information depends as well to the type of fibers that the nociceptor contains. Nociceptive fibers are divided in two principal classes [20]:

Fiber Type	Characteristics
C fibers	0.4 to 1.2 mm of diameter. They are characterized by large receptive fields for a less precise localization and unmyelinated for a slower conduction (1 m/s).
A- $\delta$ fibers	2 to 5 mm of diameter. They are characterized by small receptive fields for precise localization and myelinated for a faster conduction (5 to 30 m/s) of either thermal or mechanical nociceptive stimuli.

**Table 2.1:** Type of axons (fibers) contained in the nociceptors enabling the transmission of nociceptive information from the periphery to the central structures

## Peripheral processing

Changes in the peripheral ends of the nociceptive nerve fibers are classified as *peripheral sensitization* and are induced by inflammatory mediators or damaged cells, releasing chemicals on the site of injury. Sensitization of nociceptors in the periphery results into *primary hyperalgesia*, a clinical term implying any decrease in threshold or increase in supra-threshold and generating specific enhanced sensitivity to thermal and mechanical stimuli. When the PNS is the cause of chronic pain, the symptoms can result in spontaneous firing of nerve fibers, over-sensitivity due to denervation, and complex regional pain syndrome.

## Spinal cord

Nociceptive sensory neurons receive noxious stimuli from the peripheral terminals and transmit the signal to central centers by innervating the spinal cord in a highly orderly manner - in particular innervating the dorsal horn.

Afferent neurons terminate in different laminae of the dorsal horn, as shown in Figure 2.2, and their organizations play a crucial role in sensory processing:

- Lamina I (or marginal layer): the most superficial layer responding to noxious stimuli conveyed by  $A\delta$ - and C-fibers;
- Lamina I: another class of lamina I neurons receives signals from C-fibers activated by intense cold;
- Lamina I: another class of lamina I neurons are wide-dynamic-range neurons; thus, they respond to innocuous and noxious mechanical stimuli;
- Lamina II (or substantia gelatinosa): is a densely packed layer, containing local interneurons (some excitatory and some inhibitory). Some respond to nociceptive inputs, others to innocuous stimuli;
- Lamina III and IV: is a mixture of interneurons and supraspinal projection neurons, receiving signals from  $A\beta$ -fibers and responding to innocuous stimuli;
- Lamina V: neurons responding to a wide variety of noxious stimuli and receiving direct inputs from  $A\beta$ - and  $A\delta$ - fibers;
- Lamina IV: input from large-diameter fibers, innervating muscles and joints. Activated by innocuous joint movement and do not contribute to the transmission of nociceptive information;
- Lamina VII and VIII: intermediate and ventral regions of the spinal cord. They respond to noxious stimuli. Neurons in Lamina VII respond to stimulation of the either side of the body; on the other hand, most dorsal horn neurons receive unilateral input.

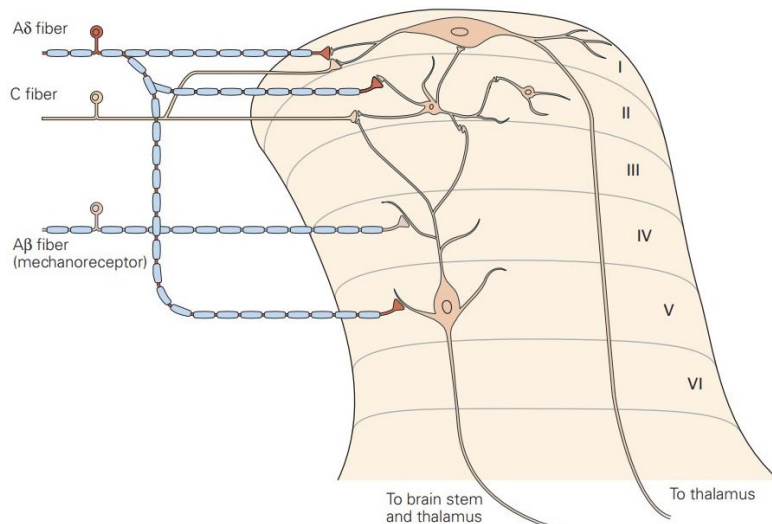


**Figure 2.2:** Neurons distribution in the laminae of the dorsal horn. Reprinted from *Principles of Neural Science* (5th Edition, p. 534), by Eric R. Kandel, James H. Schwartz, Thomas M. Jessel, Steven A. Siegelbaum, A.J. Hudspeth, 2000, USA, The McGraw-Hill Companies [20]

The activation of the neurons in the laminae is caused by the nociceptive sensory neurons releasing two classes of neurotransmitters:

- Glutamate: main neurotransmitter of all primary sensory neurons. It is commonly stored in small, electron-lucent vesicles;
- Neuropeptide: released as co-transmitter by nociceptors with unmyelinated axons. It is stored in large, dense-core vesicles at the central terminals of the nociceptive sensory neurons.

Glutamate and neuropeptides can be released under different physiological conditions and, together, act to regulate the dorsal horn neurons [20].

### Central processing in the spinal cord

An enhanced sensitivity to mechanical stimuli, when extended to surrounding regions of the skin, is known as secondary hyperalgesia [21]. Several studies have investigated the neural mechanisms that differentiate primary from secondary hyperalgesia. While primary hyperalgesia is explained by the presence of peripheral sensitization of nociceptors, the mechanism unveiling secondary hyperalgesia has been open to debate for several decades [22].

The first hypothesis on the mechanism underlying secondary hyperalgesia was introduced by Lewis (1936). According to Lewis, secondary hyperalgesia exclusively involved the peripheral nervous system (PNS), in which nerve impulses are transmitted both orthodromically and antidromically along branches to surrounding areas, evoking the activation of nociceptive terminal ending; thus, creating remote hyperalgesia [23].

However, Hardy et al. (1950) concluded that the mediating neurons causing secondary hyperalgesia are not located in the periphery, but in the CNS. The repeated exposure to noxious stimuli results into long-term changes in the dorsal horn neurons, resulting into a 'memory' of the state of C-fibers input [20]. The plasticity of the receptive fields of the dorsal horn neurons contributes to pain hypersensitivity and explains the increased excitability corresponding to central sensitization. Thus, it is responsible for amplified responses to noxious and innocuous inputs and the spread of hypersensitivity to regions beyond injured tissues [24]. Nowadays, it is well-established that secondary hyperalgesia has its origin in the CNS and is consequence of *Central Sensitization*.

Moreover, changes in the function of dorsal horn neurons are the underlying

cause of allodynia, a condition eliciting painful response to any innocuous sensory stimuli [25]. Prominent symptoms to chronic pain include allodynia and hyperalgesia. A schematic representation of allodynia and hyperalgesia is shown in Figure 2.3.

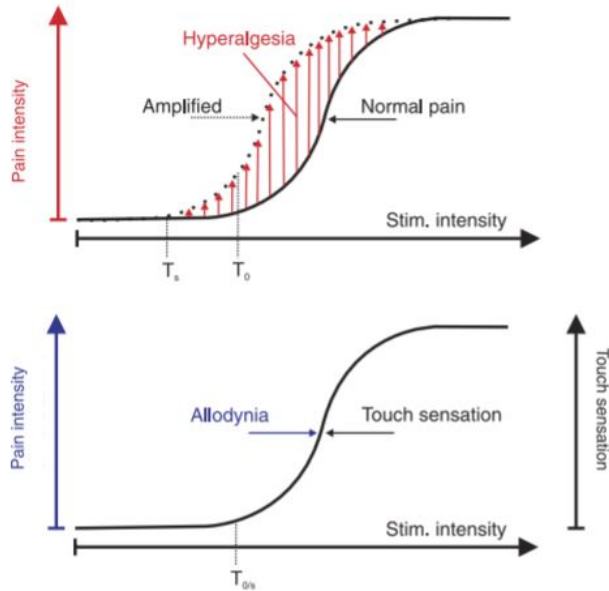


**Figure 2.3:** Representation of hyperalgesia and allodynia. Red area) increased sensitivity to noxious stimuli (hyperalgesia). Blue axis) increased pain experience to innocuous stimuli (allodynia).  $T_{0/s}$  is the threshold of touch sensation in healthy states. Adapted from "Models and mechanisms of hyperalgesia and allodynia", by Jurgen Sandkuhler, 2009, *Psychological Reviews*, 89, p. 707-758. Copyright ©2009 the American Psychological Society [25]

Thus, both allodynia and hyperalgesia are characterized by an uncontrolled change in nociceptor activity. While allodynia is usually temporary and is always triggered by an external stimulus, patients with hyperalgesia suffer from a permanent condition without the need of a sensory stimulation [20].

The red area in Figure 2.3 displays any pain amplification caused by hyperalgesia; while, in allodynia, the touch threshold overlaps with the stimulation threshold. Whenever is not clear whether the stimulus is activating or not the nociceptors, it is better to refer it as hyperalgesia [25].

Several chronic pain disorders show increased sensitivity when repetitive stimuli are applied suggesting the involvement of central processing and central sensitization. By definition, temporal summation can be obtained supplying a train of stimuli, delivered at a fast rate by controlling the inter-stimulus interval. The mechanism underlying temporal summation requires that several synaptic potentials are generated consecutively in order to be added together in the post-synaptic cell [20]. Thus, neurons with a large time constant have a greater capacity for temporal summation. Spatial summation occurs when the area of stimulation is increased generating an enhanced sensitivity to noxious stimuli. The underlying mechanism of spatial summation requires the recruitment of a larger number of nociceptors, simultaneously activated and reaching multiple receptive fields on the dorsal horn of the spinal cord [26]. A schematic representation of temporal and spatial summation is shown in Figure 2.4

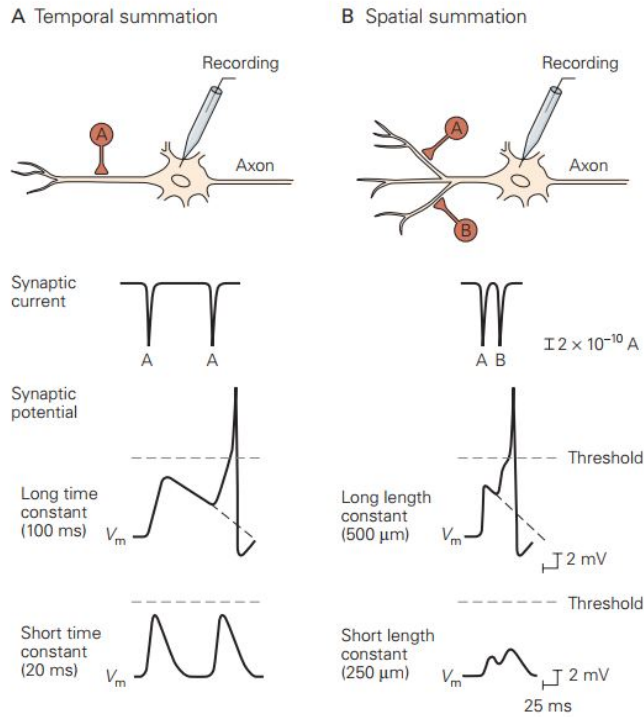


**Figure 2.4:** Representation of temporal and spatial summations on postsynaptic cells with different time constants.

A) Temporal summation. The two stimuli are under the threshold level for triggering an action potential. However, postsynaptic cells with a long time constant cause an additive effect between the two stimuli resulting in a depolarization wave.

B) Spatial summation. The distance between the sites of synaptic input and the trigger zone of the synaptic cell plays a crucial role in the production of an action potential. If the distance is equal to two length constant, 250  $\mu\text{m}$  (bottom figure), then the summation does not exceed the activation threshold.

Reprinted from *Principles of Neural Science* (5th Edition, p. 229), by Eric R. Kandel, James H. Schwartz, Thomas M. Jessel, Steven A. Siegelbaum, A.J. Hudspeth, 2000, USA, The McGraw-Hill Companies [20]

## The thalamus

From the spinal cord, information are conveyed to the thalamus via five ascending pathways [20].

- Spinothalamic ascending pathway: includes axons from neurons in Laminae I, V and VII of the dorsal horn conveying information about nociceptive and thermal information. The axons of this pathway cross the midline and have a crucial role in the transmission of noxious stimuli, Figure 2.5;

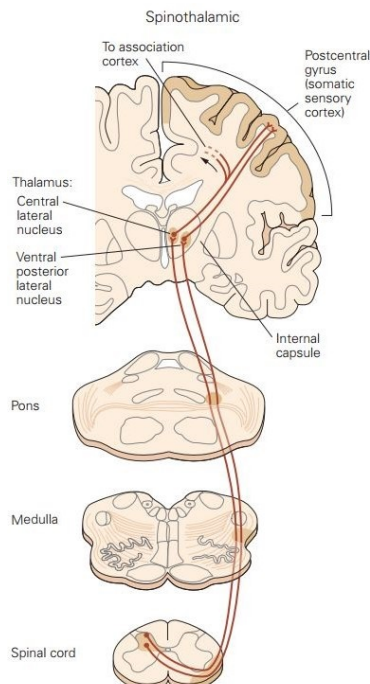


**Figure 2.5:** Spinothalamic ascending pathway. Reprinted from *Principles of Neural Science* (5th Edition, p. 544), by Eric R. Kandel, James H. Schwartz, Thomas M. Jessel, Steven A. Siegelbaum, A.J. Hudspeth, 2000, USA, The McGraw-Hill Companies [20]

- Spinoreticular ascending pathway: axons from Laminae VII and VIII terminating in the reticular formation and the thalamus without crossing the midline;
- Spinomesencephalic ascending pathway: axons contribute to the affective component of pain sensation and generate from Laminae I and V;
- Cervicothalamic ascending pathway: axons from Laminae III and IV;
- Spinohypothalamic ascending pathway: axons from Laminae I, V and VIII of the dorsal horn for the regulation of neuroendocrine and cardiovascular responses accompanying pain syndromes.

### Central processing in the thalamus

Chronic pain patients suffer from abnormal noxious processing and deafferentation, where the sensory transmission is interrupted along the pathway [27]. The underlying cause of deafferentation is related to abnormal thalamo-cortical rhythmicity. Thus, central pain states are actively correlated to thalamic dysfunctions, such as thalamocortical dysrhythmias [28].

### The cortex

Every thalamic region projects to the brain cortex and mediates the cortico-cortical communications [29]. The response to noxious stimuli is projected to several areas of the cortex, such as the primary somatosensory cortex (SI)<sup>3</sup>, the secondary somatosensory cortex (SII)<sup>4</sup>, the insular cortex (IC)<sup>5</sup> and the anterior cingulate cortex (ACC)<sup>6</sup> [30, 31].

SI is known to be the first and last region of the cortex to stay activated after an external noxious stimulus [32]. The SI is highly organized and at every location of the SI corresponds a specific location of the body. Thus, SI gives information on the location and intensity of the painful stimulus. SII also provides information on the intensity of the applied stimulus, since it is functionally connected with the posterior insular cortex (PI)<sup>7</sup> [33, 34]. In fact, PI is crucial in the chronicity of pain: its degree of activation is related to the progress of chronic pain [34]. On the other hand, the anterior side of the insular cortex (AI)<sup>8</sup>, along with the anterior cingulate cortex (ACC)<sup>9</sup>, is involved in the emotional states of the nociceptive processing and is part of the limbic system [35].

### Central processing in the cortex

Cortical projections represent the end of the ascending noxious pathway and display structural and functional abnormalities from and above the spinal cord. In chronic pain states, the perception of pain can occur also in the absence of external noxious inputs and is modulated by both cognitive and emotional states [36]. While specific brain regions are known to be involved in the processing of pain information, chronic pain might activate regions not-exclusively dedicated to pain processing [37].

Furthermore, previous research has been conducted demonstrating the relation of behavioural modulation on pain amplification, such as somatization and hyper-vigilance. These results suggest that cognitive and emotional states also influence the modulation and cause maladaptive changes to descending pain pathways [38].

- 3: SI - primary somatosensory cortex
- 4: SII - secondary somatosensory cortex
- 5: IC - insular cortex
- 6: ACC - anterior cingulate cortex
- 7: PI - posterior insular cortex
- 8: AI - anterior insular cortex
- 9: ACC - anterior cingulate cortex

## Descending pathways

Cortical regions interact with descending nociceptive pathways influencing the intensity of perception of noxious stimuli. In particular, the periaqueductal gray (PAG) produces analgesic reaction by activating an opioid-mediated inhibition of the nociceptive system. From the PAG inhibitory information travels to the dorsal horn via parabrachial nuclei, rostroventromedial medulla (RVM).

Descending pathways play a fundamental role in delivering antinociceptive effects at both presynaptical and synaptical level. For this reason, the activation of the descending system is enhanced during inflammatory processes or injuries and compensates for the amplified transmission of pain signals [39].

## 2.3 Quantitative measure of pain

Research on pain syndromes has been conducted for decades and, while several agreements have been reached, the complex nature of pain has prevented the more severe and acute stages of the syndromes to be recognized as a disease state. Stimulation of the nociceptive system can be accomplished with the use of mechanical, thermal, chemical or electrical means and the skin as easy-access and external contact point with the nociceptive system.

While qualitative studies provide an insight on the subjective experience of pain, they do not provide valuable markers that could be generalized to a larger patients' group. For this reason, a stable and objective observation of pain perception (i.e. quantitative sensory testing) is essential in pain research. The discipline aiming at finding correlations between the sensory stimuli and the individual perception of it is known as *psychophysics*. In this case, the nociceptive system is selectively activated in order to outline the characteristics and properties of it.

### 2.3.1 Peripheral stimulation

In order to activate nociceptive fibers and elicit an active perception of pain, it is necessary to apply external stimuli that exclusively activate A- $\delta$  and C-fibers. Peripheral nociceptive stimulation is commonly modulated using electrical stimulation, since the investigators can easily control over the stimulation parameters by changing waveform, frequency and duration of the electrical pulses [40].

### 2.3.2 Nociceptive detection threshold and Psychometric curve

Several paradigms are available to estimate an individual's detection threshold, defined as the stimulus amplitude at which 50% of the stimuli are detected, and based on either the low or high-threshold theory [41]. The latter theory has been known to be successful in describing detection threshold experiments [42].

Modern psychophysics uses adaptive paradigms statistically optimized to converge to the true value, despite the changes in time of detection thresholds due to habituation of the nociceptive system to applied stimuli. Therefore, these paradigms adapt new stimuli in accordance to preceding stimulus-response pairs [43]. One example of paradigm is the *method of constant* where a set of pre-determined stimuli are applied and the subject must assess whether the intensity of the present stimulus is stronger or weaker than a reference stimulus. On the other hand, the paradigm in which the stimuli adapt amplitude in either

ascending or descending steps is known as the *method of limits* [44].

The probability for a subject to recognize the intensity of a stimulus can be represented in a probability density function. This function, also known as psychometric curve (see Figure 2.6), has the shape of a cumulative normal distribution, as suggested by the *high-threshold theory* where a stimulus is perceived whenever a fixed internal criterion is exceeded thanks to the accumulation of sensory evidence [45]. The tails of a psychometric curve never tend to zero; they tend instead to a constant value either as when background activity is perceived as stimuli (*guessing*) or, on the other hand, when individuals fail to perceive a stimulus due to distractions or background activity (*lapsing*) [46]. The noise coming from the sensory evidence is normally distributed since the decision-making process is consequence of summation of a large number of neurons, each having a random firing probability [45].

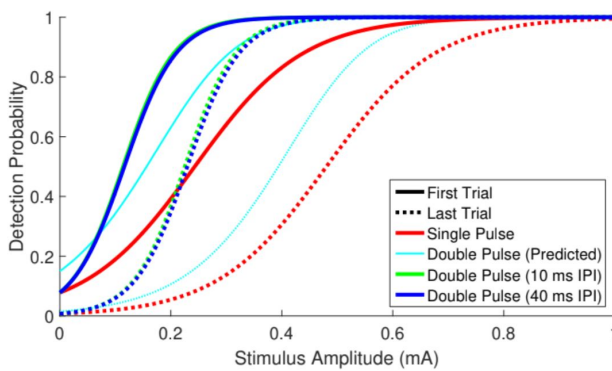


**Figure 2.6:** In the figure, several psychometric curves are shown. Each colour represents a stimulus type, while solid and dotted lines represent the beginning and the end of the experiment conducted by van den Berg et al. [41], respectively. Reprinted from "Stimulus related evoked potentials around the nociceptive detection threshold", by Boudewijn van den Berg, 2018, Enschede, The Netherlands: BSS group - University of Twente

The psychometric curve is formulated by Treutwein and Strausberger (1999) in Equation 2.1, where  $F(x; \theta; \sigma)$  is the logistic function representing the cumulative normal distribution [47].  $x$  is the external stimulus,  $\alpha$  is the threshold or position on the abscissa,  $\beta$  is the slope,  $\gamma$  and  $\lambda$  are the guessing and lapsing probability defining the lower and upper asymptote, respectively [46].

$$\psi(x; \alpha; \beta; \gamma; \lambda) = \gamma + (1 - \gamma - \lambda)F(x; \alpha, \beta) \quad (2.1)$$

According to Treutwein and Strausberger (1999), maximizing the likelihood of the logistic curve to estimate the psychometric function is a relatively unbiased estimate of the threshold and slope of the psychometric function, when paradigms such as the method of constants are used [47]. Lapsing and guessing rates are independent from the subject and usually set to some reasonable value: lapsing is zero (or almost zero), while the guessing is set to the expected chance of performance (e.g. equal to 1 in a yes/no task). However, this approach is not always a good estimate since it accurately estimates the threshold but fails in estimating the slope due to a negative bias.

### 2.3.3 Peripheral modulation

A common ground for pain research is the use of *experimental pain models* on healthy subjects, in which the investigators can induce pain and pain-related symptoms by controlling environmental factors such as location, intensity, frequency and duration of the stimulus. Another aspect is the control over both temporal and spatial summation. Conducting experiments on pain-free subjects is a common

practice to understand the pathological state of pain disorders and eliminates the biases introduced during clinical evaluations of chronic pain patients, such as comorbidity factors (e.g. psychological, cognitive and social aspects or systematic reactions) and sedation [48].

By sufficiently activating nociceptors with the correct stimulus parameters, it is possible to simulate peripheral and central sensitization inducing either allodynia or hyperalgesia, known conditions in chronic-pain, neuropathic states [49].

Among the most common techniques, there is:

### **Cold Pressor Test (CPT)**

Cold pressor test (CPT) is commonly used in pain research for clinical investigations of pain mechanisms thanks to its reliability, validity and its ability of inducing effects similar to chronic-pain symptoms [50].

Individuals subject to CPT are asked to place a limb (i.e. the hand, either dominant or non-dominant) in ice-cold water for a specific interval of time. The exposure of nociceptors to this thermal stimulation generates activation of C-fibers, known to mediate cold pain, and A- $\delta$  fibers, mediating cold sensation [48].

Temperature of the water can vary between 0° and 7°C and influences the tolerance time for the immersion of the hand. For this reason, the inconsistent methodologies used in scientific papers do not allow to have comparable results, compromising the validity and reliability of the test. Mitchell et al. (2004) confirm this hypothesis by showing that small variations in temperature result in significant differences in both tolerance times and intensity of perceived pain [50].

### **Capsaicin**

Among chemical stimulations to model neuropathic pain, capsaicin is one of the most commonly used in clinical studies. Capsaicin can be applied on the skin or injected subcutaneously and the intensity of the consequent elicited painful sensation (i.e. burning) varies depending on the concentration of the chemical substance [20]. This substance is known to generate central sensitization both by widening the receptive field of the dorsal horn and generating allodynia and by increasing the responsiveness of A- $\delta$  fibers in the surrounding areas of secondary hyperalgesia. Both dermal (capsaicin 1% moisturizing cream, applied for 30-60 minutes [48]) and intra-dermal (100  $\mu$ g capsaicin) applications are able to generate allodynia and hyperalgesia.

### **High-Frequency Stimulation (HFS)**

High-frequency stimulation (HFS) is known to induce, or at least mimic, secondary hyperalgesia on the skin. In HFS, electrical stimuli are delivered onto the skin of the individuals, using custom-built electrodes that exclusively activate nociceptive fibers (e.g. A- $\delta$  and C-fibers). The stimulus frequency of HFS is generally set at 100Hz, while the intensity is adjusted on an individual basis to 10 or 20 times the individual's detection threshold [12]. By definition, HFS-induced secondary hyperalgesia reduces pain threshold exclusively to mechanical stimuli and not thermal stimuli.

In order to evaluate the occurrence of central sensitization after experimentally inducing it with external means (e.g. CPT, capsaicin, HFS), it is necessary to conduct a quantitative testing. In particular, secondary hyperalgesia is most sensitive to mechanical stimulation generating an increased responsiveness of

the nociceptive neurons in the CNS [51]. For this reason, punctate mechanical stimulation is recommended and can be performed, before and after inducing sensitization, using monofilament devices. They are applied perpendicularly onto the skin of a subject and have different diameter's tips and normal forces. The perceived stimuli can be assessed using a Numeric Rating Scale (NRS<sup>10</sup>). NRS usually range from 0 to 10, where 0 is equivalent to 'no pain', 10 is 'the most intense pain imaginable' and 5 is usually equivalent to a 'turning point from merely a sensation to actual pain' [52]. Clinically speaking, it is interesting to investigate the NRS, since it generally indicates the changes to perceived stimuli as a function of time and determines whether a certain treatment or cure is being effective for the individuals. For example, in an experimental protocol, punctate mechanical stimulation is a standard methodology to assess the occurrence of mechanically-, chemically- or thermally-induced secondary hyperalgesia.

10: NRS: numerical rating score

### 2.3.4 Central acquisition

Physiologically speaking, pain stimuli are transmitted from the periphery to the CNS, ending into thalamic regions and projecting to the cerebral cortex. Thus, it is clinically relevant to evaluate time-locked cortical activity when a noxious stimulus is applied on the skin of individuals.

Nowadays, various techniques are available for the observation of brain activities. However, every technique presents specific limitations or lack of accuracy in either temporal or spatial variations. Among them there is, for instance, functional magnetic resonance imaging (fMRI<sup>11</sup>) known to have a high spatial accuracy and poor temporal accuracy. On the other hand, electroencephalography (EEG<sup>12</sup>) or magnetoencephalography (MEG<sup>13</sup>) are temporally very accurate with a poor spatial accuracy (e.g. EEG spatial resolution 6 to 9 cm [53]). Furthermore, additional factors must be taken into account, such as accessibility, individual compliance and invasiveness. For example, while microneurography (MN)<sup>14</sup> presents high accuracy both temporally and spatially, it is usually discarded for its invasiveness, requiring the insertion of needle electrodes inside the brain.

11: fMRI - functional magnetic resonance imaging

12: EEG - electroencephalography

13: MEG - magnetoencephalography

14: MN - microneurography

For the evaluation of the nociceptive system and assessment of cortical activity in response to noxious stimuli, temporal accuracy is one of the crucial requirement. In fact, nociceptive-evoked potentials generally occur in less than a second (~ order of milliseconds).

## 2.4 The MTT-EP protocol

At the University of Twente, an experimental protocol named 'MTT-EP protocol' has been designed to investigate and describe the mechanisms involved in the processing of nociceptive information [54]. The MTT-EP is composed of two simultaneous recordings: the individual detection thresholds using the Multiple Threshold Tracking (MTT) algorithm, and event-related potentials (EP) extracted from electroencephalographic data.

### 2.4.1 Peripheral stimulation

#### Intra-epidermal electrocutaneous stimulation (IES-5)

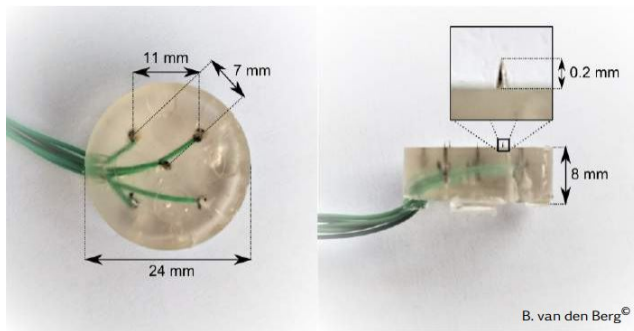
Intra-epidermal electrocutaneous stimulation (IES<sup>15</sup>) is able of selectively acti-

15: IES: intra-epidermal electrocutaneous stimulation

vating A- $\delta$  and C-fibers when applying a current close to an *individual's detection threshold*. This is fairly convenient for investigating the nociceptive system and brain activations during nociceptive stimulations. IES has positive feature including low expenses, applicability to every part of the human body and the ability of generating a single action potential inducing a time-locked response from the peripheral NS.

Once the stimulation current reaches values around  $2.5\text{mA}$ <sup>16</sup> or two times higher the detection threshold, A- $\beta$  fibers, that are usually sensitive to touch sensations, are concurrently activated [55] and overlapping cortical activation might occur. Therefore, it is important to keep the value of the stimulation under  $2.5\text{mA}$  when investigating activations of the nociceptive system.

While there exists a limit in current amplitude for nociceptive stimulation, there is no limitation in the number of pulses applicable consecutively. At the University of Twente, the electrode used for peripheral stimulation has five needles penetrating the stratum corneum for a selective activation of nociceptive fibers and it will be referred to as IES-5, Figure 2.7.



16: ma: milliAmpere

**Figure 2.7:** Electrode for intra-epidermal electrocutaneous stimulation (IES-5). The electrode was originally developed by Steenbergen et al. [56] and later used by van den Berg et al. [41] for similar purposes. The length of the needles is approximately 0.2mm ensuring the activation of A- $\delta$  and C-fibers used by the nociceptive system to transfer noxious information to the CNS. The needles penetrate the stratum corneum and interacts with the most superficial layers in the epidermis. Reprinted from "Stimulus related evoked potentials around the nociceptive detection threshold", by Boudewijn van den Berg, 2018, Enschede, The Netherlands: BSS group - University of Twente

## 2.4.2 Multiple threshold tracking

Doll et al. (2015) introduced a new paradigm, based on the method of limits, where the stimulus is randomized at every step in order to prevent the individuals from identifying the used pattern and where multiple thresholds can be simultaneously tracked [54]. In this paradigm, stimulus amplitude, number of pulses and time are all predictors for the model.

A visual representation of the latter paradigm can be found in Figure 2.8.

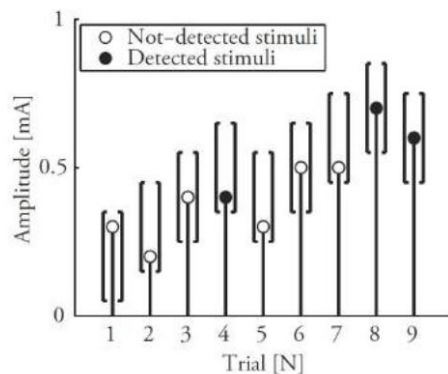


**Figure 2.8:** Detection threshold paradigm introduced by Doll et al. (2015). The square brackets represent the range within which the intensity of the stimulus can be changed. Adapted from "Observation of time-dependent psychophysical functions and accounting for threshold drifts", Robert J. Doll, Peter H. Veltink, Jan R. Buitenweg, 2015, *Atten Percept Psychophys*, 77, p. 1440-1447. ©The Author(s) 2015, [57]

Simulations of the paradigm showed a relatively unbiased estimate of both slope and threshold. According to Doll et al. (2015), the model is also able to

simultaneously track multiple psychometric thresholds when different kind of stimuli are applied. Therefore, this model is less affected by observers' and individuals' bias since it randomizes multiple types of stimuli (i.e. different amount of pulses in one stimulation. e.g. single-pulse or double-pulses) in a sequence. The use of double-pulse is justified by the need of having a quantitative assessment of pain perception using temporal summation, as described in section 2.2, [58],[57],[47],[54],[45].

Visual representation of the randomized multi-stimulation model can be found in Figure 2.9.

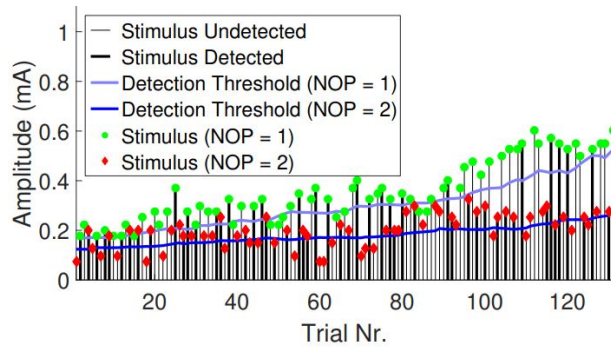


**Figure 2.9:** Multiple tracking threshold method using a randomized stimulation sequence around the nociceptive detection threshold (NDT). In the figure, the stimuli applied are either composed by single or double pulses. Reprinted from "Analysis of nociceptive evoked potentials during multi-stimulus experiments using linear mixed models", B. van den Berg, J.R. Buitenweg, 2018, *40th Annual International Conference of the IEEE Engineering in Medicine and Biology Society (EMBC)* [41]

### 2.4.3 Central acquisition

#### Electroencephalography (EEG)

At the University of Twente, the preferable measurement tool to record brain activity responding to noxious stimuli is electroencephalography (EEG): an easy-to-use, low-cost and non-invasive tool with a high temporal accuracy. It was first introduced by Hans Berger (1873-1941) who determined a dependency of brain rhythms and individuals' state of consciousness [59].

In clinical applications, EEG was first used for the evaluation of spontaneous cortical activity (i.e. during REM sleep or epileptic seizures) [60]. In the recent years, EEG has been used as tool for the assessment of event-related brain activity, also known as evoked potentials (EPs)<sup>17</sup> or event-related potentials (ERPs)<sup>18</sup>.

In the presence of nociceptive activation, EEG recordings measure electrical potentials generated in the extracellular fluid as ions cross cell membranes and neurons communicate via neurotransmitters. These potentials have to be strong enough to reach the scalp and cross layers characterized by different conductivity values. EEG measures cortical activity from both a radial and tangential orientation. Therefore, having a cohort of neurons simultaneously activated and with the same (or almost the same) direction is a necessary requirement [61].

17: EP - evoked potential

18: ERP - event-related potential

### 2.4.4 Nociceptive evoked potentials (EPs)

Analysis of EEG data for the investigation of neurocognitive processes is a common, standard procedure in pain research with valuable information both in the time and frequency domains. At the University of Twente, time-domain analysis of EEG data is the prevalent technique used to extract event-related potentials in response to noxious stimuli.

Evoked potentials (EPs) are time-dependent signals representing cortical activations time-locked to an external stimulation. Physiologically speaking, EPs are

transient post-synaptic responses of pyramidal neurons triggered by an external, in this case a noxious, stimulus [62]. Single-trial EPs have a low amplitude with respect to the rest of non-time-locked activity; therefore, multiple-trials averaging of EEG recording is necessary in order to detect stimulus responses [63]. A strong advantage of EPs is the temporal precision that can reach the order of few milliseconds without external filtering, enough resolution to determine the fast time-locked cortical activation. Positive and negative peaks characterizing the temporal evolution of EPs vary in latency, duration, scalp location and cortical distribution and they represent physiological and/or pathophysiological behaviors of the stimulated nociceptive system [64].

Time-domain representations of evoked potentials are butterfly plots where all the electrodes are superimposed [65]. An example of butterfly plot is shown in Figure 2.10, displaying characteristics of nociceptive EP components extracted from a previous research conducted at the University of Twente [41].

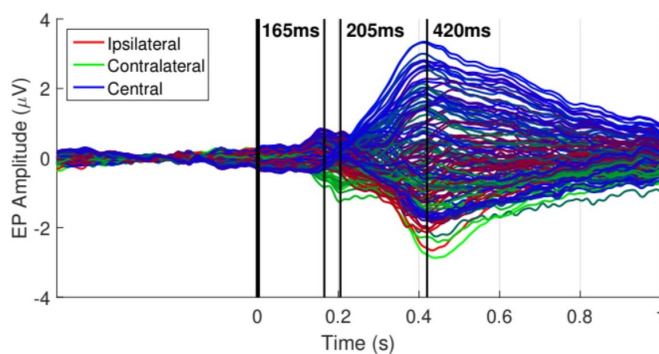


**Figure 2.10:** Representation of a butterfly plot displaying peaks of nociceptive EPs. Reprinted from "Stimulus related evoked potentials around the nociceptive detection threshold", by Boudewijn van den Berg, 2018, Enschede, The Netherlands: BSS group - University of Twente [41]

Previous research at the University of Twente has investigated the modulation of cortical activations as consequence to nociceptive stimuli in an MTT-EP protocol using a detected/undetected task around individuals' detection thresholds [41]. Three separate EP components are identified at 165ms, 205ms and 420ms (N165, N205 and P420, respectively). The variation of the P420 positive peak is directly dependent on the intensity of the stimulus. Thus, P420 is lower when the stimulus is closer to the detection threshold and is directly correlated to a conscious detection of the stimuli. In general, variations of stimulus parameters in the MTT-EP protocol, such as stimulus intensity and detection, are reflected in the components of evoked potentials.

### 2.4.5 The MTT-EP Measurement System

Previous works at the University of Twente have used the MTT-EP paradigm to measure nociceptive evoked potentials in response to noxious stimuli. Accordingly, proper instrumentation, several protocols and datasets are already available and demonstrate the possible validity of the MTT-EP paradigm. The MTT-EP measurement system is designed to acquire EEG cortical activity and synchronously measure nociceptive detection thresholds using IES, as shown in Figure 2.11.

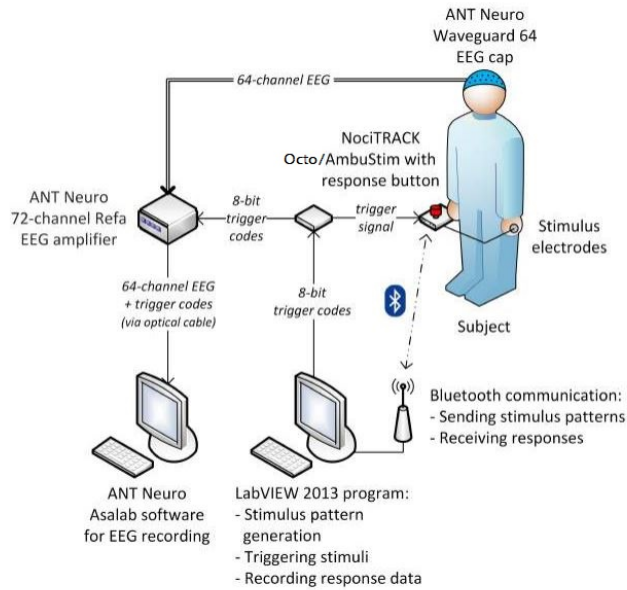


**Figure 2.11:** The MTT-EP setup. Adapted from "Stimulus related evoked potentials around the nociceptive detection threshold", by Boudewijn van den Berg, 2018, Enschede, The Netherlands: BSS group - University of Twente [41]

The multiple threshold tracking (MTT) paradigm uses a set-up including IES electrodes and a stimulator, a tracking system for stimulus responses (nociceptive detection threshold) and a recording system for EEG data (EPs).

IES are applied using an array of five micro-needle electrodes (IES-5 electrodes) protruding through the stratum corneum of the skin with a 0.2mm tip for selective activation of nociceptive skin fibers. IES-5 are sterilized before every usage and deliver stimuli consisting of one (or two) cathodic square-wave electrical currents pulse with a pulse width of 0.21 ms. The inter-stimulus interval of the double pulse waves can be modified according to experimental requirements. As mentioned in section 2.4.1, the maximum stimulus intensity is set at 2.0mA. The generation of electrical current pulses for the IES-5 electrodes is possible using either the NociTrack Ambustim or the OctoStim stimulators, both connected wirelessly using Bluetooth. The MTT system is set to deliver a randomized set of stimulus amplitudes around the individual's detection threshold.

Instead, EPs are recorded using ANT Neuro Waveguard EEG caps (32-, 64- or 128- Ag/Ag-Cl electrodes) combined with a TMSi 136-channel Refa amplifier.

The two recording systems are connected together to a computer running a LabView application controlling both the stimulator and the EEG set-ups. In this way, trigger signals will be delivered simultaneously to the two systems in order to improve the extraction of event-related potentials during the pre-processing phase.

## 2.5 Frequency-domain analysis of EEG pain-related recordings

External events are able to modulate time-locked cortical activation by creating neuronal oscillations at different frequency bands that can be investigated using time-frequency analysis [62]. The total power of single-trial EEG data represents the complex network connecting main neurons to interneurons, ranges from 3Hz to 100Hz and can be divided into relative band powers, such as theta- (4-8 Hz), alpha- (8-15 Hz), beta- (15-30 Hz) and gamma-band (30-100 Hz) [62], [66]. Existing

studies have established the relevance of relative band powers for understanding functional and perceptual processing of transient painful stimuli. In Ploner et al. (2017), theta band (4-8 Hz) activations at 150 ms - 400 ms after stimulus onset indicate the presence of a pain-related evoked potential and show altered behaviours in pathological states [66], while ipsilateral and contralateral theta-band suppressions suggest a late involvement of the sensorimotor cortex correlating to the upcoming activity of a peripheral upper limb in a motor-related task [67], [68]. Abnormalities in theta-band power became a relevant biomarker for the evaluation of neurological and psychiatric symptoms, such as ongoing pain [66]. However, the scientific community does not seem to find a common ground in the functional role of neuronal oscillations in the alpha-, beta- and gamma-bands. Hu et al. (2013) investigated the nature of both ipsilateral and contralateral alpha-band (8-15Hz) suppressions and classified them as task-related and sensory-related responses, respectively [69]. In addition, Zapala et al. (2020) and Bai et al. (2005) demonstrated a lateralization of alpha-band suppressions, being most prevalent at contralateral regions when right-handers perform motor tasks with the dominant hand, while left-hand movements results into a bilateral activation, on both contralateral and ipsilateral regions [70], [71]. Zhang et al. (2012) observed a suppression in alpha-band oscillations as a consequence to attentional biases [72]. On the other hand, Ploner et al. (2017) found a positive correlation between alpha-band suppression and placebo manipulation (i.e. variable expectations of upcoming painful stimuli) [66].

Beta-band (15-30Hz) suppressions occur in preparation of voluntary movements with most prominent components at contralateral regions [73]. Both Zhang et al. (2012) and Misra et al. (2017) detected deactivation patterns in the beta-band at 300 ms - 1000 ms after stimulus onset [72], [74]. While Zhang et al. (2012) found an active correlation between deactivation and stimulus repetitions, Misra et al. (2017) corroborated the hypothesis that beta-band suppressions are antikinetic and explain the presence of voluntary movements [72], [74].

Physiologically speaking, early-onset gamma oscillations (30-100Hz) cause first pain sensation and thus are mediated by fast A $\delta$ -fibers. However, there is disagreement in the present literature when addressing the functional role of gamma-band neuronal oscillations in relation to pain processing. While Gross et al. (2007) associated gamma-band modulations to objective changes of stimulus intensity, Zhang et al. (2012), Peng et al. (2014) and Schulz et al. (2015) argue that gamma-band oscillations are instead consequence of a subjective perception of stimulus intensity [75], [72], [76], [77].

A short summary of relative band powers and their corresponding functional role in pain processing is depicted in Table 2.2.

Relative Band Power	Role in pain processing	References
Theta Band (4-8Hz)	Equivalent to nociceptive evoked potentials Sensorimotor involvement during task-related responses Reduced lateral inhibition in chronic pain patients	Ploner et al. (2017), [66]
Alpha Band (8-15Hz)	Task-related ipsilateral suppression Sensory-related contralateral suppression	Hu et al. (2013), [69]
	Lateralization due to handedness	Zapala et al. (2020), [70] Bai et al. (2005), [71]
	Attentional biases	Zhang et al. (2012), [72]
Beta Band (15-30Hz)	Placebo manipulation	Ploner et al. (2017), [66]
	Antikinetic role during voluntary movement	Misra et al. (2017), [74]
Gamma Band (30-100Hz)	Dependent on stimulus repetition	Zhang et al. (2012), [72]
	First pain sensation	Gross et al. (2007), [75]
	Objective stimulus intensity	Zhang et al. (2012), [72] Peng et al. (2014), [76]
	Subjective perception of stimulus intensity	Schulz et al. (2015), [77]

**Table 2.2:** Functional role and modulation of relative band powers during pain processing

As Ploner et al. (2017) suggests, the most relevant frequency bands for the investigation of chronic pain are the theta and beta bands, with specific frontal activation in the beta-band [66]. For example, abnormal theta oscillations characterize chronic pain conditions by reducing lateral inhibition and influencing the appearance of gamma oscillations. Thus, time-frequency analysis is an interesting method to investigate pain-related brain activations at different time and frequency intervals, in healthy or unhealthy individuals.

### 2.5.1 Analysis of neuronal oscillations

Several methods can be used to estimate neuronal oscillations of single-trial EEG data, each characterized by advantages and disadvantages. Fourier transform is commonly used in pain research to investigate event-related neuronal oscillations. A windowed *Short-time Fourier Transform* (STFT) discards the assumption of stationarity by dividing the signal into short time intervals and produces an optimal representation of EEG data with high-resolution in both the time and frequency domain. However, a distinct characteristic of STFT is the trade-off between time and frequency resolution: a longer time-window will result into a better frequency resolution and worse time resolution. After choosing the proper resolution, results of the STFT can be displayed in spectrogram plots as power amplitude changing over frequency and time [78]. *Wavelet Convolution* or *Hilbert Transform* are alternative methodologies for extracting frequency features from EEG data. Wavelet transform overcomes the limitations of STFT over temporal localization by using a Gaussian taper window along with a sine wave, also known as Morlet (or Gabor) wavelet [65]. The trade-off between temporal and frequency accuracy is still valid and can be adjusted by changing the number of cycles the Gaussian window is constructed over: the larger the number of cycles, the stronger should be the assumption of stationarity of the EEG data. The main difference between STFT and Wavelet convolution is in the window: STFT uses a single window, while in the Wavelet transform short windows are used at higher frequencies and longer windows at lower frequencies [79]. However, STFT can be used in case of low signal-to-noise ratio and to investigate gamma-band frequency contents when combined to multitapering, a method introducing several tapers with different time and frequency characteristics to smoothen either temporal or spectral characteristics. In general, the multitaper method is not recommended for the analysis of frequencies lower than 30Hz due to temporal smoothing [65]. Hilbert transform is a decomposition method extracting complex components from EEG signals. The analytic signal obtained from a Hilbert transform is a complex time series with a large number of frequency components in which phase-angle features can be extracted along with instantaneous power and real signal. The additional information on phase-angles is a strong characteristic of Hilbert transform making it the most reliable tool for investigations related to 'phase-locked' neuronal activity.

The proper time-frequency analysis should be selected in accordance to the research question and to the type of frequency content that needs to be investigated.

# High-frequency stimulation (HFS) and the MTT-EP protocol

# 3

3.1 Methods & Materials . . . . 21

High-frequency stimulation is one of the available alternative used in experimental pain models. Previous research investigated the role of HFS in increased mechanical pinprick sensitivity, demonstrating the development of experimentally-induced secondary hyperalgesia [80]. A pilot study conducted at the University of Twente assessed the feasibility of HFS in the BSS laboratory facilities.

In this chapter, an experimental protocol combining HFS-induced secondary hyperalgesia with the MTT-EP protocol will be introduced. The aim of this experimental protocol is to investigate whether the underlying mechanisms of secondary hyperalgesia modulate cortical activations. Successful observation of maladaptive cortical activations as consequence of HFS would allow to gain a deeper understanding of the mechanisms underlying secondary hyperalgesia and to validate the MTT-EP as possible diagnostic tool for chronic pain conditions.

## 3.1 Methods & Materials

### 3.1.1 Participants

Twenty healthy subjects, between 18 and 40 years old, will be recruited at the University of Twente, The Netherlands. No additional inclusion criteria are required; however, individuals with implanted stimulation devices, with medical history of chronic pain or pregnant women will be excluded from participation to the study. All participants will be asked to read and sign an informed consent form in accordance with the declaration of Helsinki.

### 3.1.2 Equipment

#### HFS-electrodes

A fellow research group from Aalborg University developed a feasible electrode for HFS. The circular electrode has a 2cm diameter with two concentric rings; the external ring is the anode and the internal one is the cathode, as shown in Figure 3.1. Five trains of HFS are delivered to the individuals, each train lasting 1s with a frequency of 100Hz and pulse-width of 2ms.



**Figure 3.1:** Electrodes for high-frequency stimulation (HFS). The electrodes in the figure have been provided by a fellow research group from Aalborg University and later used by Snijder for a technical feasibility study [81]. Reprinted from "High frequency stimulation induced secondary hyperalgesia for validation of diagnostic tools for early detection of chronic pain development. HFS: technical feasibility study" (p. 10), by Marie-Laure Snijders, 2019, Enschede, The Netherlands: BSS group - University of Twente

### Impedance system

A 100 Ohm resistor and one oscilloscope are attached to the HFS-electrode in order to ensure that the set-up for the HFS would reach the required voltages. The electrical circuit is built to record impedance and voltage over the HFS electrode.

### Mechanical punctate stimulation

In order to evaluate the occurrence of secondary hyperalgesia, mechanical punctate stimulation is delivered before and after the HFS. Mechanical punctate stimulations are applied using a 5.18/15g Semmes-Weinstein monofilament (depicted in Figure 3.2) on the proximal, distal, radial and medial sides of the HFS and IES-5 electrodes. The 5.18/15g Semmes-Weinstein monofilament has been previously tested and used at the University of Twente, showing better force accuracy and statistically significant differences in NRS scores between the pre- and post-HFS [81]. In addition, previous literature used a comparable stimulation tool, delivering a normal force of 128mN stimulator (~ 13g), to assess increased sensitivity after HFS [80].



**Figure 3.2:** Touch Test®Sensory Evaluator by North Coast Medical Rehabilitation Products. In white: the Semmes-Weinstein monofilament used for assessing the occurrence of secondary hyperalgesia administering mechanical punctate stimulations. Reprinted from "Touch Test®Sensory Evaluators", by North Coast Medical & Rehabilitation products, 2020 (<https://www.ncmedical.com>) ©2020 North Coast Medical Inc.

The measurement used for assessing the intensity of mechanical punctate stimulations is the numerical rating score (NRS), a rate labeling the intensity of the perceived stimulus ranging from 0 to 10. The occurrence of HFS-induced secondary hyperalgesia should result in an increase in intensity of the perceived stimulus and, thus, an increase in NRS scores.

## OctoStim PT

The OctoStim PT is an 8-channel electrical stimulator for non-invasive electrical stimulation using skin electrode and developed for medical scientific research, especially for application in the field of pain diagnosis. Its system is designed to generate current pulses with adjustable width, amplitude (up to 20mA), frequency (up to 100Hz) and inter-pulse interval. In this experimental protocol, OctoStim PT is used for stimulation via both IES-5 and HFS-electrodes and for recording patients' responses through an integrated response button. OctoStim PT is battery-powered and connected to a computer via wireless connection to avoid leakage to the environment and ensure a safe stimulation.

## EEG system

Scalp electroencephalography is recorded continuously using a 1kHz sampling frequency and a 32 Ag/AgCl electrodes ANT Neuro Waveguard EEG cap combined with a TMSi Refa amplifier with up to 136 inputs. A dedicated TMSi Polybench software is integrated in order to record both trigger codes from the the OctoStim PT and the EEG data.

### 3.1.3 Experimental procedure

After signing the informed consent form, each participant to the study will be made familiar with and connected to the experimental set-up. A 32-channels EEG cap will be placed to the scalp of the subject and each electrode will be filled with conductive gel in order to maintain a scalp-electrode impedance below 5k $\Omega$ . Afterwards, the subject will be connected to the IES-5 and HFS electrodes, fixed with medical tape on the right forearm, as displayed in Figure 3.3. One IES-5 electrode will be placed on the subject's wrist and the second IES-5 will be placed on the forearm, while the OctoStim stimulation device will be placed on the left hand.

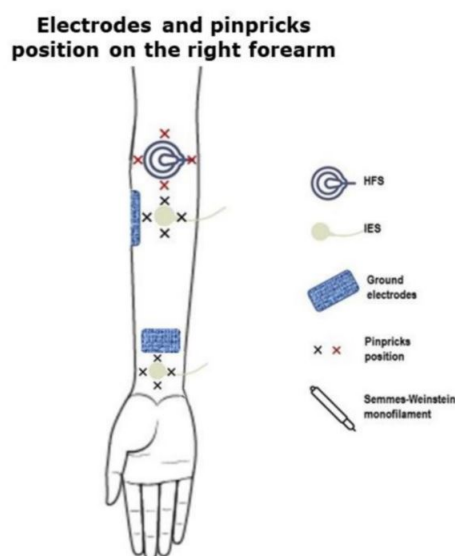


**Figure 3.3:** Electrodes and punctate stimulation positions on the right forearm of healthy subjects. This electrodes set-up is used for the HFS, MTT method and punctate mechanical stimulation.

After the set-up, a familiarization procedure will be conducted. The short method for detection threshold estimation consists of 2 series, each composed of 10 ascending single- (number of pulses (NOP) = 1) or double-pulses stimuli (NOP = 2, inter-pulse interval (IPI) = 10ms). During the first series of stimuli, the subject will be asked to release the button when the stimulus is clearly perceived. Instead, during the second series, the subject will be asked to release the button as soon as a slight sensation of a stimulus is perceived.

Subsequently, a first punctate mechanical stimulation will be conducted in order to target the baseline NRS rates to mechanical sensitivity.

This familiarization phase is crucial for a first estimation of the individual's detection threshold in order to initialize the MTT paradigm.

The protocol consists of seven items to track nociceptive detection thresholds, cortical activations, sensitivity to mechanical stimulation before and after inducing secondary hyperalgesia with HFS, Figure 3.4:

1. *First MTT-EP acquisition*: to detect nociceptive detection threshold and to simultaneously measure cortical activations from both the IES-5 electrodes on the forearm and on the hand;
2. *Second mechanical punctate stimulation*: to reject the hypothesis of inducing secondary hyperalgesia with IES-5 alone;
3. *HFS and assessment of perceived pain*: to induce secondary hyperalgesia by using a stimulation 20-times higher the individual's detection threshold and assessment of perceived pain for discomfort;
4. *Third mechanical punctate stimulation*: to assess the occurrence of HFS-induced secondary hyperalgesia;

*Break*

5. *Fourth mechanical punctate stimulation*: to confirm (or discard) the occurrence of secondary hyperalgesia
6. *Second MTT-EP acquisition*: to detect nociceptive detection threshold and to simultaneously measure cortical activations from both the IES electrodes on the forearm and on the hand;
7. *Fifth punctate mechanical stimulation*

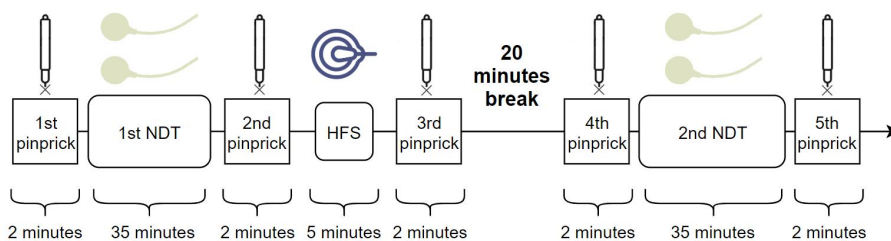


**Figure 3.4:** Timeline of experimental session

Literature suggests that occurrence of HFS-induced secondary hyperalgesia is best noticeable after 20 minutes from the stimulation [80]. For this reason, there will be a short break between the third and fourth mechanical punctate stimulation. After the fifth mechanical punctate stimulation, a final round-up phase will be conducted during which the subject will be disconnected from the set-up and provided with contact information and some time to ask questions.

### **3.1.4 Ethical approval**

In order to perform this experimental protocol, an ethical approval was submitted to the Commissie Mensgebonden Onderzoek regio Arnhem-Nijmegen (CMO Arnhem-Nijmegen) on February 26th 2020. On June 29th 2020, the experimental protocol obtained the ethical approval with Dossier number: NL72937.091.20. For more information about the experimental procedure, please refer to Appendix 5.

# Frequency-domain analysis of EEG data

# 4

4.1 Methods & Materials . . . . 26  
4.2 Results . . . . . 30  
4.3 Discussion . . . . . 54

At the University of Twente, the analysis of nociceptive evoked potentials recorded during the MTT-EP protocol is a consolidated technique. Previous results from a linear mixed model have revealed significant relations between nociceptive evoked potentials and stimulus parameters, such as stimulus intensity and detection. However, several research have demonstrated the crucial role of neuronal oscillations in pain processing. In fact, relative band powers, time-locked to nociceptive stimuli, are the reflection of the underlying mechanisms involved in the processing of the said stimuli. Time-frequency analysis has never been performed on EEG data recorded during the MTT-EP protocol. This chapter presents a first exploratory study, investigating the frequency content of EEG data recorded during the MTT-EP protocol, and the results extracted using a linear mixed model, unveiling the modulation of brain oscillations in relation to stimulation parameters.

## 4.1 Methods & Materials

### 4.1.1 Participants

Two datasets from previous experimental protocols were included in this graduation assignment.

The first dataset was provided from the experimental trials conducted by Boudewijn Van den Berg for his master’s graduation project. A total number of 25 subjects (16 males and 9 females, age  $23 \pm 3.6$ ) was included for the data analysis [41].

The second dataset is composed of healthy individuals and patients with a pain-related syndrome (i.e. FBSS, Failed-Back Surgery Syndrome) for a total number of 31 subjects, seventeen of which were pain-free subjects (14 males and 3 females, age  $35.9 \pm 11.9$ , NRS  $0.0 \pm 0.0$ ). In this assignment, the seventeen pain-free subjects from the St. Antonius Hospital were included for the analysis [82].

#### Subject characteristics

A total number of forty-two healthy subjects were included in the analysis (25 healthy subjects from UT and 17 subjects from St. Antonius Hospital). Subjects characteristics are summarized in Table 4.1.

Characteristics	Pain-free subjects	Pain-free subjects
	UT <i>N</i> = 25	St. Antonius <i>N</i> = 17
Age ( <i>years</i> )	$23.0 \pm 3.6$	$35.9 \pm 11.9$
Gender ( <i>M/F</i> )	16/9	3/14
NRS-score	-	$0.0 \pm 0.0$

Table 4.1: Subjects characteristics

Healthy subjects from University of Twente (UT) and St. Antonius Hospital had no medical history of neurological disorders.

### 4.1.2 Equipment

Electroencephalographic data were recorded using either a 128-channels electrode-cap (UT dataset) or a 64-channels cap (St. Antonius dataset), placed on the scalp of the subjects according to the international 10-20 system. The EEG recordings were amplified and digitized using a sampling rate of 1024 Hz and 1000 Hz, respectively.

Raw EEG data were corrected for horizontal and vertical eye movements using an independent component analysis (ICA) and band-pass filtered from 0.1Hz to 200Hz. The UT dataset was epoched from -500 (before stimulus onset) to 1000 ms (after stimulus onset), while the St. Antonius dataset was epoched from -1000ms (before stimulus onset) to 2000ms (after stimulus onset).

### 4.1.3 Experimental procedure

The included datasets were acquired in different location and times using the same MTT-EP protocol. The data from the first dataset were collected at the University of Twente using the MTT-EP protocol and no external intervention. The session consisted of one measurement, on the right hand.

The second dataset was collected at the St. Antonius Hospital (Utrecht, The Netherlands) where Tom Berfelo was in charge of the experimental trials using the MTT-EP protocol. The acquisition protocol consisted of two measurements, one on each hand. The pain-free subjects were tested further and obtained a pain-free NRS-score (NRS:  $0.0 \pm 0.0$ ) and CSI-score lower than 40, confirming the absence of any central sensitization syndrome (mean CSI-score  $14.6 \pm 8.8$ ).

### 4.1.4 Time-frequency analysis

Time-Frequency Analysis was conducted using a custom-built MATLAB code based on standard signal analysis methods. EEG recordings from the first dataset (hereinafter referred to as UT dataset) were time-locked and extracted using a window ranging between -0.5s (before stimulus onset) and 1s (after stimulus onset). Single-trial EEG data then were transformed using Hann-windowed Short-Time Fourier Transform (STFT).

The Hann window had a length of 200 data points, padded with zeros up to 1024 data points. The Hann window was shifted of one data point for a frequency resolution of 1 Hz and temporal resolution  $1/1024$  s.

TFR was then averaged over detected/undetected trials. Signal amplitude of averaged TFRs was computed and then transformed into percentage signal change values with respect to the single trial baseline from -400 to -100 ms. The percentage change was calculated according to equation 4.1 [83]:

$$ER\%(t, f) = \frac{[P(t, f) - R(f)]}{R(f)} \times 100 \quad (4.1)$$

Where  $P(t,f)$  is estimate of the signal amplitude at each time-frequency point and  $R(f)$  is the average of the signal amplitude before stimulus onset (between -400 and -100 ms). For each electrode, whole group TFRs were calculated averaging the individual TFRs over subjects.

### Latencies selection

Grand averages of the TFRs over subjects were divided into relative band powers: theta (3-8Hz), alpha (8-15Hz), beta (15-30Hz) and gamma band (30-100Hz). Butterfly plots were used to select latencies showing strongest neuronal responses and they were generated by averaging the grand averages TFRs over one frequency band, resulting into one time-dependent signal for every EEG electrode, as shown in equation 4.2:

$$B(t)_{electrode} = \frac{1}{N} \sum_{i=f_0}^{f_{end}} TFR\%(t, i)_{electrode}, \quad t \in [-400, 900] \text{ ms} \quad (4.2)$$

Where  $B(t)$  is the time-dependent signal depicted into the butterfly plots,  $TFR\%$  is the grand averages of the TFRs (average over trials and subjects) expressed as percentage signal changes.  $f_0$  is the lower endpoint of the relative band-power interval (e.g. in the theta-band,  $f_0 = 4\text{Hz}$ ) and  $f_{end}$  is the upper endpoint (e.g. in the theta-band,  $f_{end} = 8\text{Hz}$ ).

Due to the broad width of the gamma band (from 30Hz to 100Hz), butterfly plots of relative gamma-band powers were generated by averaging the signal over smaller frequency intervals of 5Hz-width each.

### Channel selection

Topographical maps were selected by averaging over relative frequency bands and over selected latencies, resulting into a graphical representation of cortical activations around the scalp. Electrodes showing the strongest neuronal responses, in dark blue for neuronal deactivations and dark red for neuronal activations, were used for further analysis.

At each electrode, the percentage signal change at latency  $t$  with respect to baseline interval and SNR values were computed. The SNR was computed as the ratio between the grand-average of the TFRs at latency  $t$  and the standard deviation of the grand-average of the TFRs before stimulus onset (i.e. baseline interval). Electrodes with largest amplitudes and SNR values were selected for further statistical testing.

### 4.1.5 Statistical Analysis

Previous research conducted at the BSS group of the University of Twente developed a linear mixed regression model (LMM) to investigate the role of stimulus parameters (i.e. stimulus intensity and detection), number of trials and diagnosis in the data recorded during the MTT-EP protocol. Linear mixed models are build upon a mathematical formulation including linear and random structures and detecting both within-subjects and between-subjects slopes and intercepts. The advantage of LMM over averaging is that it deals more efficiently with missing data and with a small number of subjects.

Here, LMM was used to find the influence of stimulus parameters, such as stimulus

amplitude or stimulus detection, on the relative band powers of single-trial EEG measurements. The model variables were centered and scaled based on their mean and standard deviation. In particular, we investigated which parameter influences each relative band-power by evaluating the following features: the influence of stimulus amplitude and response on the relative power and the influence of trial number due to habituation effects.

The resulting model is shown in equation 4.3:

$$TFR \sim 1 + AMP + AMP_{2_{10}} + AMP_{2_{40}} + TRL * D \\ + (1 + AMP + AMP_{2_{10}} + AMP_{2_{40}} + TRL * D | Subject) \quad (4.3)$$

The model here is described using Wilkinson notation.

Where AMP is the amplitude of the first pulse, AMP2 is the amplitude of the second pulse of a stimulus, D is the stimulus detection and TRL is the trial number. In this model, it was assumed that activity generated by a second pulse can be summed to the activity of the first pulse and it varies based on the inter-pulse intervals (either 10ms or 40 ms, AMP<sub>2<sub>10</sub></sub> and AMP<sub>2<sub>40</sub></sub>, respectively). Between-subjects random effects were introduced to the model (Subject).

#### 4.1.6 Comparison analysis

Results derived from the data analysis, channel selection and statistical testing of the UT dataset were investigated and compared to the second dataset (hereinafter referred to as St. Antonius dataset) in order to validate the analysis and detect similarities and/or discrepancies. For the purpose, single-trial TFRs at selected electrodes were extracted from the St. Antonius dataset using Hann-windowed STFT with a window length of 200 data points, padded up to 1000 data points, frequency resolution of 1Hz and a temporal resolution of 1/1000s.

Lastly, single-trial TFRs were divided into relative band-powers and the LMM model was adjusted in order to take into account the effect of handedness (HAND) on the relative band powers.

The resulting model is shown in equation 4.4:

$$TFR \sim 1 + HAND + AMP + AMP_{2_{10}} + AMP_{2_{40}} + TRL * D \\ + (1 + HAND + AMP + AMP_{2_{10}} + AMP_{2_{40}} + TRL * D | Subject) \quad (4.4)$$

The model here is described using Wilkinson notation.

Results have shown significant discrepancies between the UT and St. Antonius dataset. For these reasons, mean amplitudes and SNR values of the UT dataset were computed at selected electrodes and latencies with respect to the St. Antonius dataset. In addition, butterfly plots and scalp distributions were compared in order to exclude possible differences in temporal and regional activations.

Lastly, due to the discrepancies in subject characteristics, the distribution of significant effect sizes on individual levels were derived for both UT and St. Antonius subjects.

## 4.2 Results

### 4.2.1 Time-frequency analysis

#### Latencies selection

Butterfly plots of percentage signal changes show the relative band powers, at each frequency-band of interest, time-locked to intra-epidermal electrical stimuli delivered during the MTT-EP protocol at the University of Twente (UT dataset), as shown in Figure 4.1.

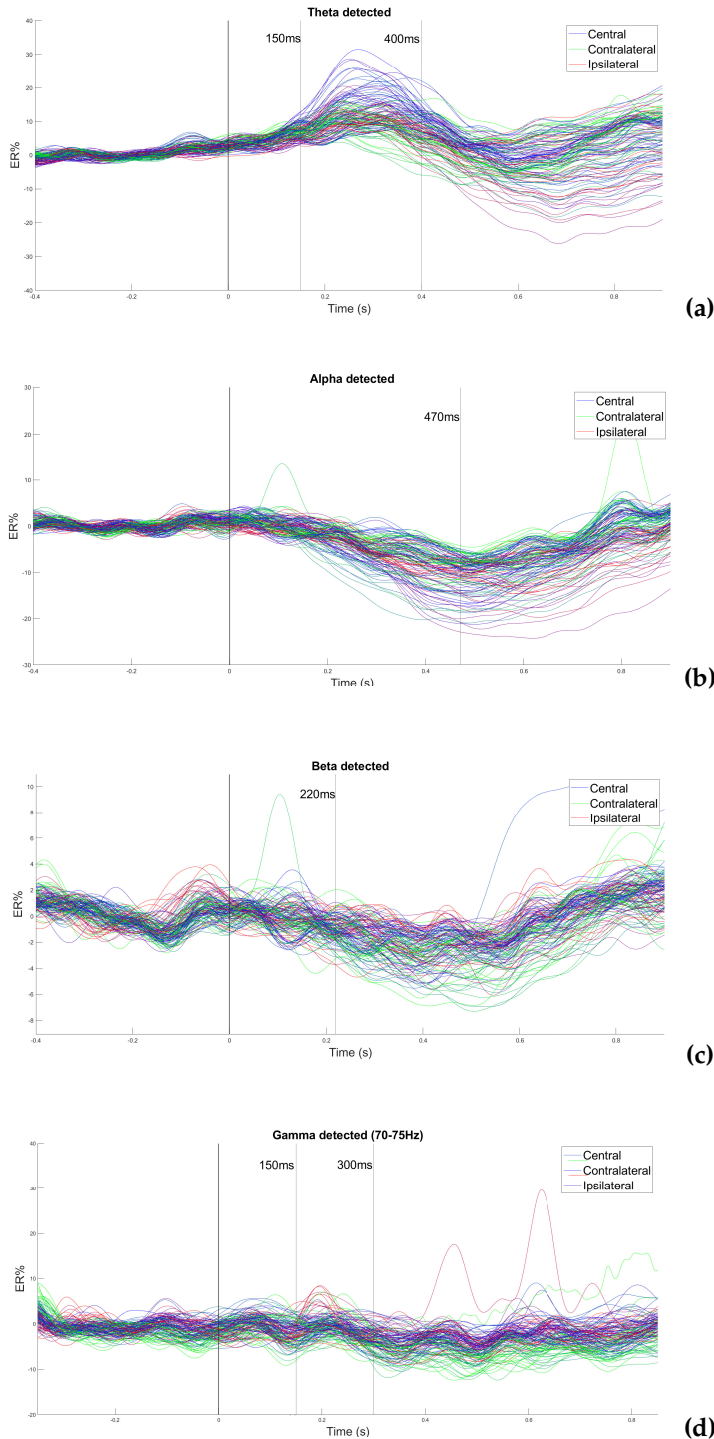


**Figure 4.1:** a) Relative *theta-band* power, as percentage signal change, of EEG channels responding to intra-epidermal stimuli around the nociceptive detection threshold. There are strongest neuronal oscillations around 150-300ms and 400-900ms. b) Relative *alpha-band* power, as percentage signal change, of EEG channels responding to intra-epidermal stimuli around the nociceptive detection threshold. Strongest neuronal oscillations are located around 470-700ms. Latency 470ms will be used for statistical testing. c) Relative *beta-band* power. The strongest neuronal oscillation is located around 200-600ms. d) Relative *gamma-band* power (70-75Hz), expressed as percentage signal change, of EEG channels responding to intra-epidermal stimuli around the nociceptive detection threshold. The strongest neuronal oscillations between 70Hz and 75Hz are located between 150ms and 300ms.

Relative theta-band power showed strongest neuronal oscillations around 150-300ms and 400-900ms. Alpha-band power had strongest neuronal oscillations at latencies around 470-700ms. At interval 200-600ms, relative beta-band power had the strongest response, while gamma-band oscillations are located around 150-300ms and 600-900ms. In Figure 4.1-d, the butterfly plot is depicted exclusively for a frequency range of 70-75Hz.

### Channel selection

At each latency, grand averages of the TFRs were computed as scalp topographies. Topographical maps were visually inspected and used to select the electrodes with the strongest positive and/or negative neuronal response. Figures from 4.2 to 4.5 display the scalp distributions at baseline intervals in comparison to relative band powers at latencies, previously selected from visual inspection of the butterfly plots.

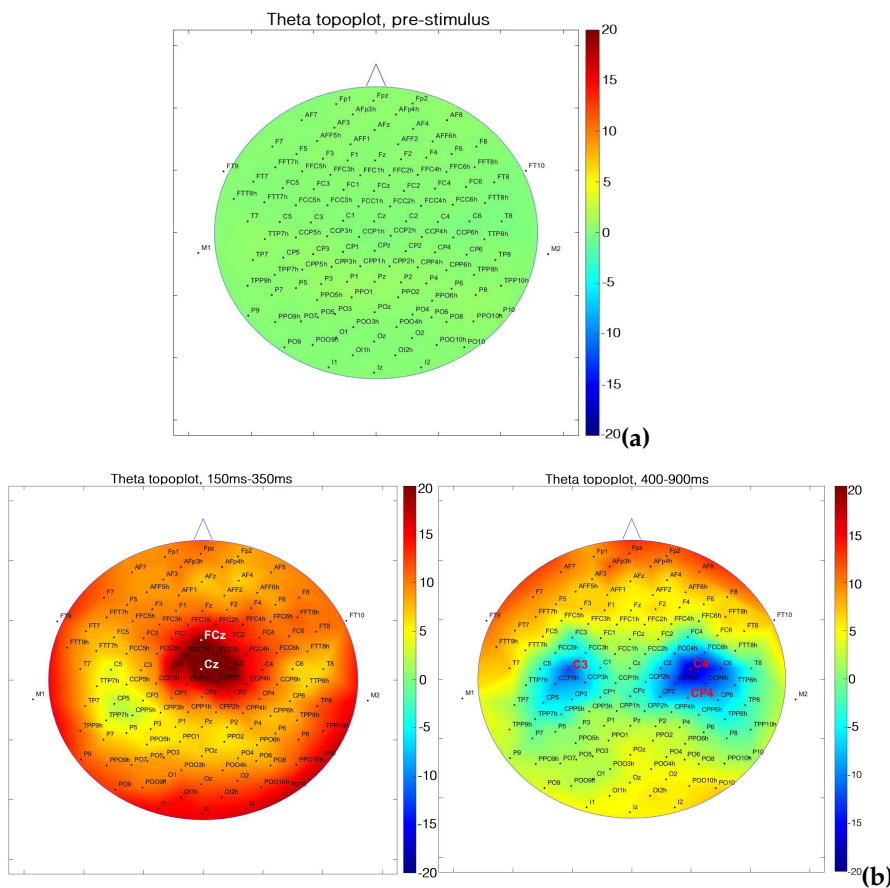


**Figure 4.2:** Scalp topography map of relative power in the theta-band. a) pre-stimulus scalp topography shows the absence of theta-band oscillations. b) theta-band oscillations are distributed along the scalp topography at latencies between 150ms-300ms (left) and 400ms-900ms (right) after stimulus onset. In the theta-band, strongest neuronal oscillations are present in the central areas, at earlier latencies, and both in the contralateral and ipsilateral regions, at later latencies.

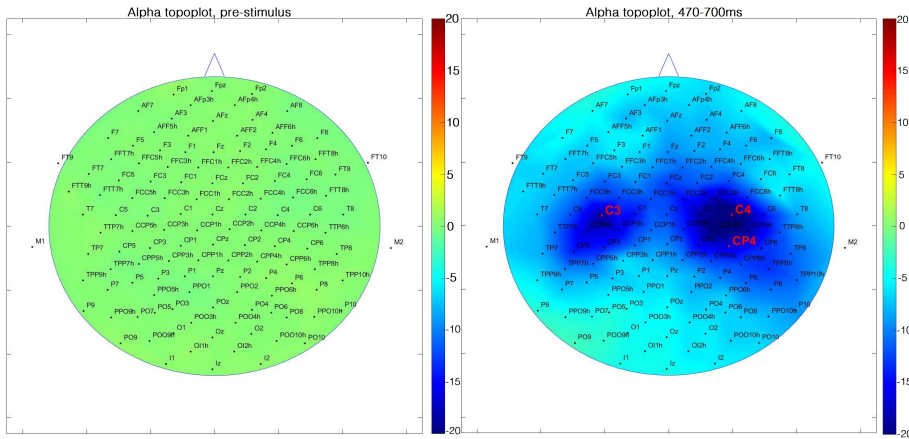


**Figure 4.3:** Scalp topography map of relative power in the alpha-band. (Left) pre-stimulus scalp topography shows the absence of alpha-band oscillations. (Right) alpha-band oscillations are distributed along the scalp topography at latencies between 470ms and 700ms after stimulus onset. In the alpha-band, strongest neuronal oscillations are present both in the contralateral and ipsilateral regions.

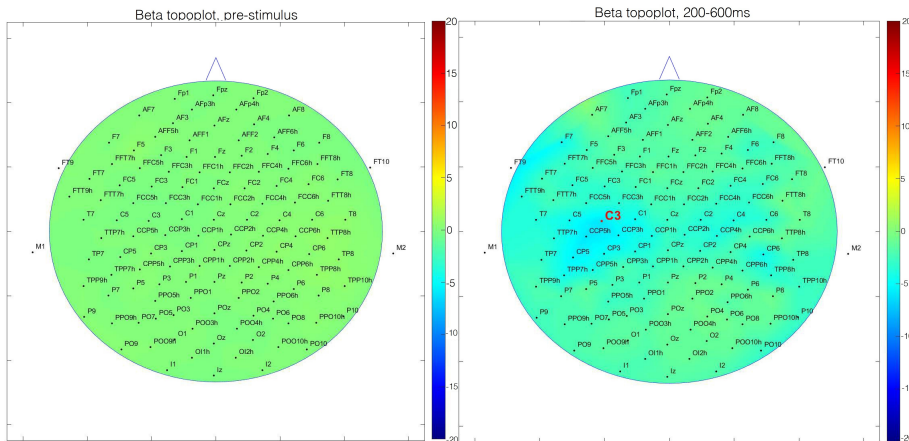


**Figure 4.4:** Scalp topography map of relative power in the beta-band. (Left) pre-stimulus scalp topography shows the absence of oscillations. (Right) beta-band oscillations are distributed along the contralateral side of the scalp at latencies between 200ms and 600ms after stimulus onset.

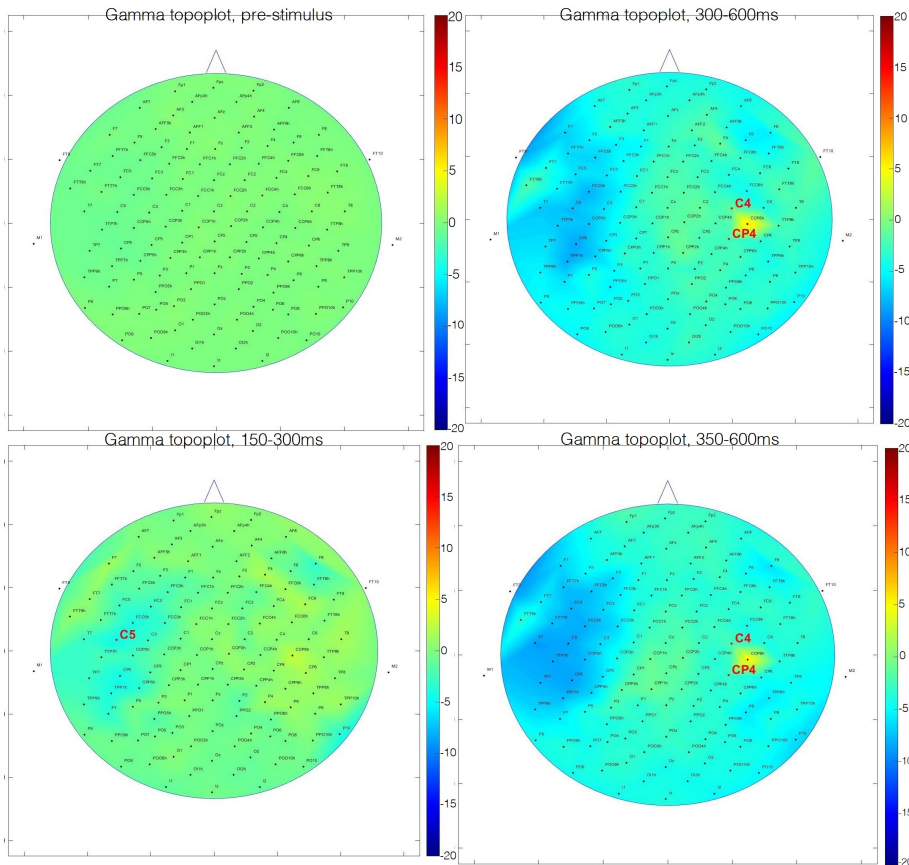


**Figure 4.5:** Scalp topography map of relative power in the gamma-band. Top row: (Left) pre-stimulus scalp topography shows the absence of oscillations. (Right) lower gamma-band (30-55Hz) oscillations are present at latencies between 300ms and 600ms after stimulus onset. Bottom row: (Left) middle gamma-band (70-85Hz) present strongest neuronal oscillations at latencies 150ms-300ms. (Right) higher gamma-band (70-95Hz) has strongest response between 350ms and 600ms after stimulus onset.

The percentage signal changes and SNR were computed at each selected electrode and latency, as shown in Table 4.2.

<b>Theta-band: 150ms-300ms</b>	<b>Amplitude</b>	<b>SNR</b>
Cz	27.65	28.36
FCz	24.09	22.55
<b>Theta-band: 400ms-900ms</b>	<b>Amplitude</b>	<b>SNR</b>
C4	-8.91	11.35
CP4	2.82	1.55
C3	-7.89	6.07
<b>Alpha-band: 470ms-700ms</b>	<b>Amplitude</b>	<b>SNR</b>
C4	-22.85	20.17
CP4	-14.67	9.76
C3	-20.75	28.38
<b>Beta-band: 200ms-600ms</b>	<b>Amplitude</b>	<b>SNR</b>
C3	-3.13	3.58
<b>Lower gamma-band: 300ms-600ms</b>	<b>Amplitude</b>	<b>SNR</b>
C4	-3.06	5.46
CP4	-2.32	3.95
<b>Middle gamma-band: 150ms-300ms</b>	<b>Amplitude</b>	<b>SNR</b>
C5	-2.99	1.96
<b>Higher gamma-band: 350ms-600ms</b>	<b>Amplitude</b>	<b>SNR</b>
C4	-1.23	2.51
CP4	-3.29	3.69

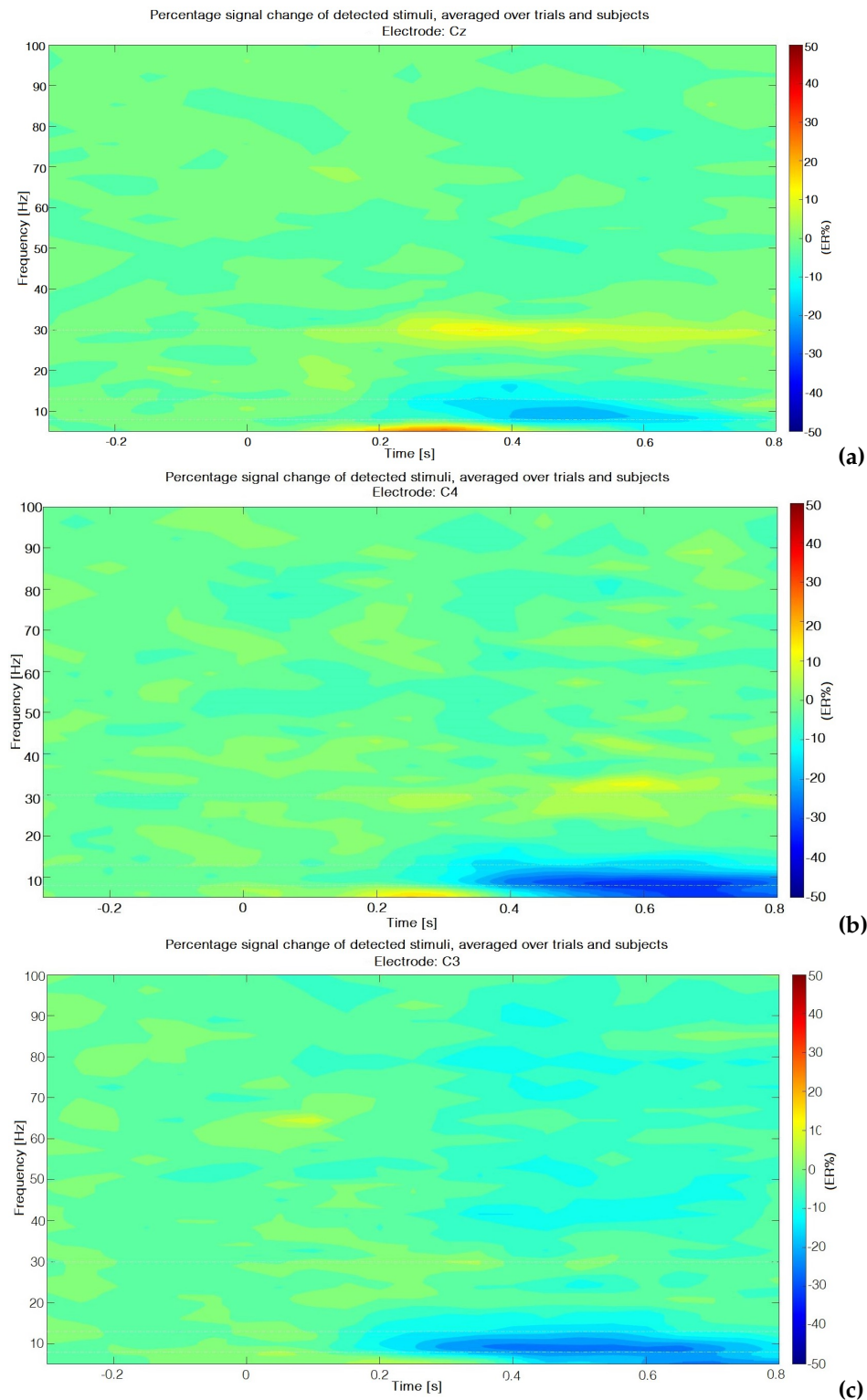
**Table 4.2:** Grand average TFRs at latencies and electrodes with strongest neuronal responses, as selected from the scalp distribution. The respective SNR is computed. The electrodes with strongest neuronal response are also the electrodes with the largest SNR values.

Scalp topographies, amplitudes and SNR values showed strongest neuronal response in the theta band (3-8 Hz) at electrode Cz (27.65 signal amplitude; SNR 28.36) and C4 (-8.91 signal amplitude; SNR 11.35). Decrease of neuronal response was pronounced in the alpha band (8-15 Hz) in both ipsilateral and contralateral regions, at electrodes C4 (-22.85 signal amplitude; SNR 20.17) and C3 (-20.75 signal amplitude; SNR 28.38), respectively. A less pronounced decrease in neuronal response was present in the beta band (15-30 Hz) at electrode C3 (-3.13 signal amplitude; SNR 3.58). The gamma-band was divided into three subgroups. The lower gamma-band (30-55 Hz) showed strongest neuronal oscillation at electrode C4 (-3.06 signal amplitude; SNR 5.46), middle gamma-band (70-85Hz) showed strongest neuronal response at electrode C5 (-2.99 signal amplitude; SNR 1.96) and high gamma-band (70-95Hz) showed strongest response at electrode CP4 (-3.29 signal amplitude; SNR 3.69).

### Grand average TFRs

Grand averages of TFRs at each electrode are displayed as percentage signal change with respect to the baseline interval in a time-frequency plot. Positive signal changes are represented in red, while negative changes in blue.

In Figure 4.6, the grand average of TFRs at electrode Cz, C4, C3, C5 and CP4 are depicted.



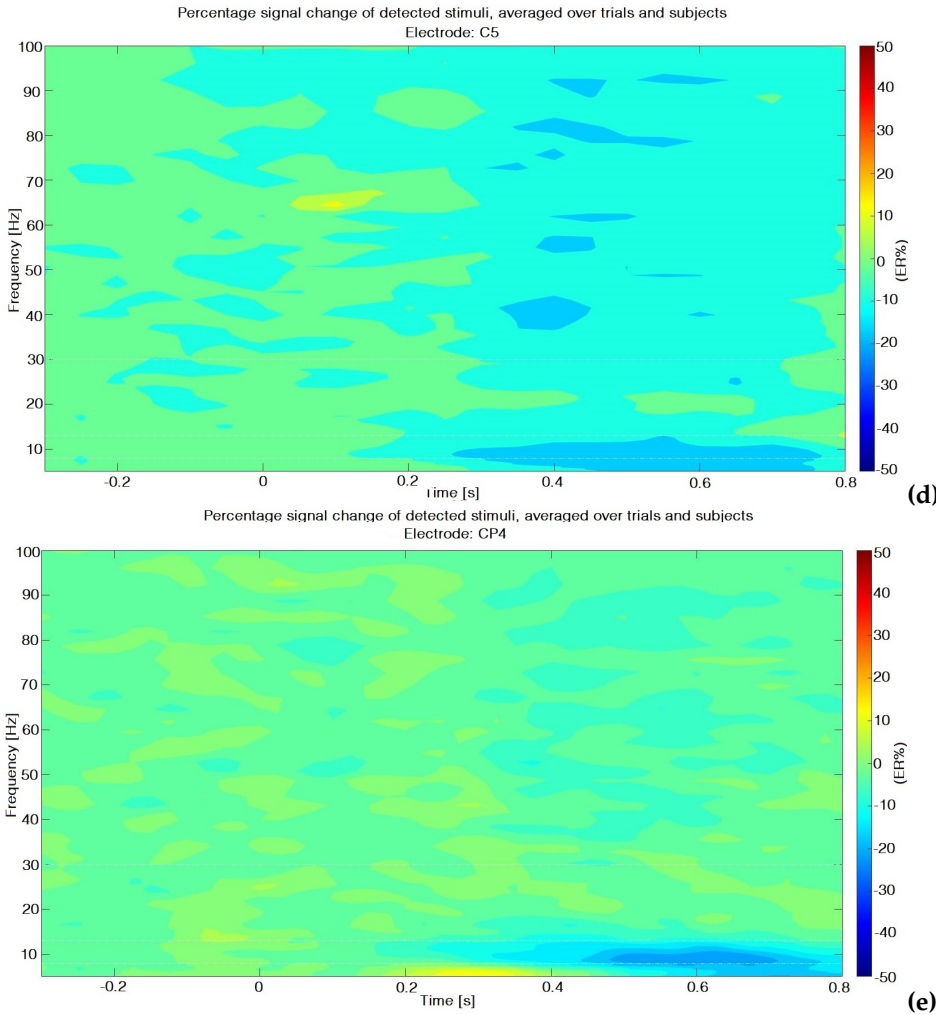


**Figure 4.6:** a) TFR of neuronal response to detected stimuli at electrode Cz represented as percentage signal change with respect to pre-stimulus baseline (-400 to -100 ms). b) TFR of neuronal response to detected stimuli at electrode C4. c) TFR of neuronal response to detected stimuli at electrode C3. d) TFR of neuronal response to detected stimuli at electrode C5. e) TFR of neuronal response to detected stimuli at electrode CP4. The TFRs in figure are the result of group averaging over detected trials and 25 subjects.

From the grand average TFRs, it was confirmed that electrode Cz has the strongest neuronal activity in the theta frequency range between 150ms and 300ms. Strong decreases in alpha-band activity are depicted both on ipsilateral and contralateral regions at electrodes C4 and C3, respectively. Furthermore, topographical scalp distributions showed a decrease in the gamma-band neuronal activity at electrode C4 and at latencies 300-600ms; this less pronounced oscillations are not depicted in the TFRs, as shown in Figure 4.6-b. A similar behaviour is seen at electrode CP4 where gamma-band oscillations are less pronounced than the alpha-band oscillatory activity, Figure 4.6-e.

Beta-band activity at electrode C3 and gamma-band activity at C5 are slightly pronounced with maximum at latencies between 200ms-600ms and 150ms-300ms, respectively. While beta-band deactivation are depicted in light blue, Figure 4.6-c, gamma-band responses at electrode C5 are neuronal activations and depicted in yellow, Figure 4.6-d.

## 4.2.2 Statistical Analysis

### Effect of stimulus properties on TFRs

The coefficients of the LMM model are extracted at previously-selected latencies and channels and are shown in Tables from 4.3 to 4.5.

Moreover, results of the statistical analysis show the model coefficients and their

significance as a function of time between pre- and post-stimulus intervals, as shown in Figure 4.7. Significant coefficients explain the modulation of relative band powers with respect to the variation of a single parameter.

### Theta-band

Coefficients	Effect size	95% Confidence Interval	Cz: 230ms	
			<i>t</i>	<i>p</i>
(Intercept)	-0.0021	[-0.0038 -0.0003]	-2.4633	0.0209
Detection (D)				
Detected	0.0046	[0.0011 0.0082]	2.7068	<b>0.0119</b>
Pulse 1 (PU1)	0.0007	[-0.0038 0.0053]	0.3322	0.7398
Pulse 2, 10ms IPI	-0.0080	[-0.0220 0.0060]	-1.1718	0.2520
Pulse 2, 40ms IPI	0.0026	[-0.0055 0.0108]	0.6273	0.5305
Trial number	-1.96e-06	[-1.10e-05 7.10e-06]	-0.4236	0.6718
Trial number x Detection				
Trial number x Detected	-1.47e-05	[-3.61e-05 6.79e-06]	-1.3856	0.1743
<b>C4: 470ms</b>				
			<i>t</i>	<i>p</i>
(Intercept)	0.0023	[0.0013; 0.0033]	4.4783	7.61e-06
Detection (D)				
Detected	-0.0051	[-0.0096 -0.0007]	-2.4019	<b>0.0234</b>
Pulse 1 (PU1)	-0.0018	[-0.0055 0.0018]	-0.9984	0.3180
Pulse 2, 10ms IPI	-0.0041	[-0.0119 0.0037]	-1.0284	0.3037
Pulse 2, 40ms IPI	0.0004	[-0.0066 0.0076]	0.1345	0.8929
Trial number	3.96e-06	[-4.36e-06 1.23e-05]	0.9326	0.3510
Trial number x Detection				
Trial number x Detected	-4.84e-06	[-1.68e-05; 7.12e-06]	-0.7938	0.4273

**Table 4.3:** Effect size, confidence interval, *t*-values and corresponding *p*-values of the effect of stimulus properties on the frequency content of EEG data at 230ms (Cz) and 470ms (C4). In the theta-band, only the detection is significant at 230ms and 470ms (electrode Cz and C4, respectively).

In the theta-band at electrode Cz and C4, stimulus detection (D) is the only significant parameters ( $p < 0.05$ , at latencies 230ms and 470ms), while none of the other stimulus properties is significant at these latencies, as shown in Table 4.3.

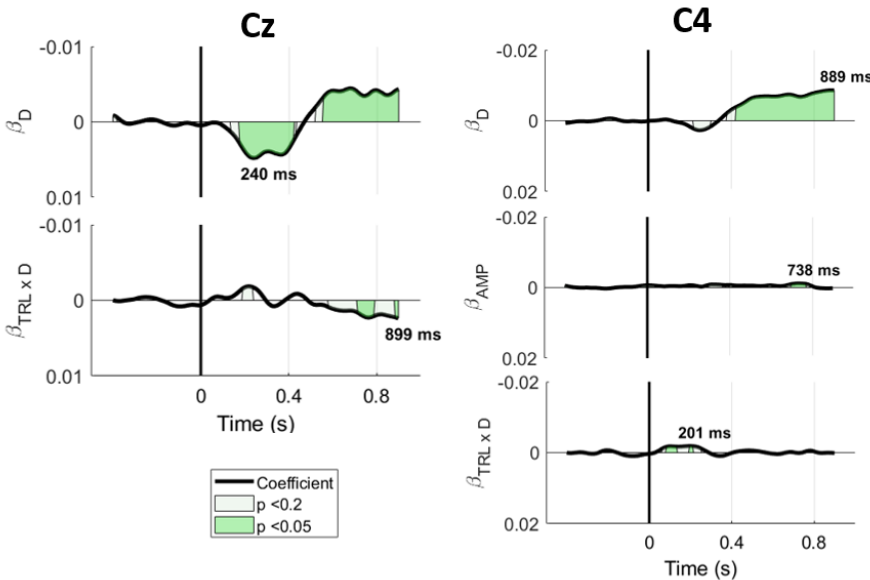


**Figure 4.7:** Significant effect of stimulus properties on theta-band of EEG frequency spectrum, computed using a LMM. The corresponding *t*-values are shown in green on a scale of 1.96 ( $p = 0.05$  with inf. DOF) to 3.29 ( $p = 0.001$  with inf. DOF). Left) At Cz, stimulus response (D) is most significant at 240ms after stimulus onset. Results from the LMM show significant effects of habituation (TRL  $\times$  D) at latency 899ms. Right) At electrode C4, stimulus response (D), amplitude of the first pulse (AMP) and habituation (TRL  $\times$  D) have significant negative effects at latencies 899ms, 738ms and 201ms, respectively.

Figure 4.7 shows the significant effect sizes and *t*-values over time at electrodes Cz and C4. At electrode Cz, the positive effect of detection starts at 200ms, lasting for several milliseconds, and is mostly concentrated at latency 240ms. A negative effect of detection is significant towards the end of the post-stimulus interval.

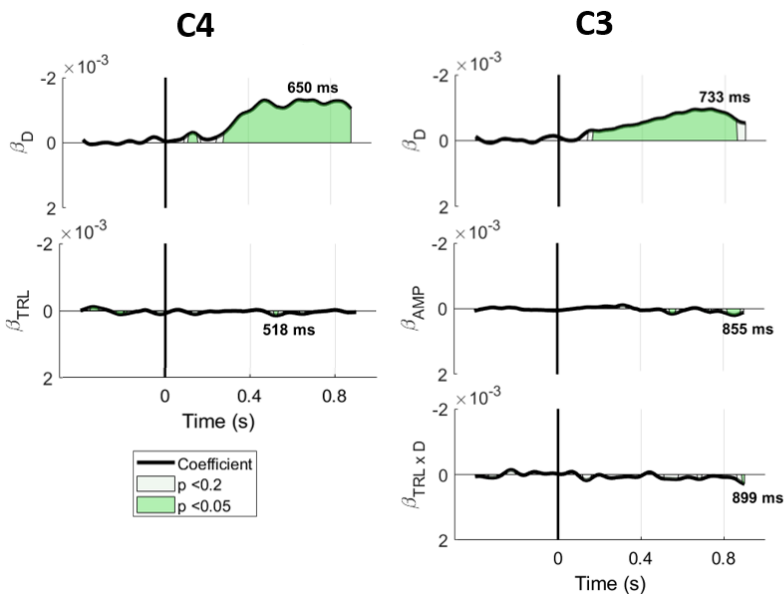
Moreover, there is an effect in the same time range as the pulse detection (D) with significant but opposite effect, consequence of the interaction between detection and trial number (TRL x D). At electrode C4, three significant effects are noticeable. Detection (D) has a negative effect towards the end of the post-stimulus interval with strongest significance at latency 899ms. At latency 738ms, the amplitude of the first pulse (AMP) has a significant negative effect. The interaction between trial number and detection (TRL x D) has a negative effect at electrode C4 and early latency (201ms after stimulus onset).

## Alpha-band

Coefficients	Effect size	95% Confidence Interval	C4: 470ms	
			<i>t</i>	<i>p</i>
(Intercept)	0.0001	[-4.58e-05 0.0002]	1.4172	0.1562
Detection (D)				
Detected	-0.0002	[-0.0005 -1.26e-05]	-2.0600	<b>0.0393</b>
Pulse 1 (PU1)	2.46e-05	[-0.0005 0.0005]	0.0866	0.9309
Pulse 2, 10ms IPI	0.0006	[-0.0006 0.0018]	0.9977	0.3184
Pulse 2, 40ms IPI	0.0001	[-0.0009 0.0012]	0.2102	0.8335
Trial number	4.13e-08	[-1.31e-06 1.39e-06]	0.0599	0.9522
Trial number x Detection				
Trial number x Detected	-7.91e-07	[-2.75e-06 1.16e-06]	-0.7933	0.4276
			C3: 470ms	
			<i>t</i>	<i>p</i>
(Intercept)	0.0002	[-0.00042; 0.0010]	0.8653	0.3967
Detection (D)				
Detected	-0.0006	[-0.0010 -0.0002]	-3.5387	<b>0.0016</b>
Pulse 1 (PU1)	0.0001	[-0.0004 0.0007]	0.5509	0.5820
Pulse 2, 10ms IPI	-0.0005	[-0.0016 0.0005]	-0.9899	0.3222
Pulse 2, 40ms IPI	-0.0001	[-0.0011 0.0009]	-0.2212	0.8249
Trial number	8.43e-07	[-2.56e-07 1.94e-06]	-0.2212	0.8249
Trial number x Detection				
Trial number x Detected	-5.63e-08	[-1.59e-06; 1.48e-06]	-0.0719	0.9426

**Table 4.4:** Effect size, confidence interval, *t*-values and corresponding *p*-values of the effect of stimulus properties on the frequency content of EEG data at 470ms (electrodes C4 and C3). In the alpha-band, only the detection is significant at 470ms.

In the alpha-band, C4 and C3 are the electrode showing the strongest ipsilateral and contralateral neuronal responses at latency 470ms. Stimulus detection is the only significant stimulus parameter ( $p < 0.05$ ), none of the other parameters are significant, as shown in Table 4.4.



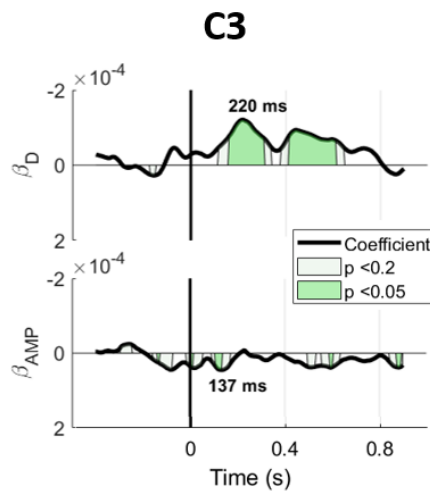
**Figure 4.8:** Significant effect of stimulus properties on alpha-band of EEG frequency spectrum, computed using a LMM. The corresponding *t*-values are shown in green on a scale of 1.96 ( $p = 0.05$  with inf. DOF) to 3.29 ( $p = 0.001$  with inf. DOF). Left) At C4, stimulus response (D) is most significant at 650ms after stimulus onset. Results from the LMM show significant effects of trial number (TRL) at latency 518ms. Right) At electrode C3, stimulus response (D), amplitude of the first pulse (AMP) and habituation (TRL x D) have significant effects at latencies 733ms (negative effect), 855ms (positive effect) and 899ms (positive effect), respectively.

Figure 4.8 shows the significant effect sizes and  $t$ -values over time in the alpha-band at C4 and C3. At electrode C4, negative effect of detection (D) has an early onset and lasts till the end of the post-stimulus interval, with most significant effect at latency 650ms. The LMM unveiled a small positive effect of trial number (TRL) at latency 518ms. Similarly, at electrode C3, detection (D) has a significant negative effect on the post-stimulus activity with maximum at latency 733ms. Two positive effects are present at electrode C3, the amplitude of the first pulse (AMP) has significant positive effect at latency 855ms and the interaction between trial number and detection (TRL  $\times$  D) has maximum significant effect at latency 899ms.

Beta-band				
Coefficients	Effect size	95% Confidence Interval	C3: 220ms	
			$t$	$p$
(Intercept)	6.37e-05	[-3.72e-05 0.0001]	1.2811	0.2084
Detection (D)				
Detected	-0.0001	[-0.0002 -2.61e-05]	-2.5016	<b>0.0123</b>
Pulse 1 (PU1)	-1.09e-05	[-0.0002 0.0002]	-0.0827	0.9341
Pulse 2, 10ms IPI	0.0005	[-0.0002 0.0014]	1.4519	0.1579
Pulse 2, 40ms IPI	0.0002	[-0.0001 0.0007]	1.1768	0.2394
Trial number	2.50e-07	[-2.73e-07 7.73e-07]	0.9365	0.3490
Trial number $\times$ Detection				
Trial number $\times$ Detected	-5.47e-07	[-1.29e-06 1.92e-07]	-1.4509	0.1468

**Table 4.5:** Effect size, confidence interval,  $t$ -values and corresponding  $p$ -values of the effect of stimulus properties on the frequency content of EEG data at 220ms (C3). In the beta-band, only stimulus detection (D) is significant.

In the beta-band, C3 is the electrode showing the strongest neuronal response at latency 220ms ( $p < 0.05$ ). Stimulus detection is the only significant effect, as shown in Table 4.5.



**Figure 4.9:** Significant effect of stimulus properties on beta-band of EEG frequency spectrum, computed using a LMM. The corresponding  $t$ -values are shown in green on a scale of 1.96 ( $p = 0.05$  with inf. DOF) to 3.29 ( $p = 0.001$  with inf. DOF). At C3, stimulus response (D) and amplitude of the first pulse (AMP) have a significant effect on the spectrum in the beta-band at 220ms and 137ms, respectively.

Figure 4.9 shows the significant effect sizes and  $t$ -values over time in the beta-band at electrode C3. Stimulus detection (D) has a significant negative effect for several millisecond after stimulus-onset with maximum at latency 220ms. Instead, the amplitude of the first pulse (AMP) has a significant positive effect mostly around 137ms.

### Gamma-band

Statistical analysis on gamma-band was divided into three subgroups. In the lower gamma-band, C4 is the electrode showing the strongest neuronal response at latency 350ms. C5 is strongest at latency 250ms and in the middle gamma-band, while the higher gamma-band shows strongest neuronal response at electrode CP4 and latency 450ms. None of the stimulus parameters has a significant effect on the lower, middle and higher gamma-band neuronal response at the selected latencies ( $p > 0.05$ ).

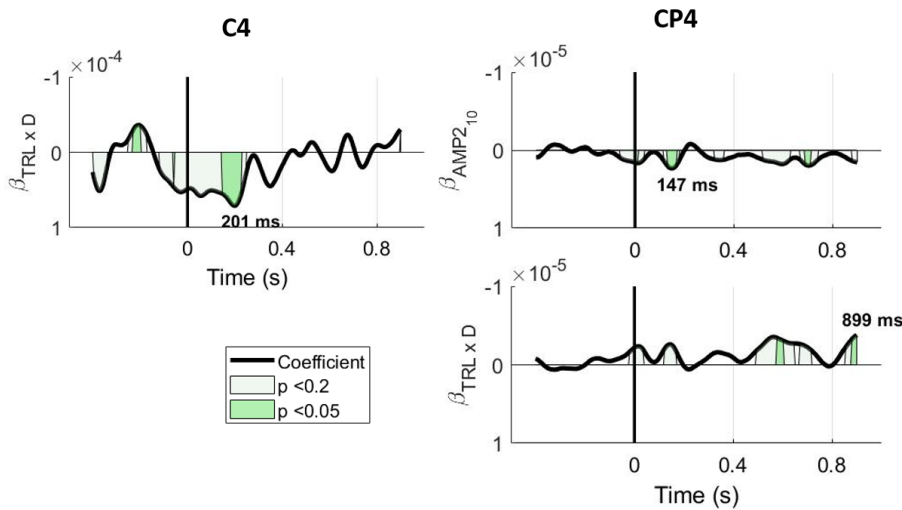


**Figure 4.10:** Significant effect of stimulus properties on gamma-band of EEG frequency spectrum, computed using a LMM. The corresponding  $t$ -values are shown in green on a scale of 1.96 ( $p = 0.05$  with inf. DOF) to 3.29 ( $p = 0.001$  with inf. DOF). At C4 (lower gamma-band), the interaction between trial number and detection (TRL  $\times$  D) has a significant effect after stimulus onset, with maximum effect at latency 210ms. At electrode CP4, amplitude of the second pulse (IPI 10ms) has a significant effect on early latencies after stimulus onset (147ms). A significant effect of interaction between trial number and detection (TRL  $\times$  D) is significant at later latencies, with maximum at 899ms.

Figure 4.10 depicts the significant effect sizes and  $t$ -values over time in the lower and higher gamma-band at electrode C4 and CP4, respectively. The LMM showed significant effect of amplitude of second pulse (IPI 10ms) at latency 147ms and electrode CP4. The interaction of trial number and detection (TRL  $\times$  D) is significant at both electrodes C4 and CP4. The LMM excluded the presence of any significant effect at electrode C5 and middle gamma-band ( $p > 0.05$ ).

### 4.2.3 Comparison analysis

The results from the LMM and time-frequency analysis on the UT dataset are tested for replicability on the St. Antonius dataset. The experimental procedure for the St. Antonius dataset is similar to the UT dataset and the same MTT-EP acquisition protocol was used in both datasets.

Single-trial TFRs, at corresponding electrodes and relative band powers, were extracted and selected for statistical analysis on the St. Antonius dataset. Due the exploratory nature of the first investigation, a second and equivalent statistical analysis was conducted on the St. Antonius dataset, exception made for the role of handedness (HAND).

Results from the LMM are shown in Tables 4.6-4.8.

## Theta-band

Coefficients	Effect size	95% Confidence Interval	Cz: 240ms	
			<i>t</i>	<i>p</i>
(Intercept)	-0.0002	[-0.0007 0.0002]	-0.8912	0.3861
Detection (D)				
Detected	0.0003	[-5.24e-05 0.0007]	1.8452	0.0824
Hand	9.23e-05	[-0.0005 0.0007]	0.3089	0.7613
Pulse 1 (PU1)	-9.01e-05	[-0.0008 0.0006]	-0.2368	0.8128
Pulse 2, 10ms IPI	0.0010	[-0.0001 0.0022]	1.7897	0.0901
Pulse 2, 40ms IPI	0.0001	[-0.0006 0.0009]	0.3061	0.7595
Trial number	-5.15e-07	[-2.37e-06 1.34e-06]	-0.5827	0.5670
Trial number x Detection				
Trial number x Detected	-2.38e-06	[-5.93e-06 1.18e-06]	-1.4122	0.1763
			C4: 470ms	
			<i>t</i>	<i>p</i>
(Intercept)	-0.0001	[-0.0003 9.50e-05]	-1.1478	0.2674
Detection (D)				
Detected	7.86e-05	[-0.0001 0.0003]	0.6199	0.5435
Hand	0.0001	[-0.0002 0.0005]	0.9260	0.3682
Pulse 1 (PU1)	0.0003	[-0.0001 0.0007]	1.4463	0.1489
Pulse 2, 10ms IPI	-0.0001	[-0.0007 0.0005]	-0.3567	0.7239
Pulse 2, 40ms IPI	-0.0003	[-0.0007 0.0001]	-1.3223	0.1861
Trial number	-3.00e-07	[-1.00e-06 4.04e-07]	-0.8522	0.3973
Trial number x Detection				
Trial number x Detected	-8.18e-07	[-1.70e-06 6.85e-08]	-1.8087	0.0705

**Table 4.6:** Effect size, confidence interval, *t*-values and corresponding *p*-values of the effect of stimulus properties on the frequency content of EEG data at 240ms (Cz) and 470ms (C4). In the theta-band of the St. Antonius dataset, none of stimulus parameters is significant.

In the theta-band at electrodes Cz (latency 240ms) and C4 (latency 470ms), none of stimulus parameters is significant.

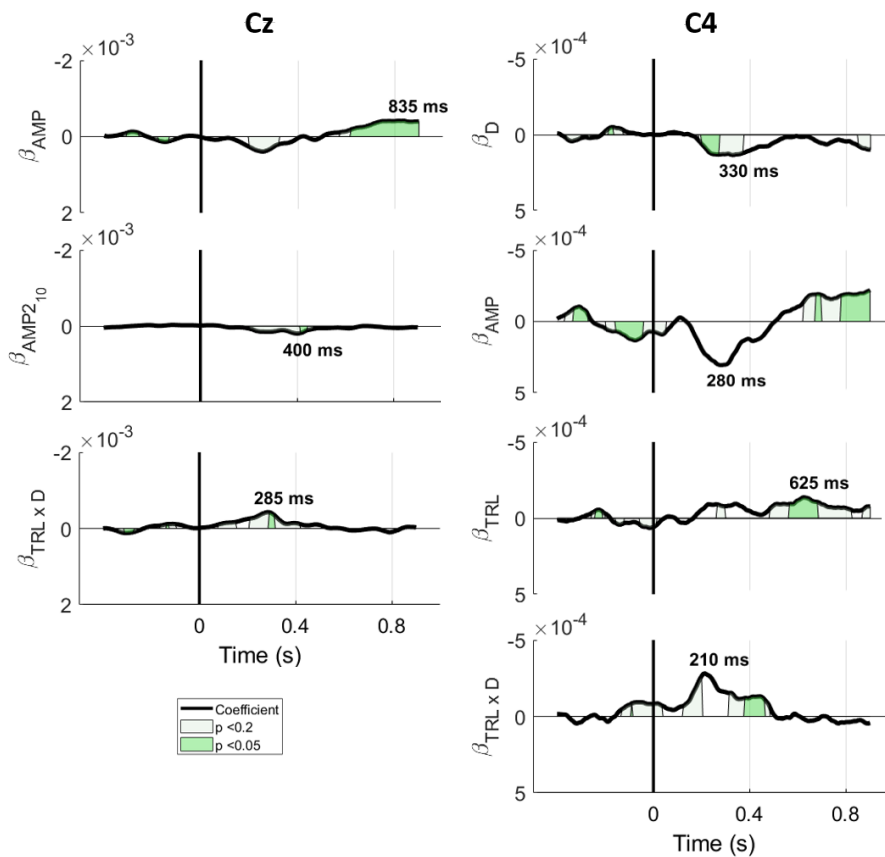


**Figure 4.11:** Significant effect of stimulus properties on theta-band of EEG frequency spectrum, computed using a LMM. The corresponding *t*-values are shown in green on a scale of 1.96 ( $p = 0.05$  with inf. DOF) to 3.29 ( $p = 0.001$  with inf. DOF). Left) At Cz, stimulus amplitude of the first and second pulse (IPI 10ms) are most significant at 835ms and 400ms, respectively. Results from the LMM show significant effects of habituation (TRL  $\times$  D) at latency 285ms. Right) At electrode C4, stimulus response (D) and amplitude of the first pulse (AMP) have significant positive effects at latencies 330ms, 280ms, respectively. Trial number (TRL) and the effect of interaction between trial number and detection (TRL  $\times$  D) are significant with largest effects at 625ms and 210ms.

Figure 4.11 shows the significant effect sizes and *t*-values over time at electrodes Cz

and C4. For Cz, the amplitude of the stimulus has negative effect on late components of the oscillations, with most significant effect at 835ms after stimulus onset. At 400ms, the amplitude of the second pulse (IPI 10ms) has a significant positive effect. Effect of habituation at Cz is negative and most significant at 285ms. At electrode C4, detection (D) and amplitude (AMP) of the first pulse have significant effects with main effect at 330ms and 280ms after stimulus onset, respectively. Trial number (TRL) and the effect of interaction between trial number and detection (TRL x D) have significant negative effects at 625ms and 210ms, respectively.

### Alpha-band

Coefficients	Effect size	95% Confidence Interval	C4: 470ms	
			<i>t</i>	<i>p</i>
(Intercept)	8.06e-05	[1.97e-05 0.0001]	2.5929	0.0095
Detection (D)				
Detected	-0.0001	[-0.0002 7.46e-06]	-1.9790	0.0623
Hand	-3.68e-05	[-0.0001 6.36e-05]	-0.7562	0.4567
Pulse 1 (PU1)	4.19e-05	[-0.0001 0.0002]	0.4119	0.6804
Pulse 2, 10ms IPI	-2.27e-05	[-0.0003 0.0002]	-0.1479	0.8824
Pulse 2, 40ms IPI	1.21e-05	[-0.0002 0.0002]	0.0874	0.9303
Trial number	-2.70e-07	[-1.32e-07 6.72e-07]	1.3175	0.1876
Trial number x Detection				
Trial number x Detected	-1.65e-07	[-7.69e-07 4.39e-07]	-0.5475	0.5862
C3: 470ms				
(Intercept)	3.67e-05	[-3.84e-05 0.0001]	1.0346	0.3161
Detection (D)				
Detected	-9.44e-05	[-0.0001 -4.06e-06]	-2.1935	<b>0.0414</b>
Hand	1.66e-05	[-8.19e-05 0.0001]	0.3608	0.7233
Pulse 1 (PU1)	3.10e-05	[-0.0001 0.0002]	0.3612	0.7183
Pulse 2, 10ms IPI	1.88e-05	[-0.0002 0.0002]	0.1647	0.8691
Pulse 2, 40ms IPI	3.48e-05	[-0.0002 0.0002]	0.3173	0.7601
Trial number	6.64e-08	[-2.48e-07 3.81e-07]	0.4235	0.6736
Trial number x Detection				
Trial number x Detected	9.85e-08	[-2.88e-07 4.85e-07]	0.5000	0.6170

**Table 4.7:** Effect size, confidence interval, *t*-values and corresponding *p*-values of the effect of stimulus properties on the frequency content of EEG data at 470ms (C3 and C4). In the alpha-band of the St. Antonius dataset, only detection (D) is significant at electrode C3.

The alpha-band frequency content of electrodes C3 and C4 is investigated at latency 470ms, Table 4.7. Results from the LMM model show significant effect of detection (D) only at electrode C3. None of the other stimulus parameters has significant effect at electrodes C3 and C4.

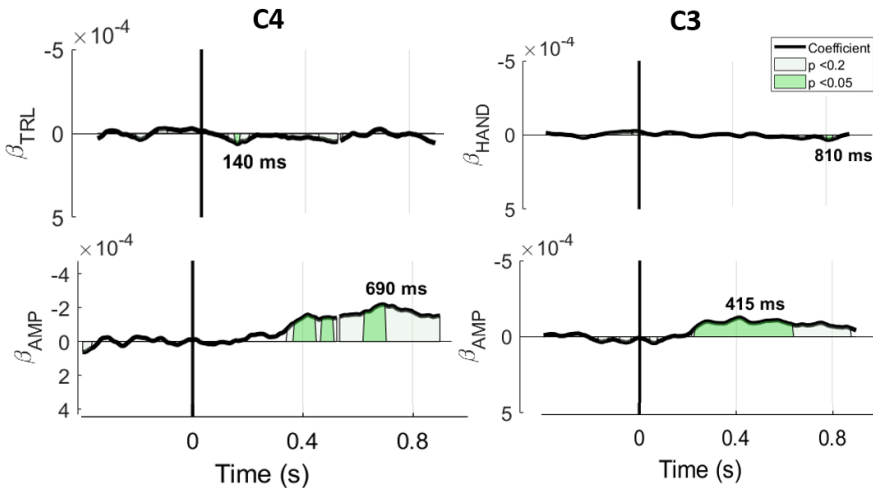


**Figure 4.12:** Significant effect of stimulus properties on alpha-band of EEG frequency spectrum, computed using a LMM. The corresponding *t*-values are shown in green on a scale of 1.96 ( $p = 0.05$  with inf. DOF) to 3.29 ( $p = 0.001$  with inf. DOF). At C4 and C3, stimulus amplitude of the first pulse (AMP) is significant after stimulus onset, with maximum negative effect at 690ms and 415ms, respectively. Left) Results from the LMM show significant effects of trial number (TRL) at electrode C4 and latency 140ms. Right) At electrode C3, the position of stimulation on either dominant or non-dominant hand has a significant effect (HAND) at later latencies of the stimulus onset, with most significance at latency 810ms.

Figure 4.12 shows the significant effect sizes and t-values over time at alpha-band frequencies and electrodes C3 and C4. Stimulus amplitude has a significant negative effect on both ipsilateral (C4) and contralateral (C3) regions with strongest effect at latencies 690ms and 415ms, respectively.

At electrode C4, the number of trials has a significant effect at early latency 140ms after stimulus onset. At 810ms and electrode C3, the position of the stimulation, either on the dominant or non-dominant hand, has a significant positive effect.

Beta-band

Coefficients	Effect size	95% Confidence Interval	C3: 220ms	
			<i>t</i>	<i>p</i>
(Intercept)	-1.67e-07	[-2.40e-05 2.37e-05]	-0.0137	0.9890
Detection (D)				
Detected	-2.18e-05	[-6.69e-05 2.33e-05]	-1.0054	0.3262
Hand	3.28e-06	[-2.31e-05 2.96e-05]	0.2437	0.8074
Pulse 1 (PU1)	-8.15e-05	[-0.0002 9.59e-05]	-0.9932	0.3388
Pulse 2, 10ms IPI	-4.79e-05	[-0.0001 5.92e-05]	-0.8763	0.3808
Pulse 2, 40ms IPI	-1.78e-05	[-0.0001 8.06e-05]	-0.3542	0.7231
Trial number	-3.67e-08	[-1.80e-07 1.07e-07]	-0.5018	0.6157
Trial number x Detection				
Trial number x Detected	1.38e-07	[-6.06e-08 3.37e-07]	1.3634	0.1727

**Table 4.8:** Effect size, confidence interval, *t*-values and corresponding *p*-values of the effect of stimulus properties on the frequency content of EEG data at 220ms and electrode C3. In the beta-band of the St. Antonius dataset, none of the stimulus parameters has significant effects at 220ms and electrode C3.

Results from the LMM in the beta-band at electrode C3 and latency 220ms are shown in Table 4.8. None of the stimulus parameters has significant effect on the St. Antonius dataset.

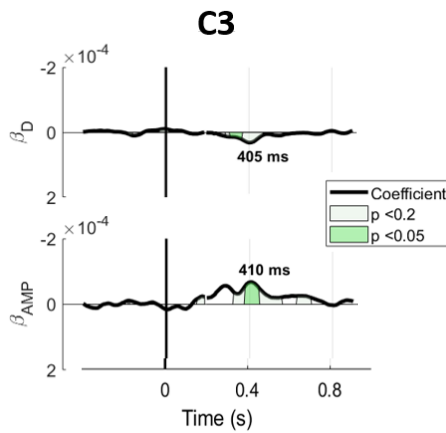
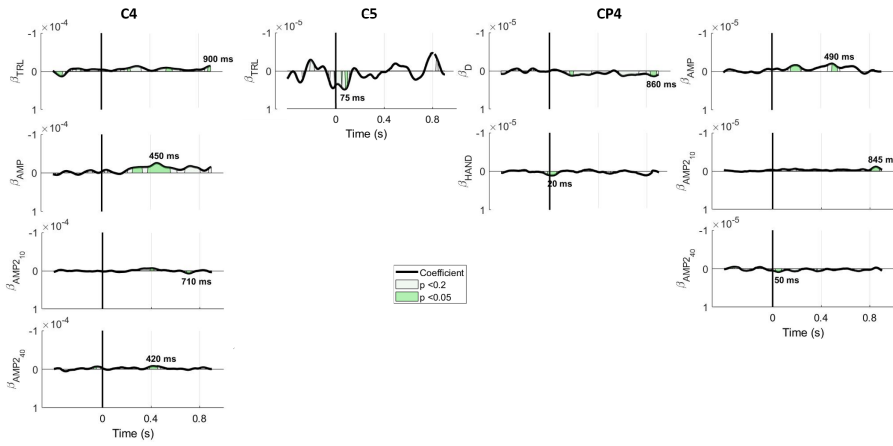


**Figure 4.13:** Significant effect of stimulus properties on beta-band of EEG frequency spectrum, computed using a LMM. The corresponding *t*-values are shown in green on a scale of 1.96 ( $p = 0.05$  with inf. DOF) to 3.29 ( $p = 0.001$  with inf. DOF). At C3, stimulus detection (D) and amplitude of the first pulse (AMP) are significant after stimulus onset, with maximum positive effect at 405ms and maximum negative effect at 410ms, respectively.

Figure 4.13 is a representation of significant effect sizes and *t*-values over time in the beta-band at electrode C3. In the beta-band, stimulus detection (D) and amplitude of the first pulse (AMP) have significant effect around latency 400ms after stimulus onset.

### Gamma-band

Results of the LMM on the gamma-band contents of the St. Antonius dataset showed no significant effects at the selected latencies.



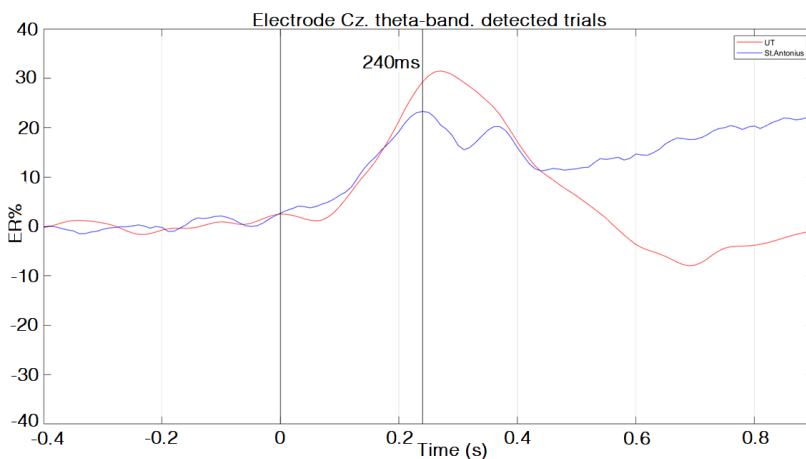
**Figure 4.14:** Significant effect of stimulus properties on gamma-band of EEG frequency spectrum, computed using a LMM. The corresponding t-values are shown in green on a scale of 1.96 ( $p = 0.05$  with inf. DOF) to 3.29 ( $p = 0.001$  with inf. DOF). At electrode C4 and CP4, trial number (TRL) and stimulus amplitudes (AMP) of both single and double pulses have significant effects. CP4 is also significantly modulated by stimulus detection (D) and handedness (HAND). At electrode C5, trial number has the only significant effect, with maximum effect at latency 75ms.

Figure 4.14 shows the significant effect sizes and t-values over time in the gamma-band at C4, C5 and CP4 (lower, middle and higher gamma-band, respectively). At electrode C4, stimulus amplitudes of both single and double pulses have significant effects at latencies 450ms (single pulse), 710ms (IPI 10ms) and 420ms (IPI 40ms). Trial number (TRL) has the most significant and negative effect at 900ms after stimulus onset.

At electrode C5, trial number (TRL) is the only significant effect, with maximum effect at latency 75ms. CP4 is the only electrode in the gamma-band being actively modulated by handedness (HAND) and stimulus detection (D) at latency 860ms and 20ms, respectively. Similarly to electrode C4, CP4 is modulated by stimulus amplitudes of both single and double pulses.

### Butterfly plots

Difference in oscillation patterns can be consequence of different activation latencies. The butterfly plot shows the differences between the UT and St. Antonius datasets. The percentage signal change at electrode Cz, electrode with strongest neuronal response in the theta-band, is displayed as a function of time in Figure 4.15.



**Figure 4.15:** Butterfly plot showing the differences between the percentage signal change extracted at electrode Cz and theta-band. Red) percentage signal change in theta-band at electrode Cz extracted from grand averages of the UT dataset. Blue) St. Antonius dataset. The displayed latency (240ms) is the result of the LMM on the UT dataset and showed the strongest significant effect for detection.

At latency 240ms, theta-band shows a positive percentage signal change. As shown in Figure 4.15, the percentage change in theta-band of the St. Antonius dataset is lower than the UT dataset. At later latencies, theta-band from the UT dataset has a negative change as opposed to the consistent increase in the St. Antonius dataset.

The percentage signal changes at electrodes C4 and C3 in the alpha-band are displayed as a function of time in Figure 4.16 and Figure 4.17, respectively.

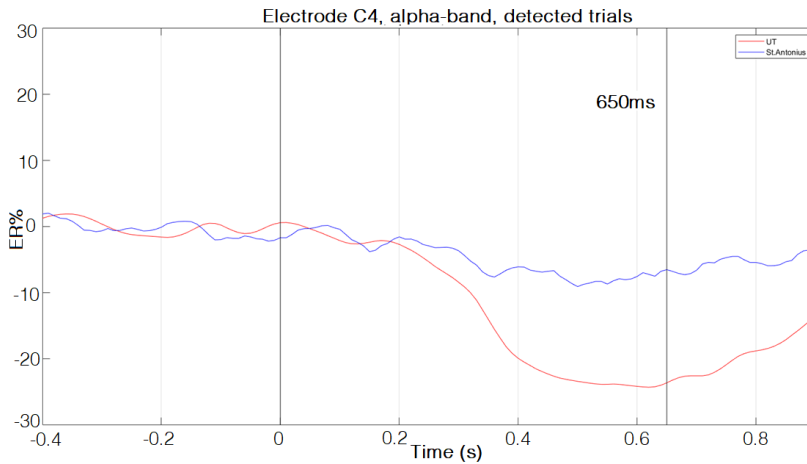


**Figure 4.16:** Butterfly plot showing the differences between the percentage signal change extracted at electrode C4 and alpha-band. Red) percentage signal change in alpha-band at electrode C4 extracted from grand averages of the UT dataset. Blue) St. Antonius dataset. The displayed latency (650ms) is the result of the LMM on the UT dataset and showed the strongest significant effects for detection and trial number.

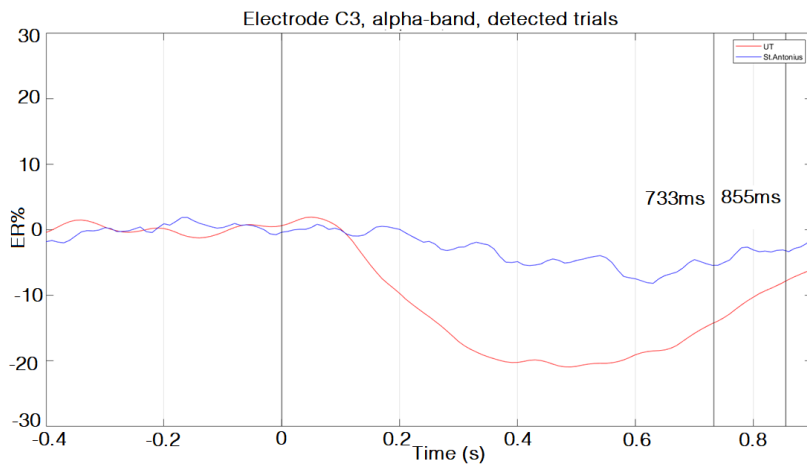


**Figure 4.17:** Butterfly plot showing the differences between the percentage signal change extracted at electrode C3 and alpha-band. Red) percentage signal change in alpha-band at electrode C3 extracted from grand averages of the UT dataset. Blue) St. Antonius dataset. The displayed latencies (733ms and 855ms) are the result of the LMM on the UT dataset and showed the strongest significant effects for detection and amplitude.

In the alpha-band, electrodes C4 and C3 shows a strongest deactivation in the UT dataset with respect to the St. Antonius dataset.

At electrode C3, the percentage signal change in the beta-band is displayed as a function of time in Figure 4.18.

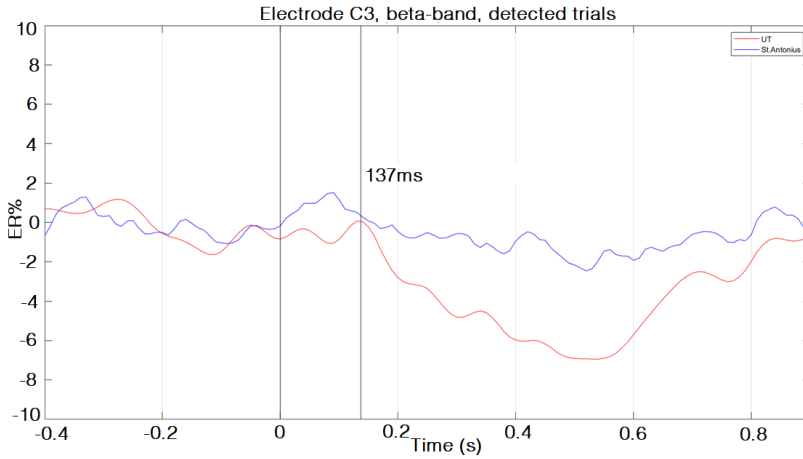


**Figure 4.18:** Butterfly plot showing the differences between the percentage signal change extracted at electrode C3 and beta-band. Red) percentage signal change in beta-band at electrode C3 extracted from grand averages of the UT dataset. Blue) St. Antonius dataset. The displayed latency (137ms) is the result of the LMM on the UT dataset and showed the strongest significant effects for detection and amplitude.

At latency 137ms where the LMM showed strongest significant effect, beta-band percentage signal change is comparable between the UT and St. Antonius dataset. However, the butterfly plot shows significant differences in beta-band responses at late latencies after stimulus onset.

#### Amplitude and SNR values

For each electrode and latency, the percentage signal change and SNR values were computed and compared between the two datasets, as shown in Table 4.9.

Theta-band: 230ms	Amplitude		SNR	
	<i>St. Antonius</i>	<i>UT</i>	<i>St. Antonius</i>	<i>UT</i>
Cz	22.65	27.65	23.76	28.36
FCz	23.52	24.09	21.61	22.55
Theta-band: 470 ms				
C4	13.46	-8.91	6.74	11.35
CP4	13.34	2.82	7.73	1.55
C3	6.98	-7.89	3.45	6.07
Alpha-band: 470 ms				
C4	-7.80	-22.85	6.50	20.17
CP4	-3.99	-14.67	2.74	9.76
C3	-4.86	-20.75	4.61	28.38
Beta-band: 220ms				
C3	-0.77	-3.13	1.20	3.58
Lower gamma-band: 350ms				
C4	0.82	-3.06	1.47	5.46
CP4	-0.11	-2.32	0.22	3.95
Middle gamma-band: 250ms				
C5	4.65	-2.99	4.64	1.96
Higher gamma-band: 450ms				
C4	3.38	-1.23	3.18	2.51
CP4	4.70	-3.29	5.02	3.69

**Table 4.9:** Grand average TFRs at latencies and electrodes with strongest neuronal responses, as selected from the scalp distribution of the UT dataset. The respective SNR is computed.

The group average of the TFRs from the St. Antonius dataset show relevant differences with respect to the UT dataset. As confirmed by previous results, at electrode Cz, the theta-band power amplitude has comparable amplitudes

and SNR values. At electrode C4, theta-band amplitudes of the St. Antonius dataset are opposite to the UT dataset. Alpha- and beta-band oscillations of the St. Antonius dataset have considerably smaller amplitudes and SNR values with respect to the UT dataset. In general, the St. Antonius dataset is characterised by positive amplitudes in the lower, middle and higher gamma-bands, opposite to the deactivations of the UT dataset.

### Scalp topographies

Results from the butterfly plots and the TFRs at selected electrodes showed significant differences of percentage signal changes between the two datasets. According to these results, a visual inspection of scalp topography is performed in order to exclude differences in scalp distribution of the neuronal oscillations, as shown in Figures 4.19, 4.20, 4.21 and 4.22.

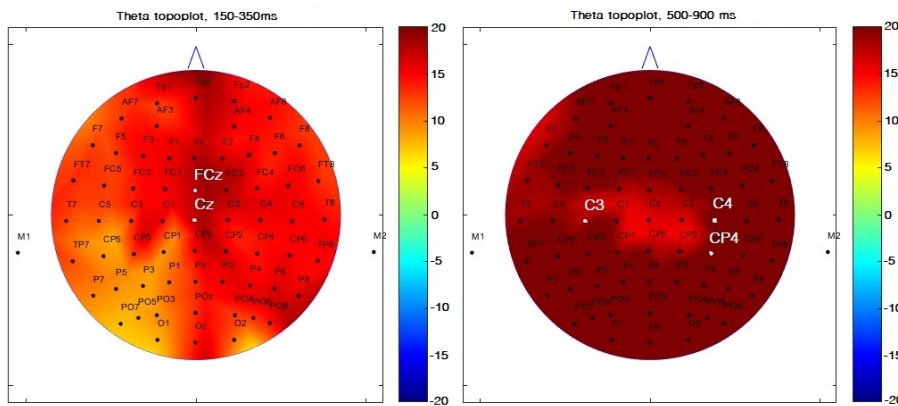


**Figure 4.19:** Scalp topography of theta-band neuronal response at selected latencies for the St. Antonius dataset. Left) scalp topography from between 150ms-350ms. Right) scalp topography at 500ms-900ms. The electrodes selected for the UT dataset are depicted in white. The activation patterns in the St. Antonius dataset are significantly different from the UT dataset.

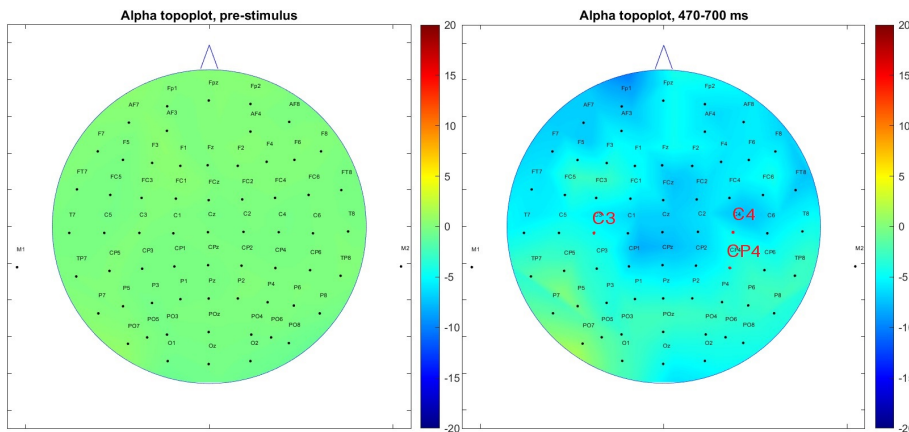


**Figure 4.20:** Scalp topography of alpha-band neuronal response at selected latencies between 470ms and 700ms. Left) scalp topography from the pre-stimulus activity. Right) scalp topography from the St. Antonius dataset. The electrodes selected for the UT dataset are depicted in red. There is a weak ipsilateral response around channel C4, while there is no contralateral activation at electrode C3.

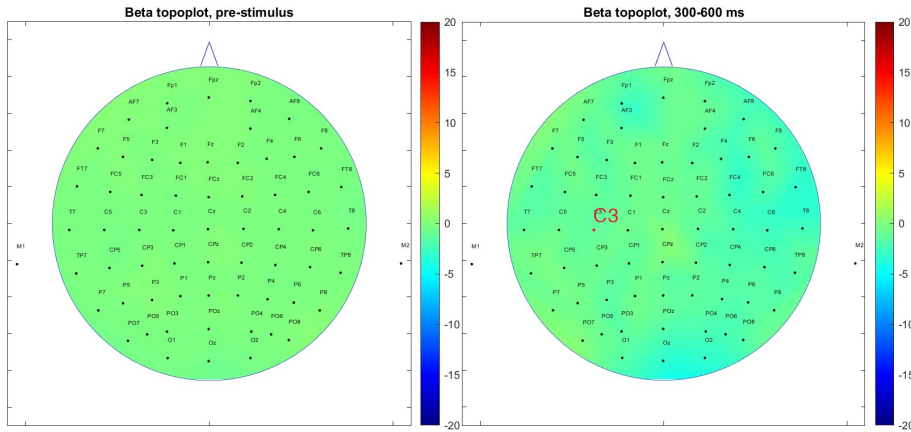


**Figure 4.21:** Scalp topography of beta-band neuronal response at selected latencies between 300ms and 600ms. Left) scalp topography from the pre-stimulus interval. Right) scalp topography from the St. Antonius dataset. The electrodes selected for the UT dataset are depicted in red.

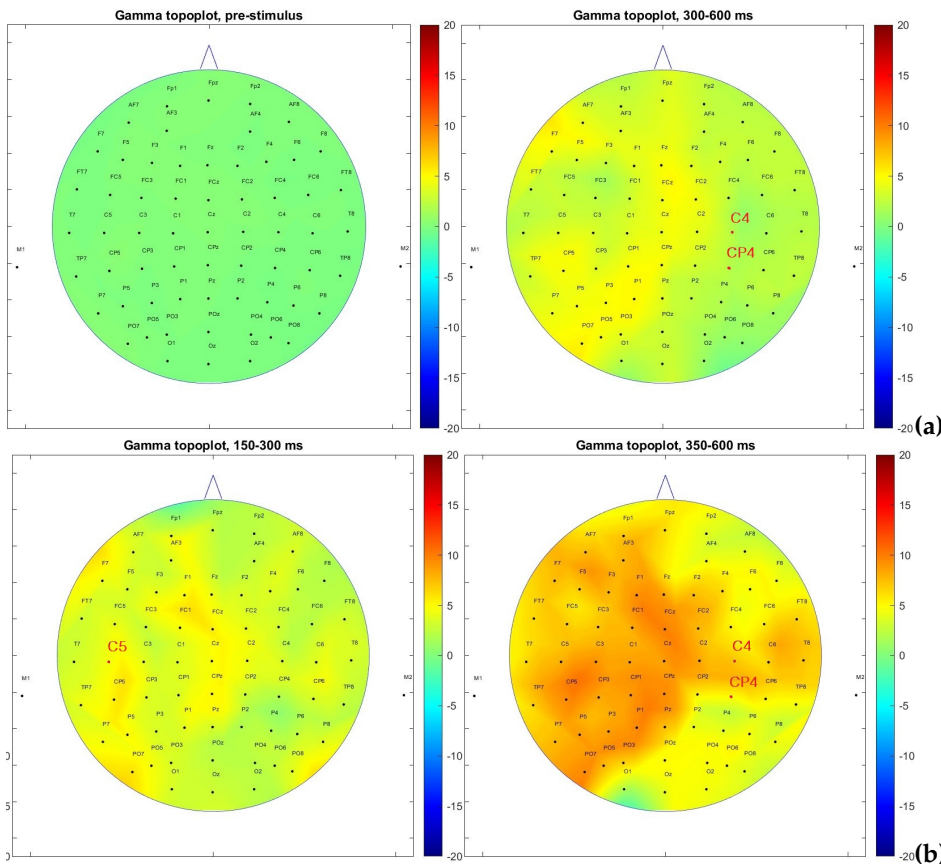


**Figure 4.22:** Scalp topography of gamma-band neuronal response at selected latencies from the St. Antonius dataset. The electrodes selected for the UT dataset are depicted in red.

In the above figures, electrodes selected for the statistical analysis of the UT dataset are depicted in either white (Figure 4.19) or red (Figures 4.20, 4.21 and 4.22).

Central activation in the theta-band is confirmed for the St. Antonius dataset at latencies between 150ms-300ms. However, the contralateral and ipsilateral theta-band deactivation at latencies 400ms-900ms present in the UT dataset is, instead, a neuronal activation in the St. Antonius dataset.

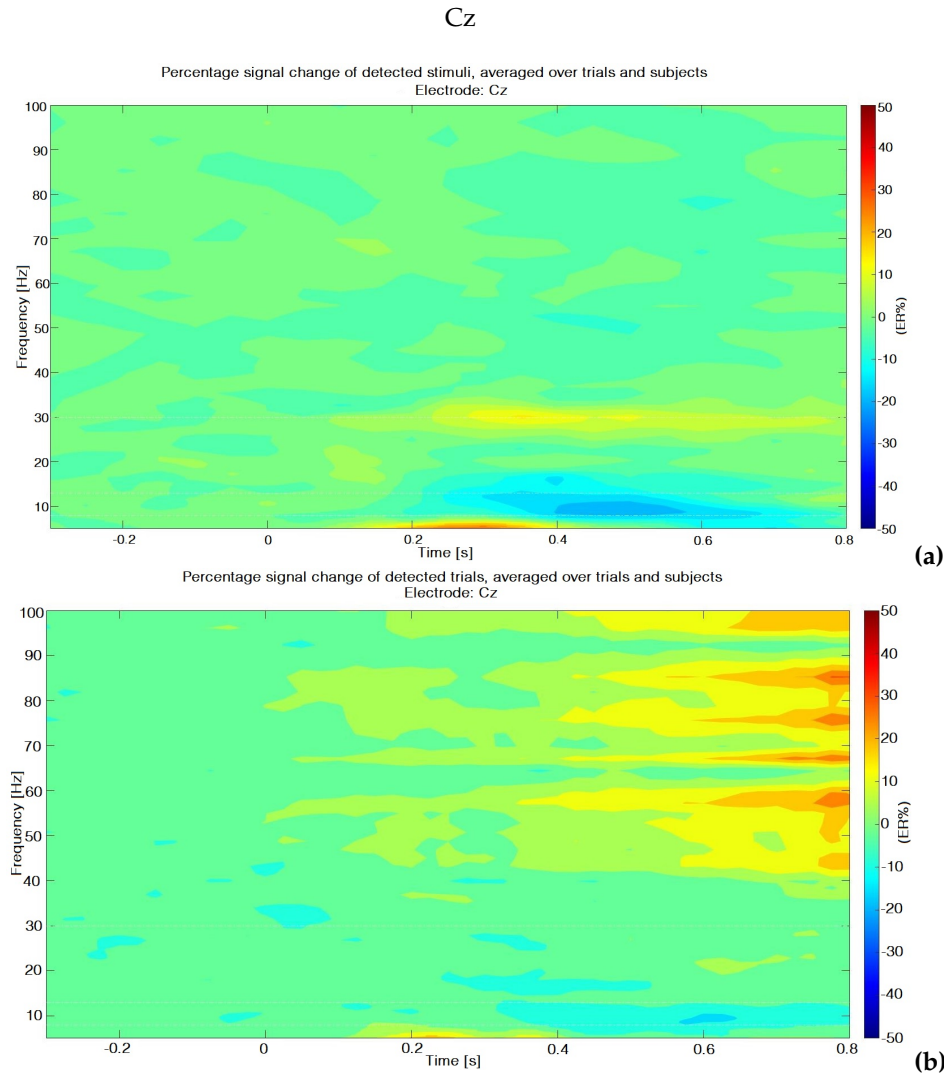
Alpha-band suppressions are mostly present at central and ipsilateral regions in the St. Antonius dataset, while there is little or none deactivation at contralateral electrodes such as electrode C3.

Beta-band power is small or completely absent in the St. Antonius dataset, while gamma-band oscillations are characterized by activation patterns. Gamma-band activations of the St. Antonius dataset are opposite to the neuronal deactivations of the UT dataset.

## Grand average of TFRs

Grand averages of TFRs at selected electrodes are displayed in a time-frequency plot as percentage signal changes with respect to the baseline interval.

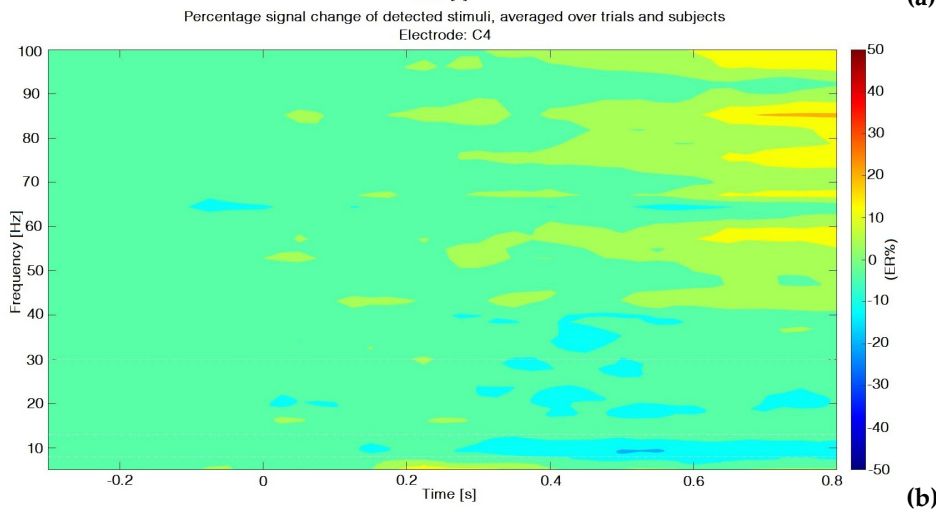
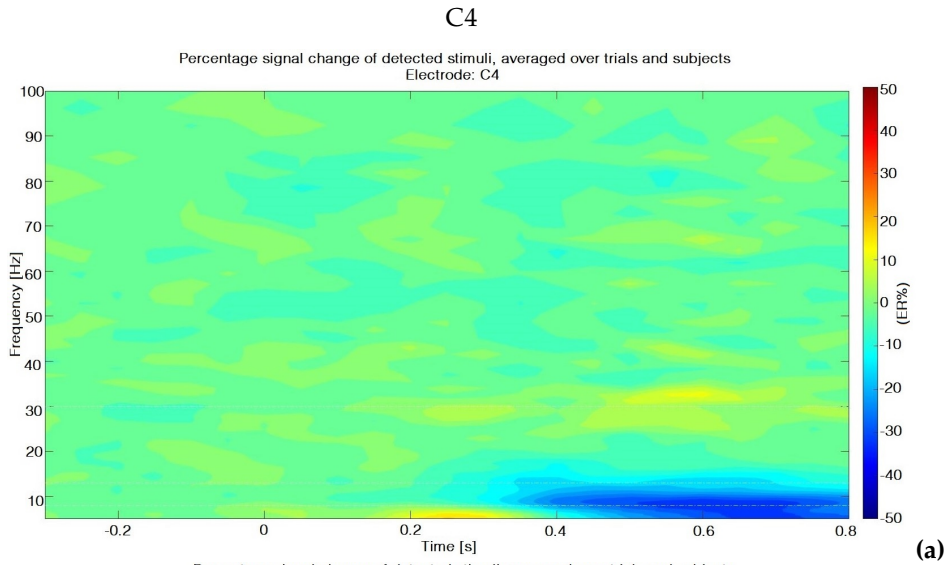
In Figure 4.23, the grand average of TFRs at electrode Cz from the UT (top) and St. Antonius datasets (bottom) are depicted.



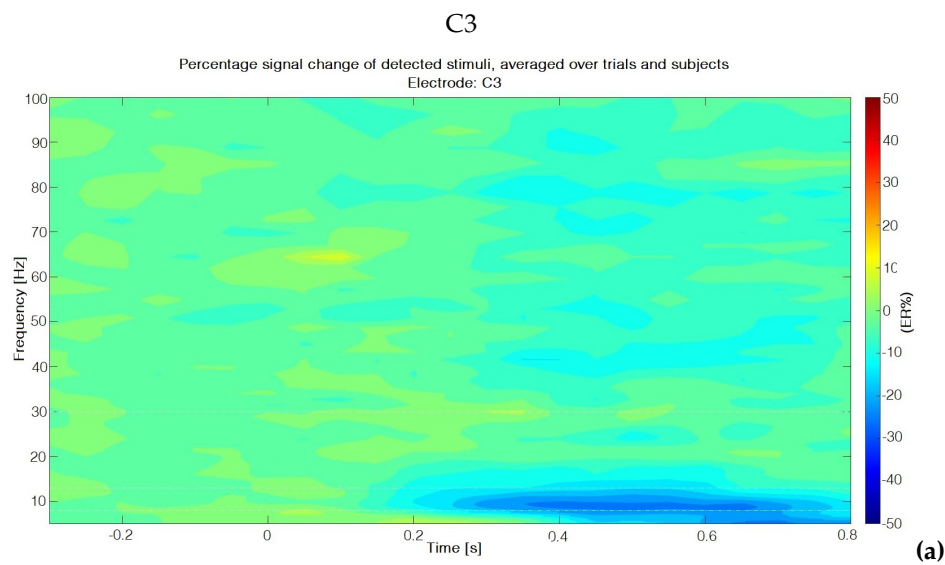
**Figure 4.23:** TFR of neuronal response to detected stimuli at electrode Cz represented as percentage signal change with respect to pre-stimulus baseline (-400 to -100 ms). The TFR in figure is the result of group averaging over detected trials and healthy subjects. a) TFR at Cz from the UT dataset. b) TFR at Cz from the St. Antonius dataset.

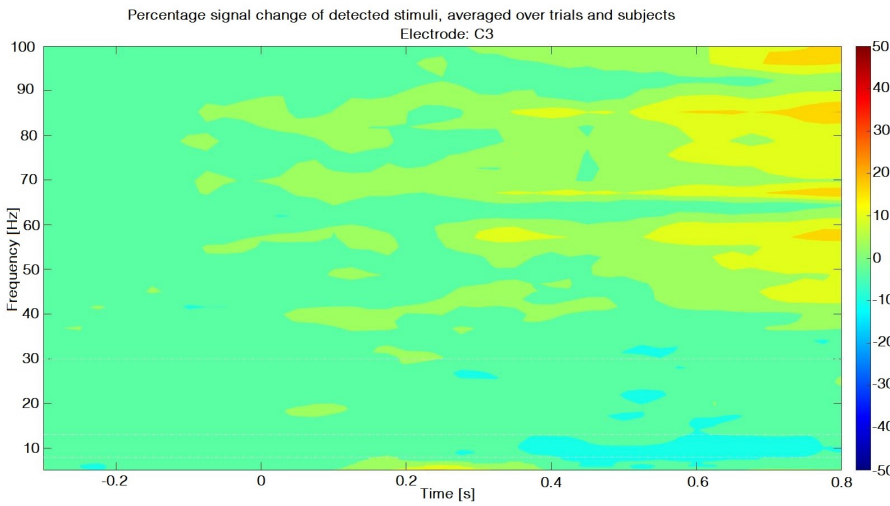
At electrode Cz, theta-band activation is present in both UT and St. Antonius dataset at latencies between 200ms and 350ms.

The relative power at other frequency bands (Figure 4.24-Figure 4.26) show considerable differences between the two datasets.

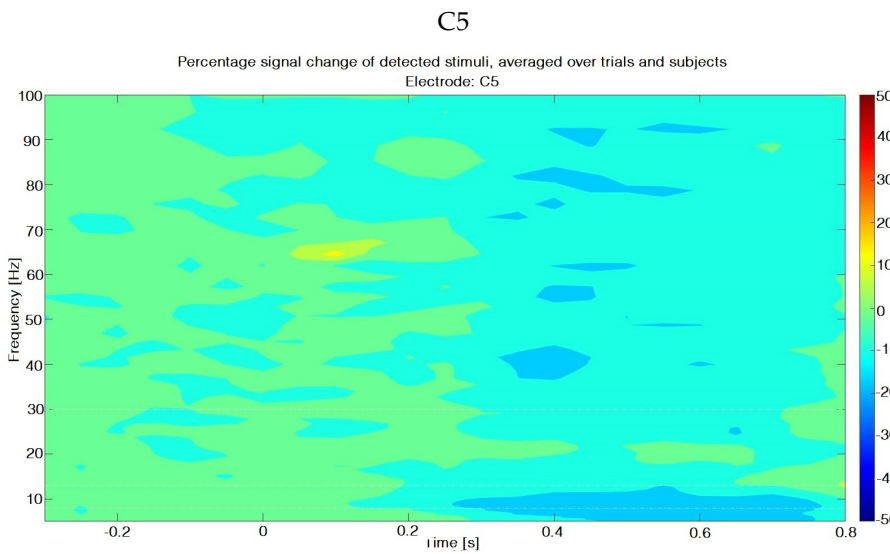


**Figure 4.24:** a) TFR at C4 from the UT dataset. b) TFR at C4 from the St. Antonius dataset.

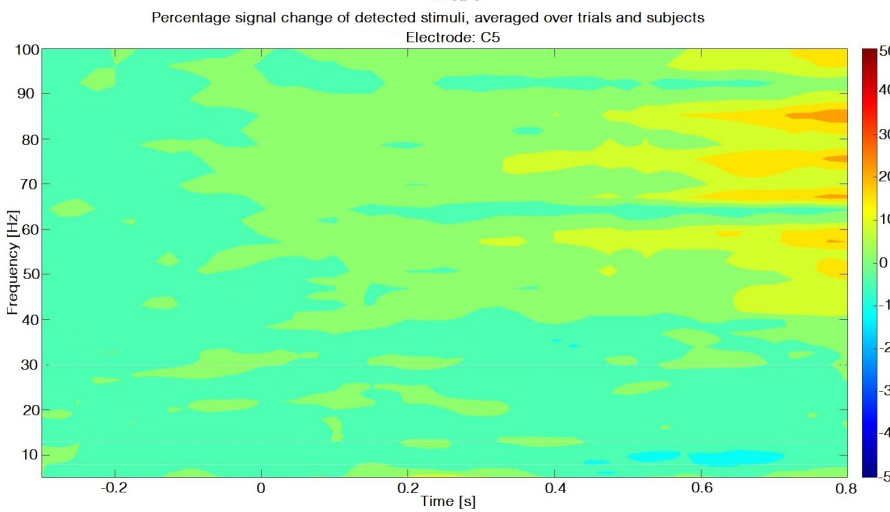




**(b)** Figure 4.25: a) TFR at C3 from the UT dataset. b) TFR at C3 from the St. Antonius dataset.



**(a)**



**(b)**

Figure 4.26: a) TFR at C5 from the UT dataset. b) TFR at C5 from the St. Antonius dataset.

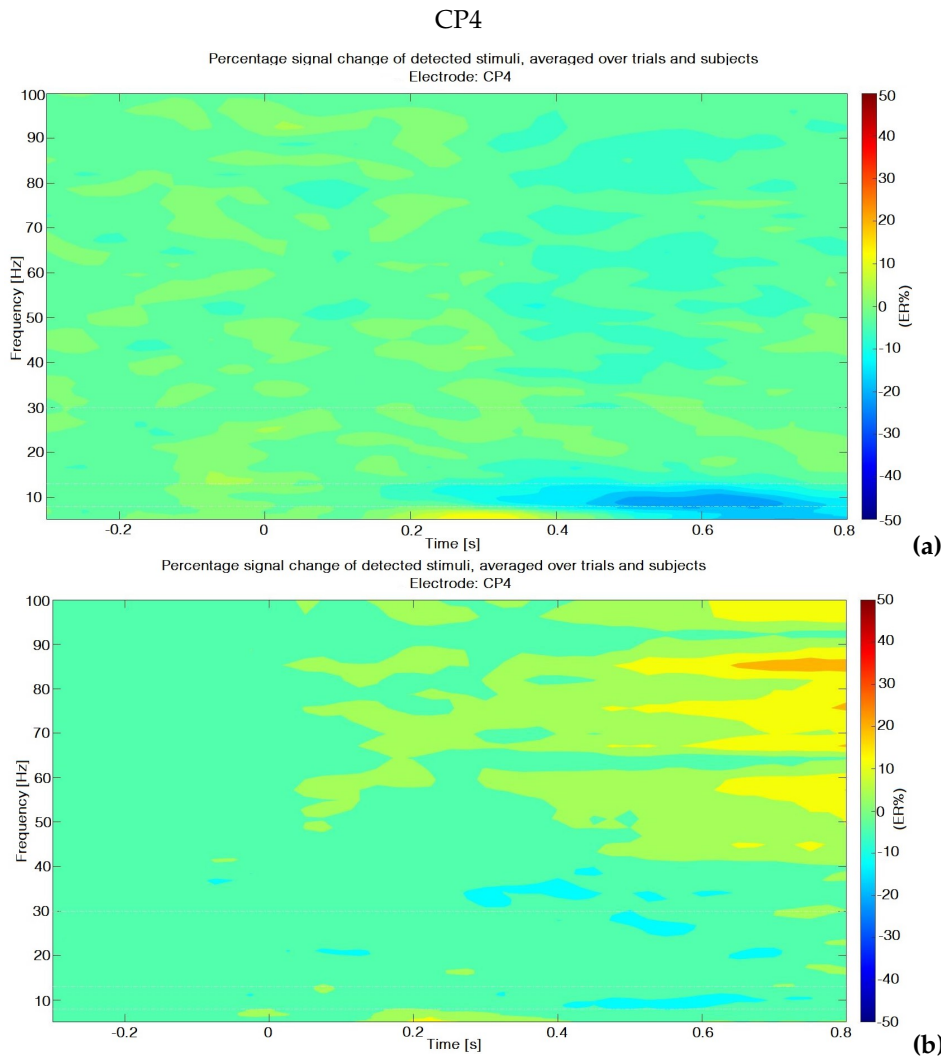


**Figure 4.27:** a) TFR at CP4 from the UT dataset. b) TFR at CP4 from the St. Antonius dataset.

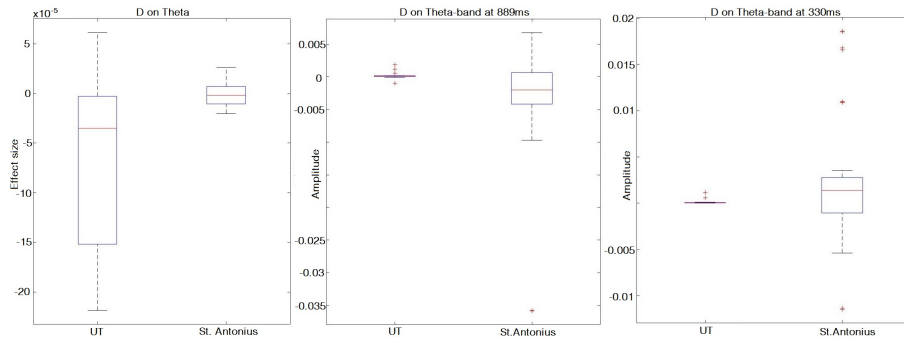
Grand average of TFRs at selected channels are depicted above with the aim of detecting similarities and/or discrepancies between the UT and St. Antonius datasets.

At electrode Cz, theta-band activation is present both in the St. Antonius and UT dataset. Alpha-band suppression is less pronounced at both contralateral and ipsilateral regions in the St. Antonius dataset. At electrode C4, the deactivation in the alpha-band is more localized around latency 500ms in the St. Antonius dataset. The low-gamma band activation for the UT dataset at latency 600ms is not present in the St. Antonius dataset, while there is a late gamma-band activation after latency 600ms and at frequencies above 60Hz at electrode C4 and in the St. Antonius dataset. The gamma-band suppressions of the UT dataset at electrode C5 are absent in the St. Antonius dataset; they are replaced instead by a late gamma-band activation (at latency 400ms). At electrode CP4, the gamma-band suppression of the UT dataset is small, while it is replaced by a late gamma-band activation in the St. Antonius dataset at latencies 600ms-900ms after stimulus onset and at frequencies 80-90Hz.

### Effect sizes on individual level

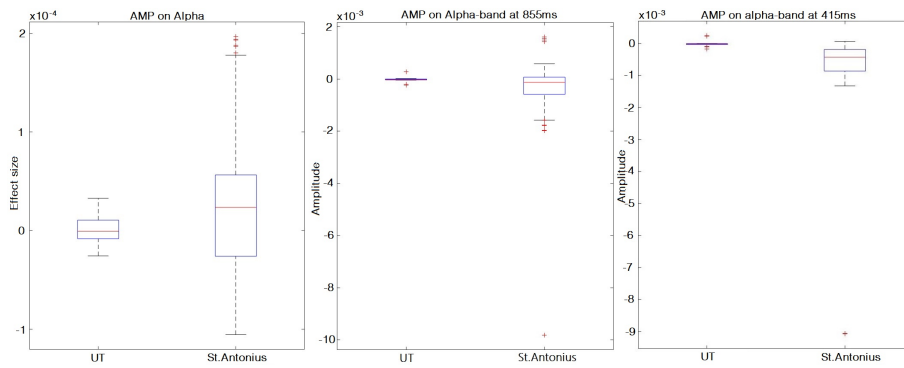
The effects sizes and mean amplitudes in relation with significant coefficients

derived from the statistical testing are depicted for both UT and St. Antonius dataset.



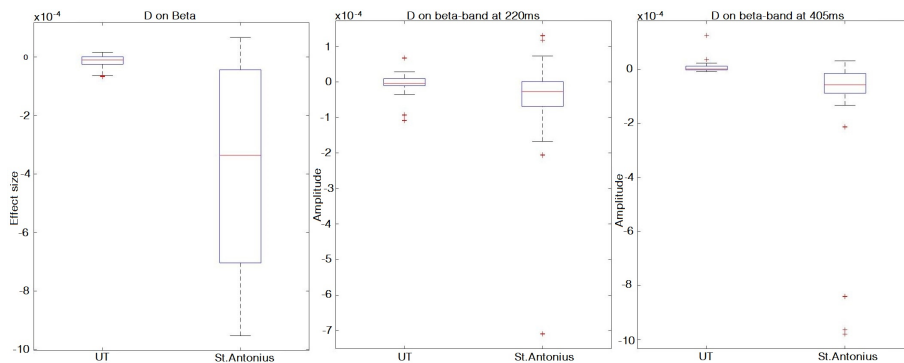
**Figure 4.28:** Left) Individual effect size of detection at electrode C4 and theta-band for the UT and St. Antonius datasets. Center) Mean power amplitude of detected trials at 889ms after stimulus onset. Right) Mean power amplitude of detected trials at latency 330ms after stimulus onset in the theta-band.

Figure 4.28 depicts the effects sizes of stimulus detection on individual level with respect to the UT and St. Antonius dataset. Results from the LMM showed that stimulus detection has strongest effect at latencies 889ms and 330ms for the UT and St. Antonius datasets, respectively. Both effect size and mean power amplitude of the UT dataset are significantly different from the values of the St. Antonius dataset.



**Figure 4.29:** Left) Individual effect size of stimulus amplitude at electrode C3 and alpha-band for the UT and St. Antonius datasets. Center) Mean power amplitude at electrode C3 and alpha-band at selected latency 853ms. Right) Mean power amplitude at latency 415ms after stimulus onset in the alpha-band and electrode C3.

Figure 4.29 shows the distribution of the effect size of stimulus amplitude and mean power amplitude at latencies where the LMM showed strongest effect of stimulus amplitude on the UT and St. Antonius datasets, 855ms and 415ms, respectively. The results are displayed on individual level at electrode C3 and in the alpha-band.



**Figure 4.30:** Left) Individual effect size of detection at electrode C3 and beta-band for the UT and St. Antonius datasets. Center) Mean power amplitude of detected trials at latency 220ms after stimulus onset in the beta-band. Right) Mean power amplitude of detected trials at latency 405ms after stimulus onset.

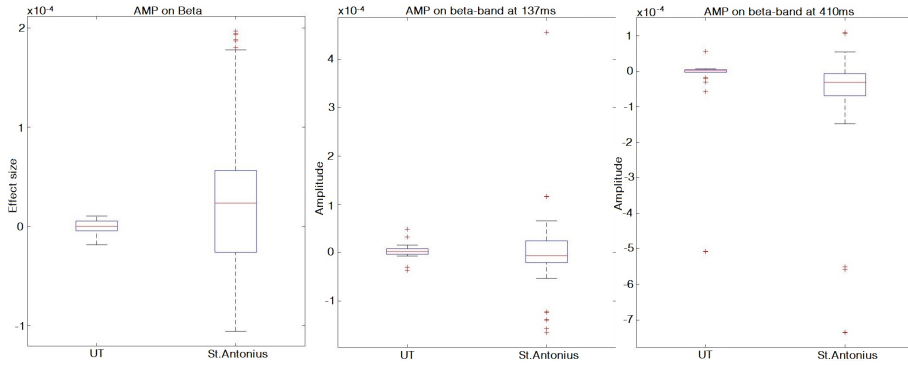


**Figure 4.31:** Left) Individual effect size of signal amplitude (first pulse) at electrode C3 and beta-band for the UT and St. Antonius datasets. Center) Mean power amplitude at latency 137ms after stimulus onset in the beta-band. Right) Mean power amplitude at latency 410ms after stimulus onset in the beta-band.

Figure 4.30 shows the distribution of the effect size of detection (D) and mean power amplitude of detected trials at latency 220ms and 405ms, where the LMM showed most significant effects of detection on the UT and St. Antonius datasets. Electrode C3 in the beta-band is depicted and values of effect sizes and mean power amplitude are displayed on individual level. Instead, Figure 4.31 shows the effect size of stimulus amplitude (first pulse) and the mean power amplitude at latencies 137ms and 410ms for the UT and St. Antonius dataset, respectively.

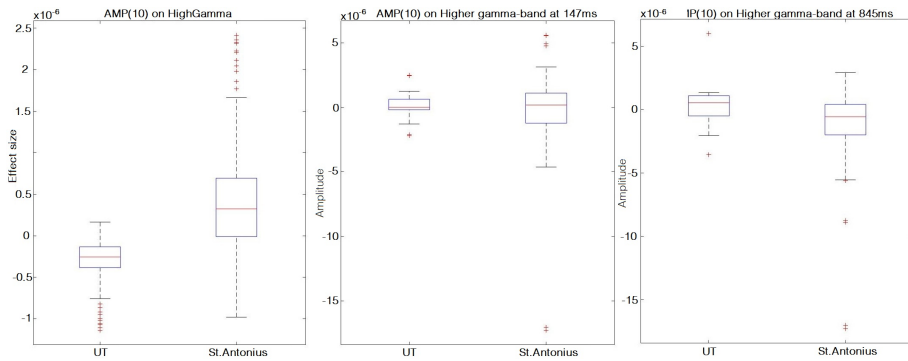


**Figure 4.32:** Left) Individual effect size of signal amplitude (second pulse, IPI 10ms) at electrode CP4 and higher gamma-band for the UT and St. Antonius datasets. Center) Mean power amplitude at latency 147ms after stimulus onset in the higher gamma-band. Right) Mean power amplitude at latency 845ms after stimulus onset in the higher gamma-band.

Figure 4.32 shows the distribution of the effect size of amplitude (AMP2, second pulse, IPI 10ms) and mean power amplitude at latencies 147ms and 845ms, where the LMM was most significant for both UT and St. Antonius datasets, respectively. The electrode depicted is CP4 in the higher frequencies of gamma-band. Effect sizes and mean power amplitudes at latency 845ms differ significantly between the two datasets on individual level. The mean power amplitude at latency 147ms is comparable with a larger variance on individual level for the St. Antonius dataset.

## 4.3 Discussion

In this assignment, time-frequency representations of single-trial EEG data were analyzed. The statistical model was designed to quantify the effect of stimulus parameters and detection probability on frequency components of cortical activations elicited by IES-5 during the MTT-EP protocol.

### 4.3.1 Time-frequency and statistical analysis

The LMM conducted on the UT dataset has revealed significant effects of stimulus parameters on relative band powers.

Our results of cortical activations in the theta-band (3 - 8Hz) are in agreement with previous results in which neuronal activations are present in the somatosensory cortex and correspond to the presence of pain-related evoked potentials in the time domain [66]. This equivalence between nociceptive EPs and theta-band oscillations is corroborated by their mutual adaptation to repeated stimulus application and mutual modulation towards the end of the experiment with respect to stimuli of the same amplitude. Thus, previous and present results reveal habituation of neurophysiological and psychophysical responses in both time- and frequency domain [41].

The decrease of ipsilateral and contralateral percentage signal changes with respect to baseline interval suggests a late involvement of the sensorimotor cortex during stimulus detection. Theta-band and alpha-band ipsilateral deactivations are result of a task-related response correlating to the upcoming activity of the hand for releasing the button after detection, while beta-band contralateral suppressions play an anti-kinetic role and promote fast motor reactions to initiate movement, in agreement with previous results [67],[74]. Instead, contralateral alpha-band deactivations are the only sensory-related responses modulated by stimulus amplitude (AMP) and, thus, represent the sensory processing of objective stimulus intensity, as already demonstrated by previous research [69].

While theta-, alpha- and beta-band neuronal oscillations are in line with previous research, results of this assignment in the gamma-band are in contrast with the literature. Gross et al. (2007) located early gamma-band activations in the contralateral regions increasing with objective stimulus intensity and subjective pain intensity [75]. Accordingly, early results of this assignment have found evidence of gamma-band activations at contralateral electrode C5 (around latency 100ms). However, our statistical analysis was unstable and did not reveal any significant effect of stimulus parameters on gamma-band neuronal oscillations. The instability of the LMM can be traced back to the nature of the signals in the gamma-band: small power amplitudes and SNR values ( as shown in Table 4.2) and merged with other background noises.

Further evidence of the literature suggested that gamma-band oscillations are most significant when the intensity of the stimulation is high [75]. This hypothesis, according to which gamma-band oscillations increase significantly when the received stimuli are perceived as painful, is a possible explanation for the results of this assignment. The absence of significant gamma-band contents may be traced back to the experimental procedure for the MTT-EP protocol, during which IES-5 induced stimuli are set around the individual's detection threshold and, thus, they are not perceived as painful. It is worth noting that results of this graduation assignment are exploratory and exclusively conducted on a cohort

group of healthy subjects. As future step of this research, it might be interesting to explore the nature of gamma-band neuronal oscillations on chronic pain patients with central sensitization. In particular, patients suffering from an enhanced sensitivity to normally innocuous stimuli (i.e. allodynia) should perceive the IES-5 stimulation as painful and exhibit an increased activity in the gamma band.

Both Gross et al. (2007) and Zhang et al. (2012) suggest that the content of gamma-band oscillations can be a predictor of subjective stimulus intensity regardless the objective stimulus amplitude [72]. In order to correlate oscillations in the gamma-frequency band to subjective stimulus intensities, it is necessary to introduce participant's rating of IES-5 during the MTT-EP protocol (i.e. numerical rating score, (NRS) where 0 is 'no pain' and 10 is 'the most intense pain imaginable'). Due to the nature of the MTT-EP, where stimuli are delivered at a fast rate and around the individual's detection threshold, it is not possible to record NRS scores at each stimulus. Recording an overall NRS score for the entire MTT-EP procedure would not provide enough evidences to discriminate the role of subjective and objective stimulus intensity on gamma-band oscillations.

### 4.3.2 Comparison analysis

Results from the LMM showed few similarities and numerous significant differences between the UT and St. Antonius datasets. For example, alpha-band oscillations showed a bivalent behavior in the UT dataset being both task-related and sensory-related responses, while in the St. Antonius dataset they are exclusively sensory-related responses, demonstrating a dependency to objective stimulus intensity. An additional significant effect on St. Antonius alpha-band power at contralateral regions is handedness (HAND), revealing a new role of stimulus location on neuronal oscillations recorded during the MTT-EP protocol. In line with this result, Zapala et al. (2020) and Bai et al. (2005) suggest that contralateral alpha-band suppressions are more prevalent when right-handers perform motor tasks with the dominant hand, while left-hand movements results into a bilateral activation, on both contralateral and ipsilateral regions [70], [71].

The contradictory results from the two datasets are confirmed during the computation of mean amplitudes and SNR values (Table 4.9) and butterfly plots at selected electrodes and latencies (Figures 4.15-4.18). Additionally, scalp topographies at selected latencies showed significant differences between the two datasets with opposite oscillation patterns, especially in the gamma-band frequencies (Figure 4.22).

A previous research conducted on the same datasets found that nociceptive evoked potentials recorded at the St. Antonius Hospital have lower amplitudes compared to the EPs from the UT dataset and could be traced back to the raw EEG data. Thus, it can be excluded that the contradictory results in this assignment were caused by either preprocessing or postprocessing algorithms. Instead, the differences might be the result of different subject characteristics, such as age or gender ratio, in the two cohort groups [84].

A preliminary evaluation of the distribution of effect sizes and power amplitudes on individual levels have shown significant differences between the two groups (Figures 4.28 - 4.32) suggesting a possible crucial role of subject's characteristic at each frequency band. Further research should be conducted using a linear mixed model to examine the data in relation to subject characteristics, by taking into account parameters such as age and gender.

The linear mixed model used in this assignment was an adapted version of a previous model that was specifically designed for the analysis of nociceptive evoked potentials. From the evidence collected during this graduation assignment, it is necessary to conduct further testing of the used LMM and of its validity in modelling time-frequency representations. A solid approach would be to test the assumption of linearity in the data by investigating the variation of the residuals over time, as suggested by van den Berg (2018) [41]. In case of high background noises, as revealed in the gamma-band frequency contents extracted during this graduation assignment, the model is not anymore able to detect errors of non-linearity. For this reason, future works should test additional and plausible models, specifically designed for the time-frequency representations of EEG data recorded during the MTT-EP protocol.

The MTT-EP protocol is an interesting tool for the investigation of the nociceptive system and its related pathologies. The aim of the ongoing research at the University of Twente is to validate the MTT-EP protocol as diagnostic tool for the assessment of chronic pain conditions.

In order to achieve this, further validating experimental protocols must be conducted.

The first objective of this assignment was to design an experimental protocol introducing high-frequency stimulation in combination with the MTT-EP protocol. HFS is an experimental pain model inducing secondary hyperalgesia through the delivery of electrical stimuli onto the skin at high frequencies. The protocol, designed during this graduation assignment, has already received ethical approval.

The second objective of this assignment was to perform an exploratory time-frequency analysis to investigate the frequency content of neuronal responses elicited using IES-5 during the MTT-EP protocol. As summary of the results presented in Section 4.3, it is possible to conclude that:

The combination of time-frequency analysis and LMM on EEG data recorded during the MTT-EP protocol provides interesting insights on the functional role of cortical activations at theta-, alpha- and beta-bands, in agreement with the available literature. Stimulus parameters, such as detection, intensity and habituation factors, play significant roles during pain processing by modulating neuronal oscillations.

The main focus of this graduation assignment was to perform time-frequency analysis on EEG data recorded during the MTT-EP protocol and to investigate their frequency contents. Additional statistical testing has been conducted with a linear mixed model, used to evaluate the role of stimulus parameters in modulating neuronal oscillations. Significant results in the theta-, alpha- and beta-bands have been found and are in line with previous research and existing literature investigating the functional role of neuronal oscillations in pain processing. The absence of gamma-band oscillatory activity may be consequence of IES-5 electrical stimulation, known to activate the nociceptive system around the individuals' detection thresholds, without eliciting painful sensations.

Contrasting results between the UT and the St. Antonius dataset, initiated a comparison analysis aiming at finding possible similarities and differences between the two datasets. Preliminary results suggest that dissimilarities depend on subject's characteristics. However, further statistical testing needs to be conducted in order to unveil the role of subject characteristics in modulating the frequency content of neuronal responses elicited by IES-5.

Furthermore, additional testing must be conducted in order to validate the LMM as plausible model for the time-frequency representations of EEG data recorded during the MTT-EP protocol.

In summary, time-frequency representations of neuronal responses to IES-5 stimuli provide meaningful insights on how sensory information are translated into cognitive responses. In order to have a comprehensive understanding of pain processing during the MTT-EP protocol, additional studies using time-frequency analysis should be conducted taking into account subjects' characteristics and a varied cohort of both pain-free subjects and chronic pain patients. Future works should also focus on validation of the most plausible LMM which would correctly model the time-frequency representations. Despite the limitations, this study showed promising results and demonstrated the feasibility of time-frequency analysis of single-trial EEG data recorded at the University of Twente during the MTT-EP protocol.

# Bibliography

Here are the references in citation order.

- [1] William Raffaelli and Elisa Arnaudo. 'Pain as a disease: an overview'. In: *Journal of Pain Research* 10 (2017), pp. 2003–2008 (cited on page 1).
- [2] Ronda G Hughes. *Patient Safety and Quality. An evidenced-based handbook for nurses*. 2008 (cited on page 1).
- [3] Sarah EE. Mills, Karen P. Nicolson, and Blair H. Smith. 'Chronic pain: a review of its epidemiology and associated factors in population-based studies'. In: *British Journal of Anaesthesia* 123.2 (2019), e273–e283. doi: [10.1016/j.bja.2019.03.023](https://doi.org/10.1016/j.bja.2019.03.023) (cited on pages 1, 4).
- [4] Paul C. Langley. 'The prevalence, correlates and treatment of pain in the European Union'. In: *Current Medical Research Opinion* 27.2 (2011), pp. 463–480. doi: [10.1185/03007995.2010.542136](https://doi.org/10.1185/03007995.2010.542136) (cited on pages 1, 4).
- [5] Lisa Goudman et al. 'Cortical mapping of painful electrical stimulation by quantitative electroencephalography: unraveling the time-frequency-channel domain'. In: *Journal of Pain Research* 10 (2017), pp. 2675–2685. doi: [10.2147/JPR.SI45783](https://doi.org/10.2147/JPR.SI45783) (cited on page 1).
- [6] R. Cowen et al. 'Assessing pain objectively: the use of physiological markers'. In: *Anaesthesia* 70 (2015), pp. 828–847. doi: [10.1111/anae.13018](https://doi.org/10.1111/anae.13018) (cited on page 1).
- [7] Marian Osterweis, Arthur Kleinman, and David Mechanic. *Pain and disability. Clinical, behavioral, and public policy perspectives*. 1987 (cited on page 1).
- [8] Sjors H. Wagemakers et al. 'A systematic review of devices and techniques that objectively measure patients' pain'. In: *Pain Physician* 22 (2019), pp. 1–13 (cited on page 2).
- [9] André Mouraux et al. 'Nociceptive Steady-State Evoked Potentials elicited by rapid periodic thermal stimulation of cutaneous nociceptors'. In: *The Journal of Neuroscience* 31.16 (2011), pp. 6079–6087. doi: [10.1523/JNEUROSCI.3977-10.2011](https://doi.org/10.1523/JNEUROSCI.3977-10.2011) (cited on page 2).
- [10] Jessica O'Neill et al. 'Unravelling the mystery of capsaicin: a tool to understand and treat pain'. In: *Pharmacological Reviews* 64 (2012), pp. 939–971. doi: [10.1124/pr.112.006163](https://doi.org/10.1124/pr.112.006163) (cited on page 2).
- [11] Matthew H McIntyre et al. 'Validity of the cold pressor test and pain sensitivity questionnaire via online self-administration'. In: *PLoS ONE* 15.4 (2020), e0231697. doi: [10.1371/journal.pone.0231697](https://doi.org/10.1371/journal.pone.0231697) (cited on page 2).
- [12] Lechi Vo and Peter D. Drummond. 'High frequency electrical stimulation concurrently induces central sensitization and ipsilateral inhibitory pain modulation'. In: *European Journal of Pain* 17.3 (2013), pp. 357–368. doi: [10.1002/j.1532-2149.2012.00208.x](https://doi.org/10.1002/j.1532-2149.2012.00208.x) (cited on pages 2, 13).
- [13] Emanuel N. van den Broeke et al. 'Characterizing pinprick-evoked brain potentials before and after experimentally induced secondary hyperalgesia'. In: *Journal of Neurophysiology* 114.5 (2015), pp. 2672–2681. doi: [10.1152/jn.00444.2015](https://doi.org/10.1152/jn.00444.2015) (cited on page 2).
- [14] Erol Basar and Aysel Duzgun. 'How is the brain working? Research on brain oscillations and connectivities in a new "Take-Off" state'. In: *International Journal of Psychophysiology* 103 (2016), pp. 3–11. doi: [10.1016/j.ijpsycho.2015.02.007](https://doi.org/10.1016/j.ijpsycho.2015.02.007) (cited on page 2).
- [15] Maeike Zijlmans et al. 'High-frequency oscillations as a new biomarker in epilepsy'. In: *Annals of Neurology* 71 (2012), pp. 169–178. doi: [10.1002/ana.22548](https://doi.org/10.1002/ana.22548) (cited on page 2).
- [16] John LK. Kramer, Jenny Haefeli, and Catherine R. Jutzeler. 'An objective measure of stimulus-evoked pain'. In: *The Journal of Neuroscience* 32.38 (2012), pp. 12981–12982. doi: [10.1523/JNEUROSCI.3175-12.2012](https://doi.org/10.1523/JNEUROSCI.3175-12.2012) (cited on page 2).

- [17] Rainer Freynhagen et al. 'Current understanding of the mixed pain concept: a brief narrative review'. In: *Current Medical Research and Opinion* 35.6 (2019), pp. 1011–1018. doi: [10.1080/03007995.2018.1552042](https://doi.org/10.1080/03007995.2018.1552042) (cited on page 4).
- [18] Albert Dahan, Monique van Velzen, and Marieke Niesters. 'Comorbidities and the complexities of chronic pain'. In: *Anesthesiology* 121.4 (2016), pp. 675–677. doi: [10.1097/ALN.000000000000402](https://doi.org/10.1097/ALN.000000000000402) (cited on page 4).
- [19] Rolf-Detlef Treede et al. 'A classification of chronic pain for ICD-11'. In: *Pain Journal Online* 156.6 (2015), pp. 1003–1007. doi: [10.1097/j.pain.000000000000160](https://doi.org/10.1097/j.pain.000000000000160) (cited on page 4).
- [20] Eric R. Kandel et al. *Principles of neural science*. 2013 (cited on pages 5, 7–9, 13).
- [21] Lisa Johannek, Boem Shim, and Richard A. Meyer. 'Primary hyperalgesia and nociceptor sensitization'. In: *Handbook of Clinical Neurology* 81 (2006), pp. 35–47. doi: [10.1016/S0072-9752\(06\)80008-4](https://doi.org/10.1016/S0072-9752(06)80008-4) (cited on page 7).
- [22] Rolf-Detlef Treede. 'Neurogenic hyperalgesia: illuminating its mechanisms with an infrared laser'. In: *The Journal of Physiology* 594.22 (2016), pp. 6441–6442. doi: [10.1113/JP273072](https://doi.org/10.1113/JP273072) (cited on page 7).
- [23] Robert H. Lamotte et al. 'Neurogenic hyperalgesia: psychophysical studies of underlying mechanisms'. In: *Journal of Neurophysiology* 66.1 (1991), pp. 190–211 (cited on page 7).
- [24] Clifford J. Woolf and Michael W. Salter. 'Neuronal plasticity: increasing the gain in pain'. In: *Science* 288.5472 (2000), pp. 1765–1768. doi: [10.1126/science.288.5472.1765](https://doi.org/10.1126/science.288.5472.1765) (cited on page 7).
- [25] Jurgen Sandkuhler. 'Models and mechanisms of hyperalgesia and allodynia'. In: *Physiological Reviews* 89 (2009), pp. 707–758. doi: [10.1152/physrev.00025.2008](https://doi.org/10.1152/physrev.00025.2008) (cited on page 8).
- [26] Emily Reid et al. 'Spatial summation of pain in humans investigated using transcutaneous electrical stimulation'. In: *The Journal of Pain* 16.1 (2015), pp. 11–18. doi: [10.1016/j.jpain.2014.10.001](https://doi.org/10.1016/j.jpain.2014.10.001) (cited on page 8).
- [27] Michael Costigan, Joachim Scholz, and Clifford J. Woolf. 'Neuropathic pain: a maladaptive response of the nervous system to damage'. In: *Annual Review of Neuroscience* 32 (2009), pp. 1–32. doi: [10.1146/annurev.neuro.051508.135531](https://doi.org/10.1146/annurev.neuro.051508.135531) (cited on page 10).
- [28] Kerry D. Walton and Rodolfo R. Llinas. *Chapter 13: Central pain as a thalamocortical dysrhythmia: a thalamic efference disconnection?* 2010 (cited on page 10).
- [29] Murray S. Sherman and Ray W. Guillery. *Functional connections of cortical areas - a new view from the thalamus*. 2013 (cited on page 10).
- [30] Didier Bouhassira et al. 'Involvement of the subnucleus reticularis dorsalis in diffuse noxious inhibitory controls in the rat'. In: *Brain Research* 595 (1992), pp. 353–357 (cited on page 10).
- [31] Rolf-Detlef Treede et al. 'The cortical representation of pain'. In: *Pain* 79.2-3 (1999), pp. 105–111. doi: [10.1016/S0304-3959\(98\)00184-5](https://doi.org/10.1016/S0304-3959(98)00184-5) (cited on page 10).
- [32] Li Hu et al. 'The primary somatosensory cortex contributes to the latest part of the cortical response elicited by nociceptive somatosensory stimuli in humans'. In: *NeuroImage* 84 (2014), pp. 383–393. doi: [10.1016/j.neuroimage.2013.08.057](https://doi.org/10.1016/j.neuroimage.2013.08.057) (cited on page 10).
- [33] Lars Timmermann et al. 'Differential coding of pain intensity in the human primary and secondary somatosensory cortex'. In: *Journal of Neurophysiology* 86 (2001), pp. 1499–1503 (cited on page 10).
- [34] Changbo Lu et al. 'Insular cortex is critical for the perception, modulation and chronification of pain'. In: *Neuroscience Bulletin* 32.2 (2016), pp. 191–201. doi: [10.1007/s12264-016-0016-y](https://doi.org/10.1007/s12264-016-0016-y) (cited on page 10).
- [35] Kamen G. Usunoff et al. *Functional neuroanatomy of pain*. 2006 (cited on page 10).
- [36] Eric L. Garland. 'Pain processing in the human nervous system: a selective review of nociceptive and behavioural pathways'. In: *Primary Care* 39.3 (2012), pp. 561–571. doi: [10.1016/j.pop.2012.06.013](https://doi.org/10.1016/j.pop.2012.06.013) (cited on page 10).
- [37] Avigail Lithwick, Shaya Lev, and Alexander M. Binshtok. 'Chronic pain-related remodeling of cerebral cortex - 'pain memory': a possible target for treatment of chronic pain'. In: *Pain Management* 3.1 (2013), pp. 35–45. doi: [10.2217/PMT.12.74](https://doi.org/10.2217/PMT.12.74) (cited on page 10).

- [38] Mira Meeus and Jo Nijs. 'Central sensitization: a biopsychosocial explanation for chronic widespread pain in patients with fibromyalgia and chronic fatigue syndrome'. In: *Clinical Rheumatology* 26 (2007), pp. 465–473. doi: [10.1007/s10067-006-0433-9](https://doi.org/10.1007/s10067-006-0433-9) (cited on page 10).
- [39] Michael H. Ossipov, Kozo Morimura, and Frank Porreca. 'Descending pain modulation and chronification of pain'. In: *Current Opinion in Supportive Palliative Care* 8.2 (2014), pp. 143–151. doi: [10.1097/SPC.000000000000055](https://doi.org/10.1097/SPC.000000000000055) (cited on page 11).
- [40] Lars Arendt-Nielsen and Hans C. Hoeck. 'Optimizing the early phase development of new analgesics by human pain biomarkers'. In: *Expert Review of Neurotherapeutics* 11.11 (2014), pp. 1631–1651. doi: [10.1586/ern.11.147](https://doi.org/10.1586/ern.11.147) (cited on page 11).
- [41] Boudewijn van den Berg and Jan R. Buitenweg. 'Analysis Of Nociceptive Evoked Potentials During Multi-Stimulus Experiments Using Linear Mixed Models'. In: *2018 40th Annual International Conference of the IEEE Engineering in Medicine and Biology Society (EMBC)* (2018), pp. 3048–3051. doi: [10.1109/EMBC.2018.8513032](https://doi.org/10.1109/EMBC.2018.8513032) (cited on pages 11, 12, 15–18, 26, 54, 56).
- [42] John Palmer, Preeti Verghese, and Misha Pavel. 'The psychophysics of visual search'. In: *Vision Research* 40 (2000), pp. 1227–1268 (cited on page 11).
- [43] Robert J. Doll, Jan R. Buitenweg, and Hil G. Meijer. 'Tracking of nociceptive thresholds using adaptive psychophysical methods'. In: *Behaviour Research Methods* 46 (2014), pp. 55–66. doi: [10.3758/s13428-013-0368-4](https://doi.org/10.3758/s13428-013-0368-4) (cited on page 11).
- [44] Andrew B. Watson and Andrew Fitzhugh. 'The method of constant stimuli is inefficient'. In: *Perception Psychophysics* 47.1 (1990), pp. 87–91 (cited on page 12).
- [45] Lewis O. jr. Harwey. 'Detection theory: sensory and decision process'. In: *Psychology of Perception* (2014) (cited on pages 12, 16).
- [46] Nicolaas Prins. 'The psychometric function: the lapse rate revisited'. In: *Journal of Vision* 12.6 (2012), pp. 1–16. doi: [10.1167/12.6.25](https://doi.org/10.1167/12.6.25) (cited on page 12).
- [47] Bernhard Treutwein and Hans Strasburger. 'Fitting the psychometric function'. In: *Perception Psychophysics* 1.1 (1999), pp. 87–106 (cited on pages 12, 16).
- [48] Camilla Staahl and Asbjorn Mohr Drewes. 'Experimental human pain models: a review of standardised methods for preclinical testing of analgesics'. In: *Basic Clinical Pharmacology Toxicology* 95 (2004), pp. 97–111 (cited on page 13).
- [49] Karin L. Petersen and Michael C. Rowbotham. 'A new human experimental pain model: the heat/capsaicin sensitization model'. In: *NeuroReport* 10 (1999), pp. 1511–1516 (cited on page 13).
- [50] Laura .A. Mitchell, Raymond A. MacDonald, and Eric E. Brodie. 'Temperature and the cold pressor test'. In: *The Journal of Pain* 5.4 (2004), pp. 233–237. doi: [10.1016/j.jpain.2004.03.004](https://doi.org/10.1016/j.jpain.2004.03.004) (cited on page 13).
- [51] Emanuel N. van den Broeke et al. 'Central sensitization of nociceptive pathways demonstrated by robot-controlled pinprick-evoked brain potentials'. In: *Clinical Neurophysiology* (2020). doi: [10.1016/j.clinph.2020.06.020](https://doi.org/10.1016/j.clinph.2020.06.020) (cited on page 14).
- [52] Craig T. Hartrick, Juliann P. Kovan, and Sharon Shapiro. 'The Numeric Rating Scale for clinical pain measurement: a ratio measure?' In: *Pain Practice* 3.4 (2003). doi: [10.1111/j.1530-7085.2003.03034.x](https://doi.org/10.1111/j.1530-7085.2003.03034.x) (cited on page 14).
- [53] Fabio Babiloni et al. 'Spatial enhancement of EEG data by surface Laplacian estimation: the use of magnetic resonance imaging-based head models'. In: *Clinical Neurophysiology* 112 (2001), pp. 724–727 (cited on page 14).
- [54] *Psychophysical methods for improved observation of nociceptive processing*. 2016 (cited on pages 14–16).
- [55] André Mouraux, GianDomenico Iannetti, and Leon Plaghki. 'Low intensity intra-epidermal electrical stimulation can activate A $\delta$ -nociceptors selectively'. In: *Pain* 150 (2010), pp. 199–207. doi: [10.1016/j.pain.2010.04.026](https://doi.org/10.1016/j.pain.2010.04.026) (cited on page 15).

- [56] Peter Steenbergen et al. 'A system for inducing concurrent tactile and nociceptive sensations at the same site using electrocutaneous stimulation'. In: *Behaviour Research Methods* 44.4 (2012), pp. 924–933. doi: [10.3758/s13428-012-0216-y](https://doi.org/10.3758/s13428-012-0216-y) (cited on page 15).
- [57] Robert Doll, Petrus H. Veltink, and Jan R. Buitenweg. 'Observation of time-dependent psychophysical functions and accounting for threshold drifts'. In: *Attention, Perception, and Psychophysics* 77.4 (2015), pp. 1440–1447 (cited on pages 15, 16).
- [58] Frederick Kingdom and Nicolaas Prins. 'Psychophysics'. In: *Academic Press* (2010) (cited on page 16).
- [59] Rumeysa Ince, Saliha Seda Adanir, and Fatma Sevmmez. 'The inventor of electroencephalography (EEG): Hans Berger (1873-1941)'. In: *Child's Nervous System* (2020). doi: [10.1007/s00381-020-04564-z](https://doi.org/10.1007/s00381-020-04564-z) (cited on page 16).
- [60] James L. Stone and John R. Hughes. 'Early history of electroencephalography and establishment of the American clinical neurophysiology society'. In: *Journal of Clinical Neurophysiology* 30.1 (2013), pp. 28–44 (cited on page 16).
- [61] Geoffrey F. Woodman. 'A brief introduction to the use of event-related potentials (ERPs) in studies of perception and attention'. In: *Attent Percept Psychophys* 72.8 (2010). doi: [10.3758/APP.72.8.2031](https://doi.org/10.3758/APP.72.8.2031) (cited on page 16).
- [62] Gert Pfurtscheller and Fernando H. Lopes da Silva. 'Event-related EEG/MEG synchronization and desynchronization: basic principles'. In: *Clinical Neurophysiology* 110 (1999), pp. 1842–1857 (cited on pages 17, 18).
- [63] Barry S. Oken and TS Phillips. 'Evoked potentials: clinical'. In: *Encyclopedia of Neuroscience* (2009), pp. 19–28. doi: [10.1016/B978-008045046-9.00587-8](https://doi.org/10.1016/B978-008045046-9.00587-8) (cited on page 17).
- [64] Melanie Boly et al. *Chapter 2 - Functional Neuroimaging Techniques*. 2016 (cited on page 17).
- [65] Mike X Cohen. *Chapter 9 - Overview of Time-Domain EEG Analyses*. 2014 (cited on pages 17, 20).
- [66] Markus Ploner, Christian Sorg, and Joachim Gross. 'Brain Rhythms of Pain'. In: *Trends in Cognitive Sciences* 21.2 (2016), pp. 100–110. doi: [10.1016/j.tics.2016.12.001](https://doi.org/10.1016/j.tics.2016.12.001) (cited on pages 18–20, 54).
- [67] Benjamin Dufour, Francois Thénault, and Pierre-Michel Bernier. 'Theta-band EEG activity over sensorimotor regions is modulated by expected visual reafferent feedback during reach planning'. In: *Neuroscience* Aug.285 (2018), pp. 47–58. doi: [10.1016/j.neuroscience.2018.06.005](https://doi.org/10.1016/j.neuroscience.2018.06.005) (cited on pages 19, 54).
- [68] James R. Hinman et al. 'Septotemporal variation in dynamics of theta: speed and habituation'. In: *Journal of Neurophysiology* 105 (2011), pp. 2675–2686. doi: [10.1152/jn.00837.2010](https://doi.org/10.1152/jn.00837.2010) (cited on page 19).
- [69] Lu Hu et al. 'Functional features of nociceptive-induced suppression of alpha band electroencephalographic oscillations'. In: *The Journal of Pain* 12.1 (2013), pp. 89–99. doi: [10.1016/j.jpain.2012.10.008](https://doi.org/10.1016/j.jpain.2012.10.008) (cited on pages 19, 54).
- [70] Dariusz Zapala et al. 'The effects of handedness on sensorimotor rhythm desynchronization and motor-imagery BCI control'. In: *Scientific Reports* 10.2087 (2020). doi: [10.1038/s41598-020-59222-w](https://doi.org/10.1038/s41598-020-59222-w) (cited on pages 19, 55).
- [71] Ou Bai et al. 'Asymmetric spatiotemporal patterns of event-related desynchronization preceding voluntary sequential finger movements: a high-resolution EEG study'. In: *Clinical Neurophysiology* 116 (2005), pp. 1213–1221 (cited on pages 19, 55).
- [72] Zhe G. Zhang et al. 'Gamma-band oscillations in the primary somatosensory cortex - a direct and obligatory correlate of subjective pain intensity'. In: *The Journal of Neuroscience* 32.22 (2012), pp. 7429–7438. doi: [10.1523/JNEUROSCI.5877-11.2012](https://doi.org/10.1523/JNEUROSCI.5877-11.2012) (cited on pages 19, 55).
- [73] Charidimos Tzagarakis et al. 'Beta-band activity during motor planning reflects response uncertainty'. In: *The Journal of Neuroscience* 30.34 (2010), pp. 11270–11277. doi: [10.1523/JNEUROSCI.6025-09.2010](https://doi.org/10.1523/JNEUROSCI.6025-09.2010) (cited on page 19).
- [74] Gaurav Misra et al. 'Pain-related suppression of beta oscillations facilitates voluntary movement'. In: *Cerebral Cortex* 27 (2017), pp. 2592–2606 (cited on pages 19, 54).

- [75] Joachim Gross et al. 'Gamma oscillations in human primary somatosensory cortex reflect pain perception'. In: *PLoS Biology* 5.5 (2007), e133. doi: [10.1371/journal.pbio.0050133](https://doi.org/10.1371/journal.pbio.0050133) (cited on pages 19, 54).
- [76] Weiwei Peng et al. 'Changes in spontaneous oscillatory activity to tonic heat pain'. In: *PLoS ONE* 9 (2014), e91052 (cited on page 19).
- [77] Enrico Schulz et al. 'Prefrontal gamma oscillations encode tonic pain in humans'. In: *Cerebral Cortex* 25 (2015), pp. 4407–4414. doi: [10.1093/cercor/bhv043](https://doi.org/10.1093/cercor/bhv043) (cited on page 19).
- [78] A. Zabidi et al. 'Short-time Fourier Transform analysis of EEG signal generated during imagined writing'. In: *2012 International Conference on System Engineering and Technology: September 11-12, 2012, Bandung, Indonesia* (2012) (cited on page 20).
- [79] Sandro A.P. Haddad and Wouter A. Serdijn. *Ultra-low power biomedical signal processing. An analog wavelet filter approach for pacemakers*. 2009 (cited on page 20).
- [80] José Biurrun Manresa et al. 'High frequency electrical stimulation induces a long-lasting enhancement of event-related potentials but does not change the perception elicited by intra-epidermal electrical stimuli delivered to the area of increased mechanical pinprick sensitivity'. In: *PLoS ONE* 13.9 (2018). doi: [10.1371/journal.pone.0203365](https://doi.org/10.1371/journal.pone.0203365) (cited on pages 21, 22, 24).
- [81] Marie-Laure Sniijders. *High frequency stimulation induced secondary hyperalgesia for validation of diagnostic tools for early detection of chronic pain development*. 2019 (cited on page 22).
- [82] Tom Berfelo et al. 'Observing electrical brain responses around the nociceptive detection threshold'. In: *Technical Innovations in Medicine Conference 2019: 10 Jaar Technische Geneeskunde - Utrecht, Netherlands* (2019) (cited on page 26).
- [83] Giulia Liberati et al. 'Gamma-band oscillations preferential for nociception can be recorded in the Human Insula'. In: *Cerebral Cortex* (2017), pp. 1–15. doi: [10.1093/cercor/bhx237](https://doi.org/10.1093/cercor/bhx237) (cited on page 27).
- [84] Tom Berfelo et al. 'Altered nociceptive detection thresholds and brain evoked potentials in Failed Back Surgery Syndrome patients'. In: *Unpublished manuscript* (2020) (cited on page 55).

---

## Appendix A

---

### **RESEARCH PROTOCOL**

Exploration of the effects of HFS-induced secondary hyperalgesia on the NDT-EP method

**(June 2020)**

**PROTOCOL TITLE** 'Exploration of the effects of HFS-induced secondary hyperalgesia on the NDT-EP method'

<b>Protocol ID</b>	<b>NL72937.091.20</b>
<b>Short title</b>	Exploration of the effects of HFS-induced secondary hyperalgesia on the NDT-EP method
<b>Version</b>	V3
<b>Date</b>	Friday, June 19 <sup>th</sup> 2020
<b>Principal Investigator and Project Leader</b>	Dr. ir. J.R. Buitenweg Universiteit Twente Biomedische Signalen en Systemen Zuidhorst 213 Postbus 217 7500 AE Enschede  Tel.: (053) 489 2705 Email: <a href="mailto:j.r.buitenweg@utwente.nl">j.r.buitenweg@utwente.nl</a>
<b>Co-investigators</b>	N. Jansen, MSc Zuidhorst 215 Postbus 217 7500AE Enschede Tel.: (053) 489 2276 Email: <a href="mailto:n.jansen@utwente.nl">n.jansen@utwente.nl</a>  F. Marsili, BSc Universiteit Twente Zuidhorst 207 Postbus 217 7500 AE Enschede Tel.: +31 (6) 30 86 9443 Email: <a href="mailto:f.marsili@student.utwente.nl">f.marsili@student.utwente.nl</a>
<b>Sponsor</b>	University of Twente Biomedical Signals en Systems (BSS) Postbus 217 7500 AE Enschede
<b>Independent expert</b>	Prof. dr. ir. M. van Putten Universiteit Twente Clinical Neurophysiology Technohal (n° 18) Room 3380  Tel.: (053) 489 4599 Email: <a href="mailto:m.j.a.m.vanputten@utwente.nl">m.j.a.m.vanputten@utwente.nl</a>

**PROTOCOL SIGNATURE SHEET**

<b>Name</b>	<b>Signature</b>	<b>Date</b>
<b>Sponsor</b> Prof. Dr. ir. Peter H. Veltink <i>Chairman Biomedical Signals and Systems</i>		
<b>Project Leader</b> Dr. ir. J.R. Buitenweg		

## Inhoudsopgave

Figures	7
1. INTRODUCTION AND RATIONALE	10
2. OBJECTIVES	13
2.1. PRIMARY OBJECTIVE	13
2.2. SECONDARY OBJECTIVE	13
3. STUDY DESIGN	14
3.1. OVERALL STUDY DESIGN AND PLAN	14
3.2. EXPERIMENTAL SETTING	15
4. STUDY POPULATION	16
4.1 POPULATION BASE	16
4.2 INCLUSION CRITERIA	16
4.3 EXCLUSION CRITERIA	16
4.4 SAMPLE SIZE CALCULATION	16
5. METHODS	17
5.1 STUDY PARAMETERS	17
5.1.1 MAIN STUDY PARAMETERS	17
5.1.2 OTHER STUDY PARAMETERS	17
5.2 MEASUREMENTS	17
5.2.1 MATERIALS AND METHODS	17
5.2.2 PROCEDURE	20
5.3 RANDOMISATION, BLINDING AND TREATMENT ALLOCATION	24
5.4 WITHDRAWAL OF INDIVIDUAL SUBJECTS	24
5.5 REPLACEMENT OF INDIVIDUAL SUBJECTS AFTER WITHDRAWAL	24
5.6 FOLLOW-UP OF SUBJECTS WITHDRAWN FROM TREATMENT	24
5.7 PREMATURE TERMINATION OF THE STUDY	24
6. SAFETY REPORTING	25
6.1 TEMPORARY HALT FOR REASONS OF SAFETY	25
6.2 AEs, SAEs and SURARs	25
6.2.1 ADVERSE EVENTS (AEs)	25
6.2.2 SERIOUS ADVERSE EVENTS (SAEs)	25
6.3 FOLLOW-UP OF ADVERSE EVENTS	26
6.4. DATA SAFETY MONITORING BOARD (DSMB)	26

7. STATISTICAL ANALYSIS	27
7.1 EEG PRE-PROCESSING	27
7.2 MODEL COMPUTATION	27
7.3 STUDY PARAMETERS	27
8. ETHICAL CONSIDERATIONS	29
8.1 REGULATION STATEMENT	29
8.2 RECRUITMENT AND CONSENT	29
8.3 BENEFITS AND RISKS ASSESSMENT, GROUP RELATEDNESS	29
8.4 COMPENSATION FOR INJURY	29
8.5 INCENTIVES	29
9. ADMINISTRATIVE ASPECTS, MONITORING AND PUBLICATION	30
9.1 HANDLING AND STORAGE OF DATA AND DOCUMENTS	30
9.2 AMENDMENTS	30
9.3 ANNUAL PROGRESS REPORT	30
9.4 TEMPORARY HALT AND (PREMATURELY) END OF STUDY REPORT	30
9.5 PUBLIC DISCLOSURE AND PUBLICATION POLICY	31
10. STRUCTURED RISK ANALYSIS	32
10.1 POTENTIAL ISSUES OF CONCERN	32
10.2 SYNTHESIS	33
11. REFERENCES	34

## LIST OF ABBREVIATIONS AND RELEVANT DEFINITIONS

<b>(S)AE</b>	<b>(Serious) Adverse Event</b>
<b>ABR</b>	<b>ABR form, General Assessment and Registration form, is the application form that is required for submission to the accredited Ethics Committee (In Dutch, ABR = Algemene Beoordeling en Registratie)</b>
<b>AE</b>	<b>Adverse Event</b>
<b>AMP</b>	<b>Stimulus Amplitude</b>
<b>AR</b>	<b>Adverse Reaction</b>
<b>CA</b>	<b>Competent Authority</b>
<b>CCMO</b>	<b>Central Committee on Research Involving Human Subjects; in Dutch: Centrale Commissie Mensgebonden Onderzoek</b>
<b>DSMB</b>	<b>Data Safety Monitoring Board</b>
<b>EEG</b>	<b>Electroencephalography</b>
<b>EP</b>	<b>Evoked Potential</b>
<b>EU</b>	<b>European Union</b>
<b>EudraCT</b>	<b>European drug regulatory affairs Clinical Trials</b>
<b>GAMM</b>	<b>Generalized Adaptive Mixed Modelling</b>
<b>GCP</b>	<b>Good Clinical Practice</b>
<b>GLMM</b>	<b>Generalized Linear Mixed-effect Model</b>
<b>IB</b>	<b>Investigator's Brochure</b>
<b>IC</b>	<b>Informed Consent</b>
<b>IMP</b>	<b>Investigational Medicinal Product</b>
<b>IMPD</b>	<b>Investigational Medicinal Product Dossier</b>
<b>IPI</b>	<b>Inter-Pulse Interval</b>
<b>LMM</b>	<b>Linear Mixed-effect Model</b>
<b>METC</b>	<b>Medical research ethics committee (MREC); in Dutch: medisch ethische toetsing commissie (METC)</b>
<b>MTT</b>	<b>Multiple Threshold Tracking</b>
<b>NOP</b>	<b>Number of Pulses</b>
<b>QST</b>	<b>Quantitative Sensory Testing</b>
<b>RT</b>	<b>Response Time</b>
<b>SPC</b>	<b>Summary of Product Characteristics (in Dutch: officiële productinformatie IB1-tekst)</b>
<b>Sponsor</b>	<b>The sponsor is the party that commissions the organisation or performance of the research, for example a pharmaceutical company, academic hospital, scientific organisation or investigator. A party that provides funding for a study but does not commission it is not regarded as the sponsor, but referred to as a subsidising party.</b>
<b>SUSAR</b>	<b>Suspected Unexpected Serious Adverse Reaction</b>
<b>Wbp</b>	<b>Personal Data Protection Act (in Dutch: Wet Bescherming Persoonsgegevens)</b>
<b>WMO</b>	<b>Medical Research Involving Human Subjects Act (in Dutch: Wet Medisch-wetenschappelijk Onderzoek met Mensen)</b>

## Figures

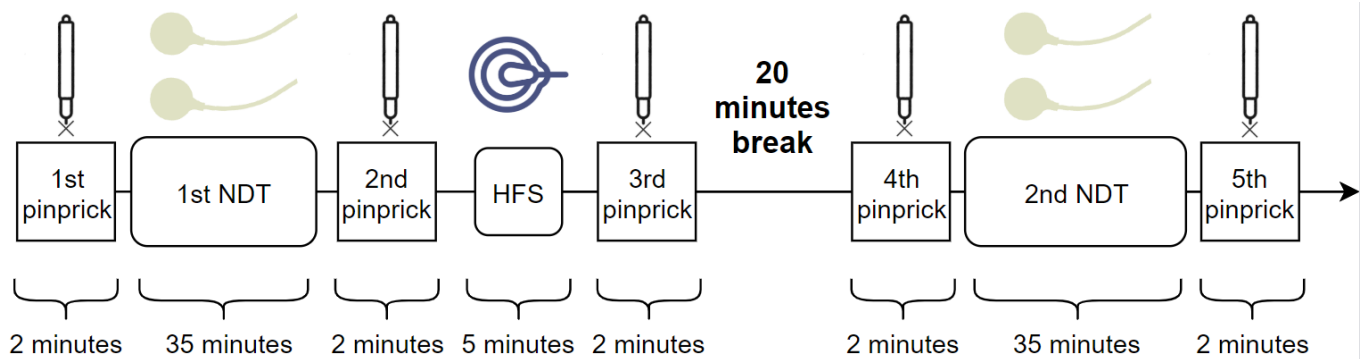


Figure 1 - Timeline of experimental session

### Electrodes and pinpricks position on the right forearm

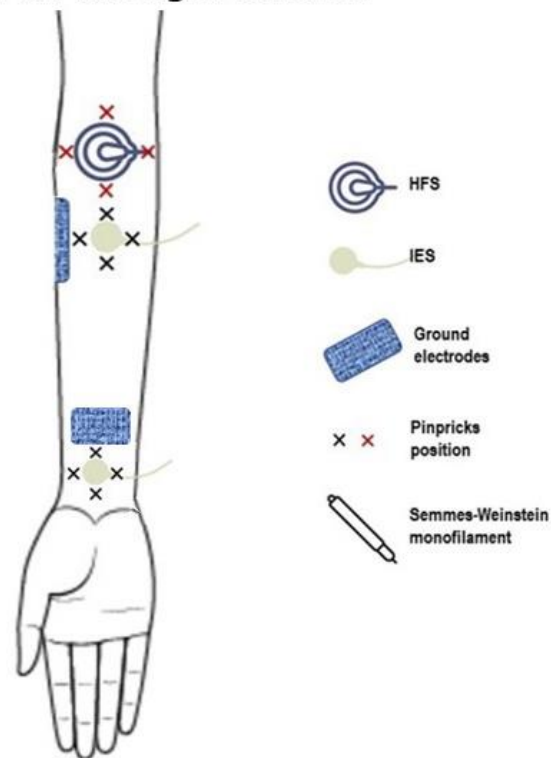


Figure 2 – Electrodes and pinpricks positions on the right forearm of healthy subjects. This set-up is used for the HFS, the MTT method and the punctate mechanical stimulation.

## SUMMARY

**Rationale:** Chronic pain often is results from disturbed processes in the central nervous system. Once chronic pain is established, treatment is relatively ineffective, with – at best – one patient in three or four achieving 50% pain intensity reduction. Early detection and therapeutic action would mean better treatment outcome and less clinical efforts per patient, but appropriate diagnostic tools are lacking. An increased sensitivity to noxious stimuli is widely recognized as a key factor in chronic pain development. Noxious stimuli are processed by neural mechanisms at several stages in the ascending pathway from periphery to brain, into a conscious pain experience. As a response to injury or disease, maladaptive changes in this pathway may result in an increased pain sensitivity. Clinical observation of the specific malfunctioning of peripheral and central components of this pathway is limited at present, but would permit a better understanding and early selection of interventions for treatment or prevention of chronic pain. Recently, we developed a new method for observing the properties of nociceptive processing utilizing subjective detection of electrocutaneous stimuli in combination with objective neurophysiological brain responses (NDT-EP). In this method, nociceptive afferents are activated by temporally defined current stimuli with varying number of pulses and varying inter pulse intervals. As these different temporal stimulus properties result in different excitation of nociceptive processing mechanisms of the ascending system, subsequent processing of stimulus-response pairs (SRPs) into estimated nociceptive detection thresholds (NDTs) and Evoked brain Potentials (EPs) of multiple stimulus types may provide information about the properties of these mechanisms.

A crucial step in exploring whether the above method could serve as a diagnostic tool is the assessment of the observability of changes in nociceptive function which are relevant for the development or maintenance of chronic pain. This can be achieved by measuring the effect of a well characterized and demonstrated alteration in nociceptive processing mechanisms on the NDTs and EPs. Other research groups have demonstrated that high frequency electrocutaneous stimulation (HFS) of sufficient duration and intensity can be used for prolonged activation of central sensitization mechanisms. These central sensitization effects are observed as a post-HFS secondary hyperalgesia to pin-prick stimuli and considered to play a key role in the development of chronic pain. Other results show that HFS also modulates the EPs obtained by electrocutaneous stimulation on the site of induced secondary hyperalgesia. Recently during a pilot study here at the University of Twente, we have assessed that HFS is technically feasible to implement in our lab. Therefore, the next step is to use HFS in an experiment together with the NDT-EP method.

**NL72937.091.20/** Exploration of the effects of HFS-induced secondary hyperalgesia on the NDT-EP method

**Objective:** The primary objective of this study is to investigate the quality and content of the MTT-EP outcomes in response to electrocutaneous stimuli by determining stimulus-related and/or physiological-related components, before and after the occurrence of HFS-induced central sensitization onto the skin of healthy subjects.

**Study design:** Mono-center, cross-sectional study.

**Study population:** 20 healthy subjects with an age between 18 and 40, recruited mostly at the University of Twente.

**Main study parameters/endpoints:** Several types of nociceptive stimuli will be applied, while the subject's response (*detected* or *not detected*) and the stimulus related EEG epochs will be measured. This data will be acquired before and after the occurrence of HFS-induced central sensitization. The modulation of NDTs and EPs as a consequence of central sensitization allows a better understanding of the underlying mechanisms of secondary hyperalgesia and chronic pain.

**Nature and extent of the burden and risks associated with participation, benefit and group relatedness:** The healthy participants will be asked to come to the Human Physiology Lab of the BSS Group at the University of Twente for one session. First, the participant is familiarized with the stimuli by stepwise application of increasing stimuli until stimulus detection. During the experiment, the participant will receive randomized stimuli around the detection threshold according to the multiple threshold tracking paradigm. Afterwards, HFS is applied to induce secondary hyperalgesia. Lastly, the subjects will receive a second series of randomized stimuli around the detection threshold according to the MTT paradigm. During the entire duration of the experimental session, cortical activity of the subject will be recorded using an EEG cap. All participants will be compensated for their participation. The participants will obtain no direct personal benefit.

## 1. INTRODUCTION AND RATIONALE

Pain is considered a major problem in modern day society, not only comprising a major physical and psychological burden for patients, but also a big economic and social burden for society. In Europe, it was found that over the range of one month 20.2 % of all people suffer a form of pain, of which 4.6 % suffer severe pain [1, 2]. Among those people is a large group that experiences chronic pain which was shown to have a prevalence of 12% to 30% depending on the country, of which 40% receives inadequate treatment for the pain [3]. These results emphasize the need for improved and new treatments for chronic pain. However, the development of those treatments requires a more profound understanding of the physiological as well as the psychological aspects of chronic pain.

Several types of chronic pain are linked to increased sensitivity of the central nervous system, including for example post-surgical pain and complex regional pain syndrome [4]. Therefore, it is important to study the underlying mechanisms of this increased sensitivity as well as how and where these changes occur. However, one major obstacle is the lack of an objective measure of peripheral and central sensitivity. Tracking psychophysical thresholds can facilitate the investigation of the underlying mechanisms of sensitization [5]. Several methods have been developed for measurement of those thresholds, which consist of application of a stimulus with a varying amplitude while measuring the subject's response to the stimulus. For example, the method of quantitative sensory testing (QST) using an ascending electrocutaneous pulse-train has been shown effective in determining post-surgical sensitization [6, 7] by measuring the electrical pain threshold (EPT). However, EPTs do not offer specific information about individual peripheral or central mechanisms. Additionally, the measured EPT highly depends on instructions provided by the observer and subjective criteria concerning pain and are therefore prone to inter-observer variability, subject-observer interactions and intra/inter-subjective psychological state and trait and variability (anxiety, depression, coping).

Recently, a method was developed for measuring psychophysical nociceptive detection thresholds (NDTs), using intra-epidermal electrocutaneous stimulation (IES) of the skin. IES preferentially activates nociceptive nerve fibers in the superficial skin (pin-prick sensation at detection level) without initial activation of tactile nerve fibers (non-painful sensation at detection level). Hence, IES permits estimation of pain sensitivity by measuring the amplitude threshold for a detectable sensation (hence called NDT), i.e. less sensitive to instruction and without the need for a subjective criterion concerning pain. Nociceptive processing of a stimulus into a detectable sensation depends on the amount of peripheral activation and the properties of central synaptic transmission. The amount of peripheral activation can be specifically modulated by variations in stimulus amplitude,

**NL72937.091.20/** Exploration of the effects of HFS-induced secondary hyperalgesia on the NDT-EP method

while central transmission is modulated by variations in the number of pulses and the inter-pulse interval, influencing synaptic summation. Therefore, measurement of NDTs using IES with multiple stimulus properties could provide information about specific peripheral and central properties of the nociceptive system.

In earlier studies, we developed a multiple threshold tracking (MTT) algorithm for measuring NDTs of IES stimuli with single and multiple pulses, and demonstrated the sensitivity to short term changes in nociceptive processing [8, 9]. We also successfully demonstrated changes of the NDT related to stimulus parameters [10] and measured the effect of capsaicin induced peripheral sensitization on the NDT [11]. However, since this method measures the subject's response, it still does not provide an objective measure of nociception.

An objective measure of nociception related activity in the central nervous system is the electroencephalographic (EEG) signal. Multiple-trial averages of this signal, referred to as evoked potentials (EPs), have been shown sensitive to changes in stimulus parameters such as the number of pulses [12, 13] or number of trials [14]. Since MTT has been shown to be effective in measuring the effect of stimulus parameters on stimulus detection, while the EP has been shown to reflect neurophysiological activity related to stimulus processing, a combination of both techniques might provide insight into the relation between neurophysiological activity and nociceptive stimuli.

One crucial step in the validation of the above-described method is the assessment of the observability of changes in the nociceptive function which are hypothesized to play a key role in the development and maintenance of chronic pain. This can be achieved by analysing the neurophysiological responses as a result of a pain model which induces a well characterized and demonstrated centrally mediated change in the nociceptive system. One such pain model is called High Frequency Stimulation (HFS).

With HFS, a train of pulses (2 ms pulsewidth, 100 Hz frequency) is provided 5 times at a stimulus strength of 20 times the detection threshold. This method has been found to induce both primary and secondary hyperalgesia [15, 16]. The effect manifests itself as a prolonged (>30 minutes), increased pain sensitivity to mechanical pinprick stimuli in the area surrounding the HFS and to electrocutaneous stimulation on the site of induced secondary hyperalgesia [17]. It has also been found that HFS modulates EPs as a result of electrocutaneous stimulation [18] and pinprick stimuli [19].

**NL72937.091.20/** Exploration of the effects of HFS-induced secondary hyperalgesia on the NDT-EP method

For the above-mentioned reasons, HFS is a promising technique to be combined with the MTT-EP method. Within pain research, HFS has been extensively used and provides consistent results in eliciting primary and secondary hyperalgesia [20-25]. Via a technical feasibility study initiated in February 2019 at the University of Twente, our setup was shown to be technically feasible to perform HFS and therefore it can now be used together with the MTT-EP.

In this study, we evaluate the responsiveness of the outcome measures of the MTT-EP method to changes in nociceptive function by evaluating the response before and after HFS.

## **2. OBJECTIVES**

### **2.1. PRIMARY OBJECTIVE**

The primary objective of this study is to investigate the quality and content of the outcomes of the multiple threshold tracking and EEG recordings from healthy subjects, before and after inducing secondary hyperalgesia onto the skin with high frequency stimulation.

### **2.2. SECONDARY OBJECTIVE**

The secondary objective of this study is to analyze if and how NDTs and/or EPs are associated to the properties of applied stimuli (e.g. stimulus amplitude, number of pulses) and/or modulated by HFS-induced secondary hyperalgesia onto the skin of healthy subjects.

### 3. STUDY DESIGN

#### 3.1. OVERALL STUDY DESIGN AND PLAN

The current study is a mono-center, cross-sectional study. Each subject will undergo a single measurement session.

Each **Measurement Session (155 minutes)** consists of:

- **Introduction (10 minutes):** The subject will be provided with information about the experiment and asked for consent to participate in the experiment.
  - **Preparation (20 minutes):** The subject will be connected to the EEG equipment and the nociceptive stimulation device.
  - **Familiarization (10 minutes):** The subject will be familiarized with the stimuli. In this phase, the subject can get used to determining whether a stimulus exceeds the stimulation threshold, and learn how to behave during the experiment.
  - **1<sup>st</sup> punctate mechanical stimulation (2 minutes):** The target for the mechanical pinpricks are marked and the first mechanical stimulation is performed.
  - **Experiment (103 minutes):** The actual experiment, in which nociceptive stimulus-response pairs will be measured for a variety of nociceptive stimuli.
    - **35 minutes:** first NDTs acquisition (both arm and hand)
    - **+2 minutes:** 2<sup>nd</sup> punctate mechanical stimulation
    - **+5 minutes:** HFS and assessment of perceived pain
    - **+2 minutes:** right after HFS for 3<sup>rd</sup> pinprick stimulation
- 20 minutes break**
- **+2 minutes:** 4<sup>th</sup> pinprick stimulation
  - **+35 minutes:** second and final NDTs acquisition (both arm and hand)
  - **+2 minutes:** 5<sup>th</sup> and final punctate mechanical stimulation
- **Round-Up (10 minutes):** Disconnection and debriefing of the subject.

A visual representation of the timeline observed during the experimental session is showed in Figure 1 - *Timeline of experimental session*. On the other hand, a more detailed description of the familiarization and the experiment will be provided in section 5.

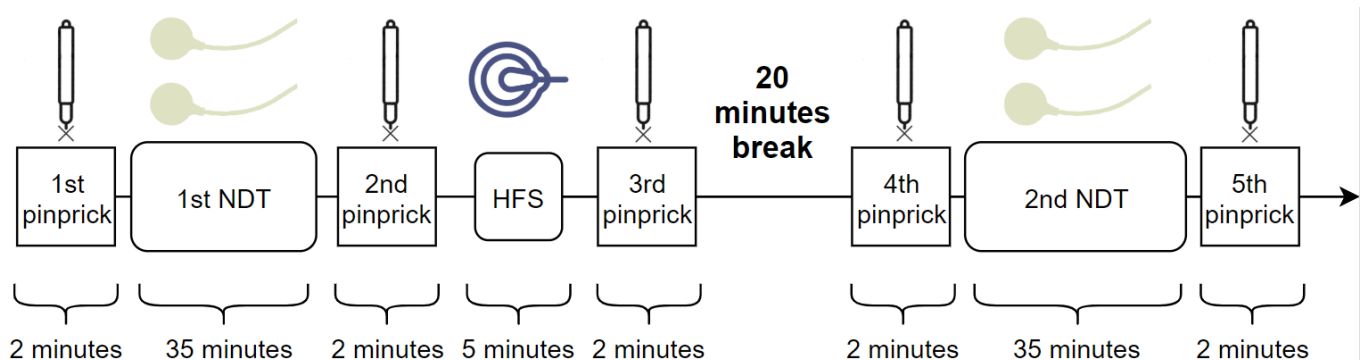


**Figure 2 - Timeline of experimental session**

### **3.2. EXPERIMENTAL SETTING**

A visual representation of the experimental set up is shown in Figure 2. The electrodes are positioned and the punctate mechanical stimulation is performed on the right forearm of each healthy subject. The pinpricks are applied using Semmes-Weinstein monofilaments and are administered on the anterior, posterior, left and right of the HFS and the two IES electrodes, where the anterior is proximal, posterior is distal, left is lateral and right is medial (right forearm).

## **4. STUDY POPULATION**

### **4.1 POPULATION BASE**

A total of 20 healthy subjects will be recruited at the University of Twente, the Netherlands, which is a realistic amount based on previous experience with experiments on nociceptive testing.

### **4.2 INCLUSION CRITERIA**

A potential participant is eligible for participation in this study if all of the following criteria are met:

- A signed, written informed consent.
- Age between 16 and 40.

### **4.3 EXCLUSION CRITERIA**

A potential participant who meets any of the following criteria will be excluded from participation in this study:

- Participant refusal during the study.
- Language problems.
- Skin problems at site of stimulation or EEG recording.
- Diabetes.
- Implanted stimulation device.
- Pregnancy.
- Usage of analgesics within 24 hours before the experiment.
- Consumption of alcohol or drugs within 24 hours before the experiment.
- Pain complaints at the time of the experiment.
- A medical history of chronic pain.
- Having a position of dependency on one or more of the researchers (i.e. being directly supervised and graded by one of the researchers).

### **4.4 SAMPLE SIZE CALCULATION**

Due to the exploratory nature of this study, no sample size calculation is performed.

## 5. METHODS

### 5.1 STUDY PARAMETERS

#### 5.1.1 MAIN STUDY PARAMETERS

*NDTs Subject Response:* The subject's response to the stimulus, *detected* or not *detected*.

*EEG Signals:* Electric signals reflecting the subject's neurophysiological activity related to the stimulus, extracted at a fixed interval around every stimulus.

*NRS after HFS stimulation:* Scoring the intensity of pinpricks by means of numerical rating score after inducing secondary hyperalgesia using high-frequency stimulation

*Punctate mechanical stimulation:* Pinprick stimulation using Semmes-Weinstein monofilaments for assessing the occurrence of secondary hyperalgesia

#### 5.1.2 OTHER STUDY PARAMETERS

*Response Time:* Subject's response time.

*Participant Characteristics:* Age and sex, handedness.

*Electrode-skin Impedance:* To assess whether the setup of the HFS was able to reach the required voltages for intensity 20 times higher the subject's detection threshold.

## 5.2 MEASUREMENTS

### 5.2.1 MATERIALS AND METHODS

#### ***IES Stimuli***

Intra-epidermal electrocutaneous stimuli are applied using an array of five micro-needle electrodes [26]. These electrodes protrude only 0.2 mm through the stratum corneum of the skin and permit specific activation of superficial (A $\delta$ ) nociceptive skin fibers. The electrodes are sterilized before every usage in a monitored autoclave process with a minimum temperature of 121 degrees Celsius for at least 15 minutes.

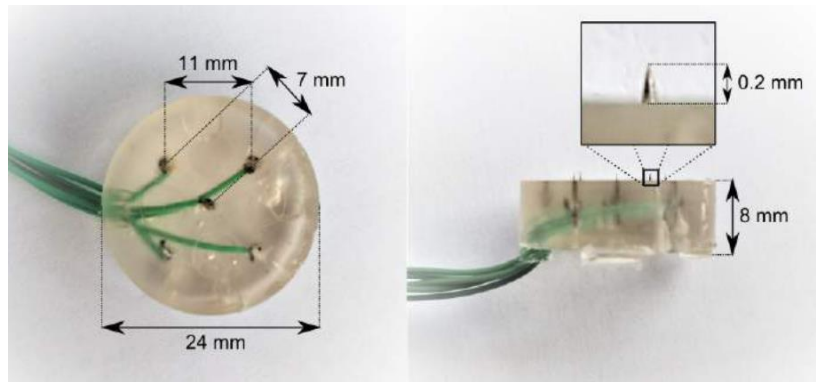


**Figure 3 - electrode for intra-epidermal electrocutaneous stimulation (IES)**

Each stimulus consists of one or two cathodic square-wave electrical currents pulse with a pulse width of 0.21 ms. The double pulse has an intra-pulse interval of 10 ms. The stimulus amplitude is limited to a maximum current of 2.0 mA.

### ***IES Stimulator***

The stimulator is a OctoStim stimulator, developed and thoroughly tested by the BSS group at the University of Twente. A desktop computer running a custom computer program written in LabVIEW 2013, SP1 controls all stimulation procedures and registers the applied stimulus amplitudes (in mA) and their trigger codes, the responses to stimuli, and the stimulus times in milliseconds. In addition to registering stimulus and threshold data, all communication between software and stimulator is logged. An IMDD of the OctoStim stimulator is available in the additional documentation

### ***EEG Recording***

To register EPs, scalp EEG is recorded continuously with a sample frequency of 1 kHz using an ANT Neuro Waveguard EEG cap containing 32 Ag/AgCl electrodes in combination with an TMSi 136-channel Refa EEG amplifier. The EEG and the trigger codes are recorded on a dedicated desktop computer running TMSi Polybench software. During the experiment, the subject sits in a comfortable chair and has to focus on a spot on the wall. The subjects are asked to blink as few times as possible during the times they press the response button and hence receive stimuli.

### ***Multiple Threshold Tracking***

Stimuli are selected according to the MTT procedure [8, 9]. The threshold for each combination of NOP and IPI is tracked simultaneously by measuring the subject's response (*detected* or *not detected*) to a randomized set of stimulus amplitudes, resulting in 2 simultaneously tracked nociceptive detection thresholds. All types of stimuli are selected the same number of times but in a random order.

### ***Punctate mechanical stimulation***

Pinpricks are applied using a 5.18/15g Semmes-Weinstein monofilament. The punctate mechanical stimulation is administered on the proximal, distal, radial and medial sides of the HFS and the two IES electrodes and every pinprick is applied at slightly displaced locations, to prevent mechanical sensitization, Figure 2. Thus, three areas will be tested: the ventral side of the forearm where the HFS electrode is placed, the ventral side of the forearm where the IES electrode is placed and the dorsal side of the hand where the last IES electrode is applied.



***Figure 4 - Semmes-Weinstein monofilament***

The order of the areas (proximal, distal, lateral and medial) where the pinpricks will be applied, will be randomized at every stage and for all the five punctate mechanical stimulations performed throughout the experimental session. This should prevent anticipation of the subjects on the position of the pinpricks. Furthermore, the subjects are asked to look away when the punctate mechanical stimulation is performed in order to ensure that blinding is as effective as possible. A visual representation of the position of the administered pinpricks can be seen in Figure 2

The subjects will be asked to assess the intensity of the perceived pinpricks, taking in consideration all the pinpricks (north-south, east-west) for each region of interest. The intensity will be evaluated with the NRS score. The numerical scores range from 0 (equal to 'no pain') to 10 (equal to 'the most intense pain imaginable'), where 5 is the turning point between 'merely a sensation' to 'actual pain'.

### ***HFS Stimuli***

**NL72937.091.20/** Exploration of the effects of HFS-induced secondary hyperalgesia on the NDT-EP method

High-frequency electrocutaneous stimuli are applied using a circular electrode with a 2cm diameter composed of two concentric rings. The external ring is the anode, while the internal ring is a cathode. While applying HFS, the electrode-skin impedance will be monitored in order to ensure whether the setup of the HFS was able to reach the required voltages for intensity 20 times higher the subject's detection threshold.

Each stimulus consists of 5 trains: each lasting 1s, frequency of 100Hz and pulse-width 2ms. The time interval between each train is 10s.



**Figure 5 - Two electrodes used for High-frequency stimulation. In this experimental protocol, only one electrode will be used.**

The subjects will be asked to assess the intensity of the perceived stimulation. The intensity will be evaluated with the NRS score. The numerical scores range from 0 (equal to 'no pain') to 10 (equal to 'the most intense pain imaginable'), where 5 is the turning point between 'merely a sensation' to 'actual pain'.

## **5.2.2 PROCEDURE**

### **Introduction (10 minutes)**

The subject will be asked to read and sign the informed consent form (document E2).

### **Preparation (20 minutes)**

The subject will be connected to the EEG equipment by connecting the EEG cap to the head of the subject and filling EEG electrodes with conductive gel. After applying the cap, it is verified if the scalp-electrode impedance is less than 5 k $\Omega$ . The first IES electrode will be

placed on the backside of the hand of the right arm, while the second IES electrode will be placed on the ventral side of the right forearm. The connected stimulation device will be held by the hand on the contralateral side. The stimulation device is wirelessly connected to the controlling computer using Bluetooth.

The HFS electrode will be placed proximal to the second IES electrode, on the subject's ventral side of the right forearm.

### ***Familiarization (10 minutes)***

To learn recognizing the barely detectable stimuli, the subjects receive test stimuli using a short detection threshold estimation method consisting of 2 series of 10 ascending stimuli for each stimulus type, as described by Steenbergen et al.[27]. The subjects are asked to press and hold the button on the stimulator triggering a series of stimuli with rising amplitude applied at a rate of 1 stimulus per second. During the first series, the subjects are instructed to release the button (terminating the series of stimuli) when they have been able to clearly feel and recognize the stimulus-related sensation. During the second series, the subjects are instructed to release the button as soon as they feel any sensation which they ascribe to the application of a stimulus. An initial estimate of the sensation threshold, which is the value at which the MTT paradigm will initialize tracking, will be obtained using the value of the last measurement.

### ***1<sup>st</sup> punctate mechanical stimulation (2 minutes)***

Before starting the procedure, a marker is used on the subject's right forearm and hand to target the exact position where pinpricks will be performed throughout the entire session. The position of the pinpricks are on the north, south, east and west side of imaginary HFS-electrode and both IES-electrodes, as shown in Figure 2. The order of the regions to apply the pinpricks will be randomized at every stage.

The subjects will be asked to assess the intensity of the perceived pinpricks, taking in consideration all the pinpricks (north-south, east-west) for each region of interest. The intensity will be evaluated with the NRS score. The numerical scores range from 0 (equal to 'no pain') to 10 (equal to 'the most intense pain imaginable'), where 5 is the turning point between 'merely a sensation' to 'actual pain'.

### ***Nociceptive perception task (35 minutes)***

Nociceptive perception thresholds are tracked over time. Subjects are instructed to press and hold a button, and release the button as soon as they feel a sensation that they ascribe to the application of a stimulus. A stimulus is identified as not detected if the subject does not release the response button within 1 second after the stimulus is given. While the

button is pressed, the stimulator applies stimuli to the subject with randomized amplitudes according to the MTT paradigm. Subjects are instructed to re-press and hold the button again after approximately second. The subject is allowed to take short breaks during the stimulus series, by releasing the button for a longer time after application of a stimulus. This procedure repeats until the end of the experiment. The stimuli are applied alternating between the first and second IES electrode.

The total experiment will consist of one block of 400 stimuli with equal amount of each stimulus type. To prevent discomfort, the total MTT paradigm duration (including familiarization) is limited to 50 minutes, which is expected to be sufficient for collection of all SRPs, based on previous experiments [10, 11].

<b>STIMULI</b>		<b>Familiarization</b>	<b>Experiment</b>
<b>Amplitude</b>		0 to 1 (stepsize 0.1) mA	randomized (max. 2.0 mA)
<b>NOP = 1</b>		3 times 10	100 (hand, dorsal side) 100 (forearm, ventral side)
<b>NOP = 2</b>	<b>IPI = 10 ms</b>	3 times 10	100 (hand, dorsal side) 100 (forearm, ventral side)
<b>Total</b>		60 stimuli	400 stimuli

**Table 1: Stimuli in the planned experiment, which will be applied in a randomized sequence according to the MTT paradigm. NOP refers to Number of Pulses and IPI refers to Inter-Pulse Interval.**

### **2<sup>nd</sup> punctate mechanical stimulation (2 minutes)**

The mechanical pinpricks are performed again to exclude any sensitization that might occur as consequence of the IES stimulation. The position of the pinprick is again randomized, as established for the first punctate stimulation (see at the start of the procedure, after the section called **Familiarization**).

### **HFS stimulation (5 minutes)**

Secondary hyperalgesia can be induced by applying high-frequency stimulation. The electrode is placed on the ventral side of the subject's right forearm, see Figure 2

Before starting this phase a new detection threshold is measured, specifically for the high frequency stimulation. The amplitude of the HFS is now set at 20 times the detection threshold estimated. The applied stimulus consists of 5 trains: each lasting 1s, frequency of 100Hz and pulse-width 2ms. The time interval between each train is 10s. After the first train, the stimulation is stopped and the subject is asked whether they would like to continue with the experiment or to stop due to discomfort, consequence of the high-frequency stimulation. If the subject agrees, the experiment will proceed.

While applying HFS, the electrode-skin impedance is measured to assess whether the setup of the HFS was able to reach the required voltages for intensity 20 times higher the subject's detection threshold.

<b>STIMULI</b>	<b>Frequency</b>	<b>Width</b>	<b>Length</b>	<b>Inter-train interval</b>	<b>Amount</b>
<b>Train pulses</b>	100 Hz	2 ms	1 s	10 s	5

Table 2: High frequency stimuli in the planned experiment.

### ***3<sup>rd</sup> punctate mechanical stimulation (2 minutes, right after HFS)***

The mechanical pinpricks are performed again to confirm (or discard) the occurrence of secondary hyperalgesia.

### ***20 minutes break***

As suggested by the literature, the occurrence of HFS-induced secondary hyperalgesia is best noticeable after 20 minutes from the stimulation[28],[29].

In this phase, the subjects will be asked to remain seated in position since the EEG cap and the electrodes will not be removed. However, the subjects will be allowed to check their phones, interact with the people in the room, read a book and cautiously drink something.

### ***4<sup>th</sup> punctate mechanical stimulation (2 minutes)***

The mechanical pinpricks are performed again to confirm (or discard) the occurrence of secondary hyperalgesia.

### ***Nociceptive perception task (35 minutes)***

A second Nociceptive perception task is required. The protocol for this second nociceptive perception task is equal to the one presented in the previous ***Nociceptive perception task*** section.

### ***5<sup>th</sup> punctate mechanical stimulation (2 minutes, right after last NDT)***

The mechanical pinpricks are performed once again.

### ***Round-up (10 minutes)***

The subject will be disconnected from the set-up, after which the subject will be given the opportunity to wash-out conductive EEG gel from the hair. Subsequently the subject will be given the Bol.com voucher, be provided with contact information, and given the chance to ask questions.

A visual representation of the timeline observed during the experimental session is showed in *Figure 1 - Timeline of experimental session*.

### **5.3 RANDOMISATION, BLINDING AND TREATMENT ALLOCATION**

Since this study does not include any comparison between groups of subjects, randomization and blinding of the study design is not relevant for this study.

However, the mechanical pinprick stimulation will require the subjects to be blinded. The Semmes-Weinstein filament used in this protocol is a 5.18 / 15g, but the subjects will not be informed that the filament will be the same throughout the whole session. Furthermore, the participants will be blinded to location of applied pinpricks. This should allow the subjects to give a more objective score.

### **5.4 WITHDRAWAL OF INDIVIDUAL SUBJECTS**

Participants can leave the study at any time for any reason if they wish to do so without any consequences. The investigator can decide to withdraw a subject from the study for urgent medical reasons.

### **5.5 REPLACEMENT OF INDIVIDUAL SUBJECTS AFTER WITHDRAWAL**

If participants discontinue the study, additional participants will be recruited to have the planned number of evaluable participants. A maximum of 5 included participants will be replaced. In case more than this maximum has to be replaced, the study will be stopped. For further information about this, see section 5.7.

### **5.6 FOLLOW-UP OF SUBJECTS WITHDRAWN FROM TREATMENT**

The follow-up of participants due to adverse events is described in section 8.3. The investigator and participant will decide if and what kind of follow-up is indicated in other situations.

### **5.7 PREMATURE TERMINATION OF THE STUDY**

The investigator reserves the right to close an investigational site or terminate the trial at any time for any reason. In case of an early termination of the trial or temporary halt, the competent authority will be notified by the investigator within 15 calendar days, including a detailed written explanation of the reasons for the termination/halt. The end of trial is defined as the last participant's measurement.

## 6. SAFETY REPORTING

### 6.1 TEMPORARY HALT FOR REASONS OF SAFETY

In accordance to section 10, subsection 4, of the WMO, the sponsor will suspend the study if there is sufficient ground that continuation of the study will jeopardise subject health or safety. The sponsor will notify the accredited METC without undue delay of a temporary halt including the reason for such an action. The study will be suspended pending a further positive decision by the accredited METC. The investigator will take care that all subjects are kept informed.

### 6.2 AEs, SAEs and SURARs

#### 6.2.1 ADVERSE EVENTS (AEs)

Adverse events are defined as any undesirable experience occurring to a subject during the study, whether or not considered related to the experimental procedure. All adverse events reported spontaneously by the subject or observed by the investigator or his staff will be recorded.

#### 6.2.2 SERIOUS ADVERSE EVENTS (SAEs)

A serious adverse event is any untoward medical occurrence or effect that at any dose:

- results in death;
- is life threatening (at the time of the event);
- requires hospitalization or prolongation of existing inpatients' hospitalization;
- results in persistent or significant disability or incapacity;
- is a congenital anomaly or birth defect;
- Any other important medical event that may not result in death, be life threatening, or require hospitalization, may be considered a serious adverse experience when, based upon appropriate medical judgement, the event may jeopardize the subject or may require an intervention to prevent one of the outcomes listed above.

The sponsor will report the SAEs through the web portal *ToetsingOnline* to the accredited METC that approved the protocol within 15 days after the sponsor has first knowledge of the serious adverse reactions.

SAEs that result in death or are life threatening should be reported expedited. The expedited reporting will occur not later than 7 days after the responsible investigator has first knowledge of the adverse reaction. This is for a preliminary report with another 8 days for completion of the report.

**NL72937.091.20/** Exploration of the effects of HFS-induced secondary hyperalgesia on the NDT-EP method

### **6.3 FOLLOW-UP OF ADVERSE EVENTS**

All AEs will be followed until they have abated, or until a stable situation has been reached. Depending on the event, follow up may require additional tests or medical procedures as indicated, and/or referral to the general physician or a medical specialist.

SAEs need to be reported till end of study within the Netherlands, as defined in the protocol.

### **6.4. DATA SAFETY MONITORING BOARD (DSMB)**

The need for a DSMB is assessed taking the EMEA guidelines on data monitoring committees into consideration. In the current study, aspects such as indication, study endpoints, study duration and study population do not trigger the need of a DSMB. Therefore, a DSMB is not considered beneficial for this study and will therefore not be established.

## 7. STATISTICAL ANALYSIS

Statistical analysis will be performed at the University of Twente, using appropriate statistical software (Matlab, Fieldtrip [30] and R).

### 7.1 EEG PRE-PROCESSING

EEG data is pre-processed using FieldTrip, a third-party Matlab toolbox for MEG and EEG analysis. Contamination of the EEG by eye-blinks or movements is corrected using an independent component analysis algorithm [31], with which components with a clear EOG component and a frontal scalp distribution are removed. Trials are extracted from the continuous EEG by taking a fixed time-window around every stimulus. Trials are baseline corrected and filtered to achieve an optimal signal-to-noise ratio. The resulting trial signals are stored together with the stimulus parameters.

### 7.2 MODEL COMPUTATION

EEG data is downsampled to 200 Hz to increase computational speed. Subsequently, the EP will be modelled as a function of the stimulus parameters by a LMM. The model variables are centered and scaled to a variance of one. The mixed-model is computed for every time point, similar to Vossen et al. [32],[33],[34].

In the mixed-model, to prevent confounding by subject-specific variables (e.g. age, gender etc.), subject is modelled as a random factor including a random intercept and a random slope for every main effect. No assumptions, despite the assumption of multivariate normality and independence between subjects, are made on the covariance or correlation structures of the random effects. Furthermore, no correlation structure is assumed for the residual, allowing for an unconstrained residual distribution in every time-point.

Model computation and analysis is performed in R, using the 'lme4' [35] and the 'lmerTest' library, which is an extension to 'lme4' for statistical testing. To compute the model, parameters are estimated for every point in time by optimization of the restricted maximum likelihood with the 'lmer' function. Model coefficients are tested against the null-hypothesis, which is that the coefficient has no effect (is equal to 0), by the Wald Chi-Square test. To check for validity of the linearity and normality assumptions the residuals of the models are checked.

### 7.3 STUDY PARAMETERS

**Describe the quality and content of the multiple threshold tracking and EEG recordings before and after inducing secondary hyperalgesia onto the skin of healthy subjects with high-frequency stimulation**

This objective is achieved by:

**NL72937.091.20/** Exploration of the effects of HFS-induced secondary hyperalgesia on the NDT-EP method

- 1) Showing that the MTT-EP model successfully extracts parameter-related components from the original signal, demonstrating parameter-related functional activity.

*Parameters: stimulus related variations of the signal (as predicted by model).*

- 2) Showing that HFS-induced secondary hyperalgesia occurred by performing punctate mechanical stimulation.

*Parameters: stimulus-related variation of the NRS scores.*

**Analyze if and how NDTs and/or EPs are associated to the properties of applied stimuli (e.g. stimulus amplitude, number of pulses) and/or modulated by HFS-induced secondary hyperalgesia onto the skin of healthy subjects.**

This objective is achieved by:

- 1) Showing that the MTT-EP model, expressing psychophysical measurements and cortical activity, can successfully extract parameter-related components, demonstrating influences of stimuli type on functional activity.

*Parameters: stimulus related variations of the signal.*

- 2) Showing that the MTT-EP paradigm successfully extracts physiological-related components, demonstrating influences of central sensitization on functional activity.

*Parameters: variations of the signal related to central sensitization.*

## **8. ETHICAL CONSIDERATIONS**

### **8.1 REGULATION STATEMENT**

This study will be conducted according to the principle of the Declaration of Helsinki (October 2013) and the Medical Research Involving Human Subjects Act (WMO) and Good Clinical Practice (GCP) guidelines.

### **8.2 RECRUITMENT AND CONSENT**

Participants will be recruited at the University of Twente. Students and employees of the university meeting the inclusion criteria will be asked to participate in the study. Furthermore, a recruitment poster will be placed at the University to advertise the study, where contact information will be available in order for volunteers to reach out to our research group. Participants will receive written information about the study and are asked for their consent. After providing the information letter, participants are given a one-week reflection time in order to decide whether they would like to take part of the study.

### **8.3 BENEFITS AND RISKS ASSESSMENT, GROUP RELATEDNESS**

Participants of this study will obtain no direct personal benefit. However, measuring accurate, reliable pain sensitivity in combination with a mathematical model of the nociceptive system, can be used to detect and distinguish malfunctioning of either ascending and/or descending mechanisms, e.g. in chronic post-surgical pain. The possibility of harm or injury for participating subjects is negligible although some parts of the stimulation, especially the intervention (HFS), can be experienced as (very) painful. Furthermore, the HFS can lead to a red skin and sensitivity of the lower right arm for some hours after the experiment.

### **8.4 COMPENSATION FOR INJURY**

The sponsor/investigator has a liability insurance which is in accordance with article 7, subsection 6 of the WMO.

Due to the negligible risk related to this study, an exemption is requested for an insurance which is in accordance with the legal requirements in the Netherlands (Article 7 WMO and the Measure regarding Compulsory Insurance for Clinical Research in Humans of 23th June 2003).

### **8.5 INCENTIVES**

All participants will receive compensation for participation via Bol.com vouchers worthy of approximately €10. Only participants who completed the study will receive the compensation.

## **9. ADMINISTRATIVE ASPECTS, MONITORING AND PUBLICATION**

### **9.1 HANDLING AND STORAGE OF DATA AND DOCUMENTS**

Participants will be coded by a numeric code in order to create a coded dataset. This code will be reported in the collected dataset. The investigators will have access to this code, and will store the subject identification code list at a separate location from the dataset. The principal investigator will store the source files, CRF's and the trial master file (TMF) for 15 years in a locked cupboard.

All endpoints will be directly recorded on a paper data collection forms and put into a paper CRF. Copies of this CRF will be made at the site of the investigation, which is equal to the site of the sponsor.

### **9.2 AMENDMENTS**

A 'substantial amendment' is defined as an amendment to the terms of the METC application, or to the protocol or any other supporting documentation, that is likely to affect to a significant degree:

- The safety or physical or mental integrity of the subjects of the trial;
- The scientific value of the trial;
- The conduct or management of the trial;
- The quality of safety of any intervention used in the trial.

All substantial amendments will be notified to the METC and to the competent authority.

Non-substantial amendments will not be notified to the accredited METC and the competent authority, but will be recorded and filed by the sponsor.

### **9.3 ANNUAL PROGRESS REPORT**

The sponsor/investigator will submit a summary of the progress of the trial to the accredited METC once a year. Information will be provided on the date of inclusion of the first subject, numbers of subjects included and numbers of subjects that have completed the trial, serious adverse events/ serious adverse reactions, other problems, and amendments.

### **9.4 TEMPORARY HALT AND (PREMATURELY) END OF STUDY REPORT**

The investigator will notify the accredited METC of the end of the study within a period of 8 weeks. The end of the study is defined as the last participant's last visit.

**NL72937.091.20/** Exploration of the effects of HFS-induced secondary hyperalgesia on the NDT-EP method

In case the study is ended prematurely, the investigator will notify the accredited METC within 15 days, including the reasons for the premature termination.

Within one year after the end of the study the investigator/sponsor will submit a final study report with the results of the study, including any publications/abstracts of the study, to the accredited METC

## **9.5 PUBLIC DISCLOSURE AND PUBLICATION POLICY**

All publication rights belong to the principal investigator. Positive as well as negative trial results will be published in international peer-reviewed journals in the field of pain, neurophysiology and engineering. A primary author will be denoted according to the Vancouver system. A report will be submitted for the Independent Ethic Committee (CMO) at the end of the study as requested by law.

## 10. STRUCTURED RISK ANALYSIS

### 10.1 POTENTIAL ISSUES OF CONCERN

#### a. Level of knowledge about mechanism of action

The only possible mechanism of action involved with high-frequency and intra-epidermal electrical stimulation is the activation of skin fibres, which are mainly A $\beta$ , A $\delta$  and C fibres. The device with which the stimulation will be provided, is unable to provide currents that are above the legal maximum (IEC 601-2-10: effective current density may not be higher than 2 mA/cm<sup>2</sup>). This is the case since within the stimulator, there is one hardware component that is physically unable to provide more than 6 mA continuous DC. This was proven once this component was tested in isolation. The produced current is too low to produce heat at the skin.

#### b. Previous exposure of human beings with the test product(s) and/or products with a similar biological mechanism

Extensive of literature is available regarding high-frequency and intra-epidermal electrical stimulation. The electrode and a mono-channel version of the stimulator (the AmbuStim) used for electrical stimulation have been used in several previous studies [36],[37]. The MTT procedure has been used in several published (and unpublished) studies [37]. The HFS electrode is used in several studies by other research groups. In this study, a duplicate of this electrode will be used, which is obtained from the research group producing the electrode. Technical compliance of this electrode with our setup has been positively evaluated in a technical pilot study.

#### c. Analysis of potential effect

In none of the studies listed above, or in other studies on the subject, negative effects of the electrical stimulation either through needle electrodes or flat-plate electrodes have been described. It is not expected that electrical stimulation would cause any negative effects when stimulation duration and intensity is kept low.

#### g. Study population

Out of precaution, pregnancy is an exclusion factor, even though there is no real indication of increased risks related to pregnancy.

#### h. Interaction with other products

**NL72937.091.20/** Exploration of the effects of HFS-induced secondary hyperalgesia on the NDT-EP method

Possible interaction with implanted electrical devices, such as pacemakers or neuromodulation devices cannot be excluded. Therefore, participants with an implanted stimulation device are excluded from participation.

## **10.2 SYNTHESIS**

The stimulator is a prototype and does not have a CE mark, but an IMDD brochure is available (in D2). The stimulator is powered by an internal rechargeable battery and is not connected to the 220V power-supply.

Participants control the device by pressing a button. Electrical stimulation will pass through 2 electrodes attached to the skin. The maximum current of the stimulation procedure is limited to 2.0 mA. Stimulation immediately stops when the button is released. In addition, the examiner can switch off the stimulator at all times.

The electrodes used for the measurements are reusable electrodes and consist of 5 small needles with a length of about 0.4 mm. After each use, the electrodes are put in a sterilization pouch and sterilized in an autoclave with a minimum temperature of 121 degrees Celsius for at least 15 minutes.

Participants do not control the high-frequency electrical stimulation. The train pulses are delivered through an electrode attached to the skin. The maximum current of the stimulation procedure is limited to 2.0 mA.

From the information above, we conclude that it is highly unlikely that there are serious risks involved in the use of electrical stimulation.

## 11. REFERENCES

1. Langley, P.C., *The prevalence, correlates and treatment of pain in the European Union*. Current Medical Research and Opinion, 2011. **27**(2): p. 463-480.
2. Langley, P.C., *The prevalence, correlates and treatment of pain in the European Union*. Curr Med Res Opin, 2011. **27**(2): p. 463-80.
3. Breivik, H., et al., *Survey of chronic pain in Europe: Prevalence, impact on daily life, and treatment*. European Journal of Pain, 2006. **10**(4): p. 287-333.
4. Woolf, C.J., *Central sensitization: Implications for the diagnosis and treatment of pain*. Pain, 2011. **152**(SUPPL.3).
5. Doll, R.J., et al., *Tracking of nociceptive thresholds using adaptive psychophysical methods*. Behavior Research Methods, 2014. **46**(1): p. 55-66.
6. Wright, A., et al., *Abnormal Quantitative Sensory Testing is Associated With Persistent Pain One Year After TKA*. Clinical Orthopaedics and Related Research, 2015. **473**(1): p. 246-254.
7. Wylde, V., et al., *The association between pre-operative pain sensitisation and chronic pain after knee replacement: An exploratory study*. Osteoarthritis and Cartilage, 2013. **21**(9): p. 1253-1256.
8. Doll, R.J., P.H. Veltink, and J.R. Buitenweg, *Observation of time-dependent psychophysical functions and accounting for threshold drifts*. Attention, Perception, and Psychophysics, 2015. **77**(4): p. 1440-1447.
9. Doll, R.J., *Psychophysical Methods for Improved Observation of Nociceptive Processing*. 2016, University of Twente: Enschede.
10. Doll, R.J., et al., *Effect of temporal stimulus properties on the nociceptive detection probability using intra-epidermal electrical stimulation*. Experimental Brain Research, 2016. **234**(1): p. 219-227.
11. Doll, R.J., et al., *Responsiveness of electrical nociceptive detection thresholds to capsaicin (8 %)-induced changes in nociceptive processing*. Experimental Brain Research, 2016. **234**(9): p. 2505-2514.
12. van der Heide, E.M., et al., *Single pulse and pulse train modulation of cutaneous electrical stimulation: a comparison of methods*. J Clin Neurophysiol, 2009. **26**(1): p. 54-60.
13. Mouraux, A., E. Marot, and V. Legrain, *Short trains of intra-epidermal electrical stimulation to elicit reliable behavioral and electrophysiological responses to the selective activation of nociceptors in humans* Neuroscience Letters 2014. **561**: p. 69 - 73.
14. Vossen, C.J., et al., *Does habituation differ in chronic low back pain subjects compared to pain-free controls? A cross-sectional pain rating ERP study reanalyzed with the ERFIA multilevel method*. Medicine (United States), 2015. **94**(19).
15. Klein, T., et al., *Perceptual correlates of nociceptive long-term potentiation and long-term depression in humans*. J Neurosci, 2004. **24**(4): p. 964-71.
16. Lang, S., et al., *Modality-specific sensory changes in humans after the induction of long-term potentiation (LTP) in cutaneous nociceptive pathways*. Pain, 2007. **128**(3): p. 254-63.
17. Pfau, D.B., et al., *Analysis of hyperalgesia time courses in humans after painful electrical high-frequency stimulation identifies a possible transition from early to late LTP-like pain plasticity*. Pain, 2011. **152**(7): p. 1532-9.
18. Biurrun Manresa, J., et al., *High frequency electrical stimulation induces a long-lasting enhancement of event-related potentials but does not change the perception elicited by intra-epidermal electrical stimuli delivered to the area of increased mechanical pinprick sensitivity*. PLoS One, 2018. **13**(9): p. e0203365.
19. van den Broeke, E.N., et al., *Central Sensitization of Mechanical Nociceptive Pathways Is Associated with a Long-Lasting Increase of Pinprick-Evoked Brain Potentials*. Front Hum Neurosci, 2016. **10**: p. 531.
20. Klein, T., et al., *The role of heterosynaptic facilitation in long-term potentiation (LTP) of human pain sensation*. Pain, 2008. **139**(3): p. 507-19.

21. van den Broeke, E.N., C. Lenoir, and A. Mouraux, *Secondary hyperalgesia is mediated by heat-insensitive A-fibre nociceptors*. J Physiol, 2016. **594**(22): p. 6767-6776.
22. van den Broeke, E.N. and A. Mouraux, *Enhanced brain responses to C-fiber input in the area of secondary hyperalgesia induced by high-frequency electrical stimulation of the skin*. J Neurophysiol, 2014. **112**(9): p. 2059-66.
23. van den Broeke, E.N. and A. Mouraux, *High-frequency electrical stimulation of the human skin induces heterotopical mechanical hyperalgesia, heat hyperalgesia, and enhanced responses to nonnociceptive vibrotactile input*. J Neurophysiol, 2014. **111**(8): p. 1564-73.
24. van den Broeke, E.N., et al., *Neurophysiological correlates of nociceptive heterosynaptic long-term potentiation in humans*. J Neurophysiol, 2010. **103**(4): p. 2107-13.
25. Vo, L. and P.D. Drummond, *High frequency electrical stimulation concurrently induces central sensitization and ipsilateral inhibitory pain modulation*. European Journal of Pain, 2013. **17**(3): p. 357-368 % @ 1090-3801.
26. Steenbergen, P., et al., *Characterization of a bimodal electrocutaneous stimulation device*, in *4th European Conference of the International Federation for Medical and Biological Engineering*. 2008, EMBEC2008, Antwerp: Antwerp. p. 230-234.
27. Steenbergen, P., et al., *A system for inducing concurrent tactile and nociceptive sensations at the same site using electrocutaneous stimulation*. Behavior Research Methods, 2012. **44**: p. 924-933.
28. Pfau, D.B., et al., *Analysis of hyperalgesia time courses in humans after painful electrical high-frequency stimulation identifies a possible transition from early to late LTP-like pain plasticity*. Pain, 2011. **152**: p. 1532-1539.
29. Manresa, J.B., et al., *High frequency electrical stimulation induces a long-lasting enhancement of event-related potentials but does not change the perception elicited by intra-epidermal electrical stimuli delivered to the area of increased mechanical pinprick sensitivity*. PLoS ONE, 2018. **13**(9).
30. Oostenveld, R., et al., *FieldTrip: Open source software for advanced analysis of MEG, EEG, and invasive electrophysiological data*. Computational Intelligence and Neuroscience, 2011. **2011**.
31. Delorme, A. and S. Makeig, *EEGLAB: an open source toolbox for analysis of single-trial EEG dynamics including independent component analysis*. Journal of Neuroscience Methods, 2004. **134**: p. 9-21.
32. Vossen, C.J., et al., *Does habituation differ in chronic low back pain subjects compared to pain-free controls? A cross-sectional pain rating ERP study reanalyzed with the ERFIA multilevel method*. Medicine, 2015. **94**(19).
33. Vossen, C.J., et al., *Introducing the event related fixed interval area (ERFIA) multilevel technique: a method to analyze the complete epoch of event-related potentials at single trial level*. PLoS ONE, 2013. **8**(11).
34. Vossen, H., et al., *More potential in statistical analyses of event-related potentials: a mixed regression approach*. International Journal of Methods in Psychiatric Research, 2011. **20**(3): p. e56-e68.
35. Bates, D., et al., *Fitting linear mixed-effects models using lme4*. Journal of Statistical Software, 2015. **67**(1).
36. Doll, R.J., et al., *Tracking of nociceptive thresholds using adaptive psychophysical methods*. Behavior Research Methods, 2014. **46**: p. 55-66.
37. Doll, R.J., et al., *Effect of temporal stimulus properties on the nociceptive detection probability using intra-epidermal electrical stimulation*. Experimental Brain Research, 2016. **234**: p. 219-277.